

University of Kentucky

UKnowledge

Theses and Dissertations--Neuroscience

Neuroscience

2023

THERAPEUTIC IMPLICATIONS OF THE GUT-CNS AXIS IN PROMOTING RECOVERY FOLLOWING CERVICAL SPINAL CORD INJURY

Jessica Wilson

University of Kentucky, jsne223@uky.edu

Author ORCID Identifier:

 <https://orcid.org/0009-0003-8453-1270>

Digital Object Identifier: <https://doi.org/10.13023/etd.2023.164>

[Right click to open a feedback form in a new tab to let us know how this document benefits you.](#)

Recommended Citation

Wilson, Jessica, "THERAPEUTIC IMPLICATIONS OF THE GUT-CNS AXIS IN PROMOTING RECOVERY FOLLOWING CERVICAL SPINAL CORD INJURY" (2023). *Theses and Dissertations--Neuroscience*. 31. https://uknowledge.uky.edu/neurobio_etds/31

This Doctoral Dissertation is brought to you for free and open access by the Neuroscience at UKnowledge. It has been accepted for inclusion in Theses and Dissertations--Neuroscience by an authorized administrator of UKnowledge. For more information, please contact UKnowledge@lsv.uky.edu.

STUDENT AGREEMENT:

I represent that my thesis or dissertation and abstract are my original work. Proper attribution has been given to all outside sources. I understand that I am solely responsible for obtaining any needed copyright permissions. I have obtained needed written permission statement(s) from the owner(s) of each third-party copyrighted matter to be included in my work, allowing electronic distribution (if such use is not permitted by the fair use doctrine) which will be submitted to UKnowledge as Additional File.

I hereby grant to The University of Kentucky and its agents the irrevocable, non-exclusive, and royalty-free license to archive and make accessible my work in whole or in part in all forms of media, now or hereafter known. I agree that the document mentioned above may be made available immediately for worldwide access unless an embargo applies.

I retain all other ownership rights to the copyright of my work. I also retain the right to use in future works (such as articles or books) all or part of my work. I understand that I am free to register the copyright to my work.

REVIEW, APPROVAL AND ACCEPTANCE

The document mentioned above has been reviewed and accepted by the student's advisor, on behalf of the advisory committee, and by the Director of Graduate Studies (DGS), on behalf of the program; we verify that this is the final, approved version of the student's thesis including all changes required by the advisory committee. The undersigned agree to abide by the statements above.

Jessica Wilson, Student

Dr. Warren Alilain, Major Professor

Dr. Warren Alilain, Director of Graduate Studies

THERAPEUTIC IMPLICATIONS OF THE GUT-CNS AXIS IN PROMOTING
RECOVERY FOLLOWING CERVICAL SPINAL CORD INJURY

DISSERTATION

A dissertation submitted in partial fulfillment of the
requirements for the degree of Doctor of Philosophy in the
College of Medicine
at the University of Kentucky

By
Jessica Newton Wilson
Lexington, Kentucky
Director: Dr. Warren Alilain, Professor of Neuroscience
Lexington, Kentucky
2023

Copyright © Jessica Newton Wilson 2023
<https://orcid.org/0009-0003-8453-1270>

ABSTRACT OF DISSERTATION

THERAPEUTIC IMPLICATIONS OF THE GUT-CNS AXIS IN PROMOTING RECOVERY FOLLOWING SPINAL CORD INJURY

Nearly 60% of all spinal cord injuries (SCI) occur at the cervical level. These high-level injuries can interrupt the descending respiratory pathways required for breathing. Indeed, therapies in animal studies have been successful at restoring breathing after SCI; however, these interventions appear to be more effective at chronic time points. One potential cause for this observation is the impact of the injury on the gut microbiome. Neurotrauma can induce gut dysbiosis, an imbalance of pathogenic and beneficial gut microbiota, which has previously been shown to negatively impact the central nervous system (CNS) and impair recovery. We aimed to build upon these findings and investigate 1.) the impact of cervical SCI (cSCI) on the gut microbiome and 2.) how treating the resulting gut dysbiosis may improve respiratory recovery after cSCI. We hypothesized that cSCI leads to dynamic changes in the gut microbiome, which are most severe acutely after injury. Further, we hypothesized that this dysbiosis impedes functional recovery of breathing in the acute phase. As the dysbiosis resolves at chronic time points, treatments result in a more profound recovery.

To test our hypothesis, we performed a left C2 hemisection (LC2Hx) on adult female rats. We assessed the gut microbiome pre- and post-injury as well as the effects of treating gut dysbiosis following cSCI on respiratory outcomes. Our data suggest that LC2Hx results in transient changes in the gut microbiome that returns to preinjury levels over time. There were also inter-institutional differences in the Firmicutes-to-Bacteroidetes ratio when comparing animals that received cervical hemisection injuries at the University of Kentucky versus Drexel University. Further, gut tissue pathology indicated damage and dysregulation following LC2Hx. Performing a fecal matter transplant led to mixed results in functional outcomes. However, when we treated animals with high-dose probiotics following LC2Hx there were minimal deficits in minute ventilation when compared to vehicle. Additionally, the high-dose probiotic group also exhibited an increase in neurite sprouting and regenerative potential of neurons when compared to all other groups. Interestingly, we also observed a reduction in systemic TNF-alpha in all LC2Hx animals treated with probiotics, regardless of dose level, at 3dpi compared to vehicle. Our work suggests that treating gut dysbiosis in individuals with cSCI could improve functional outcomes and allow for interventions to be more efficacious at acute time points.

KEYWORDS: Spinal cord injury, Breathing, Gut microbiome, Gut-CNS Axis

Jessica Newton Wilson
(Name of Student)

04/12/2023
Date

THERAPEUTIC IMPLICATIONS OF THE GUT-CNS AXIS IN PROMOTING
RECOVERY FOLLOWING CERVICAL SPINAL CORD INJURY

By
Jessica Newton Wilson

Warren J. Alilain, Ph.D.

Director of Dissertation

Warren J. Alilain, Ph.D.

Director of Graduate Studies

04/12/2023

Date

DEDICATION

To my family, friends, and husband. This work would not have been possible without your unwavering support, encouragement, and good humor.

ACKNOWLEDGMENTS

The following dissertation, while an individual work, benefited from the insights and direction of several people. First, my Dissertation Chair, Dr. Warren Alilain, exemplifies the high-quality scholarship to which I aspire. In addition, Dr. Kristina Kigerl provided timely and instructive comments and evaluations at every stage of the dissertation process, allowing me to complete this project on schedule. Next, I wish to thank the complete Dissertation Committee, and outside reader, respectively: Drs. Ann Stowe, Jamie Sturgill, Ai-Ling Lin, Joe Springer, and John McCarthy. Each individual provided insights that guided and challenged my thinking, substantially improving the finished product. Further, my lab mates provided technical, scientific, and emotional support that was critical for completing the project in a timely manner. I am especially grateful for the friendships I have made throughout this experience, and that made my time doing this work enjoyable.

In addition to the technical and instrumental assistance above, I received equally important assistance from family and friends. Their support through phone calls, inspirational texts, and making me take breaks really allowed me to push through the tough times and persevere. Additionally, my grandmother, mother, and sister have been wonderful examples of strong women in STEM and inspire me every day. Finally, I wish to thank my husband, Dr. Billy Wilson, for providing ongoing support throughout the dissertation process. I wouldn't have been able to do this without your love, support, and numerous pie runs.

TABLE OF CONTENTS

TITLE PAGE i

ABSTRACT OF DISSERTATION ii

ACKNOWLEDGMENTS vi

TABLE OF CONTENTS vii

LIST OF TABLES x

LIST OF FIGURES xi

CHAPTER 1. INTRODUCTION 1

 1.1 *Spinal cord injury (SCI)* 1

 1.1.1 SCI pathophysiology 2

 1.1.2 Assessment of injury severity 5

 1.1.3 History of SCI and treatment recommendations 8

 1.1.4 Current management and therapeutic strategies 9

 1.1.5 Clinical trials and experimental approaches for SCI 13

 1.1.5.1 Neuroprotection 14

 1.1.5.2 Neuroregeneration and plasticity 15

 1.1.5.3 Neurorehabilitation 18

 1.2 *Neural control of breathing* 19

 1.2.1 Respiratory Complications Following SCI 21

 1.2.2 Spontaneous recovery of breathing 22

 1.2.3 The lateral C2 hemisection (LC2Hx) model of SCI 22

 1.3 *Gut Microbiome* 23

 1.3.1 Gut-CNS Axis 25

 1.3.2 Gut-CNS Axis and SCI 26

 1.3.3 Gut-CNS Axis, SCI, and the restoration of breathing 31

CHAPTER 2. Targeting the Microbiome to Improve Gut Health and Breathing After Spinal Cord Injury 34

 2.1 *Introduction* 34

 2.2 *Materials and Methods* 35

 2.2.1 Animals and Housing 35

 2.2.1.1 Groups 35

 2.2.2 Fecal Matter Transplant 36

2.2.3	Probiotics	37
2.2.4	Left C2 Hemisection (LC2Hx)	37
2.2.5	Whole Body Plethysmography	38
2.2.6	Diaphragmatic Electromyogram (DiaEMG).....	39
2.2.7	16S rRNA Sequencing	40
2.2.8	Sectioning and Staining	42
2.2.8.1	CNS.....	42
2.2.8.1.1	Cresyl Violet	43
2.2.8.1.2	Immunohistochemistry (IHC).....	43
2.2.8.2	Gut Tissue (Swiss Roll)	44
2.2.9	Systemic Inflammation	45
2.2.10	Lung Health	45
2.2.11	Open Field Chamber	46
2.2.12	Dorsal Root Ganglia (DRG) Outgrowth	46
2.2.13	Statistical Analysis.....	48
2.3	<i>Results</i>	49
2.3.1	Cervical SCI leads to acute gut dysbiosis and gastrointestinal tract pathology. 49	
2.3.2	Targeting gut dysbiosis improves ventilatory function and gut health.	53
2.3.3	Probiotic Treatment after SCI reduces the systemic inflammatory response and increases the sprouting and regeneration potential of neurons.	57
2.4	<i>Discussion</i>	60
CHAPTER 3. Interinstitutional Comparisons of the Gut Microbiome Following Cervical Spinal Cord Injury..... 86		
3.1	<i>Introduction</i>	86
3.2	<i>Methods</i>	87
3.2.1	Animals and Housing.....	87
3.2.2	Left C2 Hemisection (LC2Hx)	87
3.2.2.1	University of Kentucky	87
3.2.2.2	Drexel University	89
3.2.3	16S rRNA Sequencing.....	90
3.2.4	Sectioning and Staining	91
3.2.4.1	Cresyl Violet	92
3.3	<i>Results</i>	92
3.3.1	Institution-specific gut microbiome profiles following cervical SCI.	92
3.3.2	Inter-institutional variables impact the gut microbiome.	94
3.4	<i>Discussion</i>	95
CHAPTER 4. DISCUSSION..... 103		

4.1	<i>Major Finding #1: Targeting gut dysbiosis following SCI improves functional and pathological outcomes.</i>	104
4.2	<i>Major finding #2: Cervical SCI induces distinct gut microbiome profiles at separate institutions and potentially influences outcomes.</i>	106
4.3	<i>Methodological Considerations and Limitations.</i>	108
4.4	<i>Future Directions.</i>	109
4.5	<i>Conclusion</i>	111
	APPENDIX	114
	<i>List of Abbreviations</i>	114
	REFERENCES	116
	VITA	134

LIST OF TABLES

Table 2.1 Summary of 16S sequencing reads processing	41
Table 2.2. Summary of Statistical Analyses	48
Table 3.1. Interinstitutional differences using the LC2Hx model.	102

LIST OF FIGURES

Figure 2.1 Injury model and experimental design.	63
Figure 2.2 Cervical SCI leads to acute dysbiosis and GI tract pathology.....	65
Figure 2.3. FMT treatment does not improve ventilatory function following LC2Hx.	67
Figure 2.4. High-dose probiotic treatment mitigates decline in respiratory rate following SCI.	69
Figure 2.5. Hypoxic whole-body plethysmography and lung mechanic measurements following SCI and probiotic treatment.	71
Figure 2.6 Confirmation of LC2Hx in Experiment 3: Probiotic treatment following LC2Hx.....	73
Figure 2.7 Probiotics treatment does not affect locomotor activity following LC2Hx. ...	75
Figure 2.8 Targeting gut dysbiosis improves gut health.....	77
Figure 2.9 Treating gut dysbiosis reduces the systemic inflammatory response.....	80
Figure 2.10 Probiotic treatment following SCI increases the sprouting and regenerative potential of neurons.....	82
Figure 2.11 Probiotics treatment does not alter serotonin levels at the level of the phrenic motor nucleus.....	85
Figure 3.1 The gut microbiome has distinct profiles between institutions and following cervical spinal cord injury.....	99
Figure 3.2 Interinstitutional confirmation of injury	101
Figure 4.1 Schematic summary of the proposed mechanism of gut dysbiosis impeding the functional recovery of breathing	113

CHAPTER 1. INTRODUCTION

1.1 Spinal cord injury (SCI)

The spinal cord is an extension of nervous tissue from the base of the brain that runs through the spinal column and terminates at the lumbar level as the conus medullaris. Its main functions are allowing bi-directional communication of motor commands and sensory experience between the brain and body, coordinating reflexes, and providing autonomic control of life-sustaining peripheral organs. Injury to the spinal cord can therefore be a life-threatening event that can result in permanent damage to these essential pathways. Survival from this damage can cause loss of sensory, motor, reflex, and autonomic function at and below the level of injury, dramatically impairing an individual's quality of life.

Worldwide, an estimated 500,000 people suffer a spinal cord injury (SCI) each year¹. In the United States alone, there are approximately 18,000 new cases each year and nearly 300,000 people currently living with an SCI. The leading causes of SCI are vehicle crashes (37.7%) and falls (31.4%), followed by violence, particularly from gunshot wounds (15.3%), and lastly, sports/recreation (8.3%)². Since 2015, 78% of new cases have been males, with the average age at the time of injury increasing from 29 years old in the 1970s to 43 years old in 2015².

Unfortunately, the average life expectancy of a person with an SCI has not improved since the 1980s². Higher-level injuries reduce life expectancy by almost half and increase mortality risk due to complications in vital organ functions, such as respiration. Further, pneumonia and septicemia are the leading causes of death of individuals with an SCI. The mortality rate due to respiratory disease has only slightly decreased, while there has been no change in the septicemia mortality rate for the past 48 years². In addition to life

expectancy stress, individuals with an SCI are also faced with financial burdens. Healthcare costs and living expenses for persons with higher tetraplegia have an average yearly expense reaching over \$1 million, with each subsequent year averaging over \$200,000 ².

Due to these daily-life and financial difficulties, researchers and clinicians have worked to develop experimental strategies to improve outcomes and effectively restore function following SCI. While many of these strategies have shown promise in preclinical animal models and several have entered clinical trials, there are still no approved treatments for SCI. The lack of success in clinical translation to the human SCI population may indicate that there are unique and understudied factors that influence the recovery process. It is becoming more apparent that individual differences can influence the propensity for recovery and efficacy of treatment strategies ³⁻⁵. One potential variable undermining recovery is the gut microbiome, or the trillions of microorganisms that populate the gastrointestinal tract. These gut microbes have been shown to regulate host physiology while disruption, or gut dysbiosis, can exacerbate disease and impact recovery potential following neurotrauma ⁶⁻¹⁰. Fully elucidating the role of the gut microbiome and its influence on recovery may provide a novel therapeutic target to enhance the efficacy of previous experimental therapeutic techniques and overcome translational barriers by emphasizing personalized medicine and a holistic approach.

1.1.1 SCI pathophysiology

The pathophysiology of SCI is divided into primary and secondary phases. The primary injury phase describes the direct mechanical insult of physical trauma to the spinal

cord. The most common type of primary injury is a compressive-contusive-type injury in which the fracture and/or dislocation of the vertebral column causes a blow to the cord, followed by sustained compression ¹¹. This primary injury results in axon disruption, hemorrhage, and cell membrane destruction. Although there may be a complete functional loss, rarely does this injury cause a complete transection of the spinal cord ^{11,12}. Importantly, the presence of spared axons is a major focus of therapeutic strategies. Therefore, the severity of the primary injury is significant in determining the outcome of SCI ¹³.

The secondary phase of SCI was initially introduced over a century ago in 1911 and describes the cascade of intra- and extracellular insults that cause further damage to the spinal cord ¹⁴. This phase is further categorized into three additional subphases: acute, sub-acute, and chronic phases. The acute phase begins at the time of injury and describes the subsequent events of hemorrhage and ischemia that result in ionic imbalances, calcium influx, excitotoxicity, formation of free radicals, lipid peroxidation, inflammatory cell infiltration, edema, and necrosis. These processes and inflammatory responses lead to progressive tissue degeneration and orchestrate the mechanisms in the subacute and chronic phases of secondary injury.

The subacute phase encompasses the resulting apoptosis, demyelination, Wallerian degeneration, inflammatory cascade, and the formation of a glial scar. Within the first 48 hours after the injury, resident astrocytes and microglia, and blood-born neutrophils are recruited to the injury site ¹⁵. These cells begin to clear the debris resulting from cell death, axonal demyelination, and Wallerian degeneration, which begin to form a cystic cavitation at the lesion epicenter ¹⁶. By 72 hours post-injury, blood-born macrophages, B- and T-

lymphocytes begin infiltrating the injury site ¹⁷⁻¹⁹. In order to contain the injury, astroglia begin to hypertrophy to become activated and overlap to form a barrier, or scar, around the lesion cavity. Astrocytes play an immunomodulatory role and promote the pro-inflammatory M1-like phenotype of microglia and macrophages in favor of the anti-inflammatory, pro-regenerative M2-like phenotype through mechanisms of TNF-alpha signaling and intracellular iron accumulation ^{19,20}. Of note, the classification of M1- and M2-like phenotypes as pro- and anti-inflammatory may not be as straightforward as previously accepted. In traumatic brain injury studies, it has been shown that microglia and macrophages simultaneously express M1 and M2 phenotypic markers following neurotrauma ²¹. This finding suggests that the microglia and macrophage response to injury is complex and cannot be easily categorized under such multifaceted events. These immune cells are capable of adopting a pro-inflammatory or an anti-inflammatory, regenerative phenotype in the injured spinal cord ¹⁹. While neuroinflammation is typically considered to be detrimental to outcomes, it is now well-recognized that some inflammation is beneficial to recovery ^{22,23}. Overall, inflammation is multiphasic following SCI. This inflammatory response is most pronounced acutely after injury, although it continues into the subacute and chronic phases and may persist throughout a patient's life ¹⁸.

Finally, the chronic phase describes the continued axonal die-back, formation of a cystic cavity, and the maturation of the glial scar ¹³. Within the first two weeks post-injury, the lesion epicenter forms an extracellular matrix (ECM) consisting of fibronectin, collagen, and laminin ¹³. As the glial scar matures, these cells become replaced by pericytes, macrophages, and fibroblasts and form the inner fibrotic scar. Additional cells are also recruited from the periphery, and the maturation of the glial scar consists of

astrocytes, NG2+ oligodendrocyte precursor cells (OPCs), microglia, fibroblasts, and pericytes in penumbra^{24,25 26}. The mature scar is described as the formation of a fibrotic scar in the lesion core surrounded by a glial scar²⁷. Additionally, lectin-family chondroitin-sulfate proteoglycans (CSPGs) are upregulated by astrocytes and surround the lesion in a gradient pattern²⁶. By nature, CSPGs inhibit axon outgrowth due to their glycosaminoglycan (GAG) moieties^{26,28}. CSPGs link together to form a perineuronal net (PNN) that surrounds the neuronal soma and proximal neurites, further limiting growth and plasticity within the CNS after injury²⁶. While the glial scar is important for containing damage after injury, it also prevents beneficial axonal regenerative and sprouting potential. Importantly for recovery, enzymatic degradation of these inhibitory molecules using chondroitinase ABC (ChABC) can promote axonal outgrowth and sprouting, leading to significant improvement of locomotor and proprioceptive function²⁹. The use of ChABC to degrade CSPGs was also found to promote the plasticity of spared pathways and induce functional regeneration of respiratory pathways after cervical SCI³⁰. These findings provide further evidence that while the innate repair process is necessary, modulation of the intensity and duration of these mechanisms may allow for greater functional restoration.

1.1.2 Assessment of injury severity

Due to the heterogeneous nature of SCIs, the development of a standardized assessment to classify injury level and severity was essential for medical providers to diagnose patients and make clinical decisions. In 1982, the International Standards for Neurological Classification of Spinal Injury was published by the American Spinal Injury Association (ASIA) and provided a grading and classification system for assessing spinal

cord injury. Known today as the ASIA Impairment Scale (AIS), this clinical exam has become the gold standard for evaluating spinal cord injuries and identifying the neurological level of injury ³¹. The neurological level refers to the most caudal segment of the spinal cord with normal sensory and motor function bilaterally. Sensory and motor function are assessed using dermatomes and myotomes. The sensory examination tests 28 dermatomes bilaterally using light touch and pinprick. The motor examination consists of bilaterally grading ten muscle groups, five in the upper extremity and five in the lower extremity, using a six-point scale (0-5) ranging from total paralysis (0) to normal (5). Following these exams, the injury can be designated as “complete” or “incomplete”. If there is no sparing of sensory or motor function in the lowest sacral segment of the cord, the injury is deemed complete and given an AIS score of A. An incomplete injury is described as having a “partial preservation of sensory and/or motor functions below the neurological level and includes the lowest sacral segment”, and AIS scores range between B – D ³². The classification of AIS B describes sensory but no motor function, while AIS C and D are described as having 50% of muscle function below the neurological level with either less (C) or more (D) than a grade 3 on the six-point scale. Finally, an AIS score of E indicates normal sensory and motor function.

While the AIS is a useful tool in assessing the level and severity of an SCI, this test requires extensive training by the examiner and may have some sensitivity, reliability, and validity issues ³³. In recent years, the use of biomarkers to assess SCI severity has become an exciting area of research. The use of biomarkers has been proposed to be used in conjunction with the AIS assessment to provide unbiased outcomes and strengthen the predictive scores and potential for functional recovery. Additionally, biomarkers have the

potential to be used to track SCI progression and assess therapeutic efficacy. A clinical trial assessing inflammatory cytokines, structural proteins, and microRNA in the cerebral spinal fluid (CSF) following acute SCI resulted in distinct differences between AIS A, B, and C grades ³⁴⁻³⁶. Specifically, interleukin (IL)-6, IL-8, monocyte chemoattractant protein 1 (MCP-1/CCL2), tau, S100 β , and glial fibrillary acidic protein (GFAP) exhibited time-dependent changes that could classify AIS grades with 89% accuracy ^{35,36}. Additionally, subsequent studies by the same group determined that these biomarkers were significantly higher at 24 hours post-injury in patients that did not convert, or improve, their AIS score than those who did convert ³⁷.

Serum biomarkers have also been used clinically to assess SCI. Regardless of injury level or severity, migration inhibitory factor (MIF), several inflammatory cytokines, and High-Motility Group Box 1 (HMGB1) have all been shown to be elevated in patients acutely following SCI, with the HMGB1 elevation persisting in patients with chronic SCI (approximately 15 years post-injury) ^{38,39}. Though serum samples are much easier to access than CSF samples, they are less specific in differentiating injury level and severity and are found at levels that are several orders of magnitude lower when compared to CSF samples ³⁵. Interestingly, a recent study assessed both serum and CSF levels of neurofilament light (NF-L) and GFAP and found both to be increased with injury severity in patients with SCI and distinct between baseline AIS grades ⁴⁰. Overall, the utilization of biomarkers can be a powerful tool in the assessment and management of SCI.

1.1.3 History of SCI and treatment recommendations

Documentation of spinal cord injury is dated back to the seventeenth century B.C. in the Edwin Smith surgical papyrus⁴¹. This document not only describes the signs and symptoms of spinal injury with high accuracy but is the earliest known treatise on trauma, illustrating the advanced medical knowledge of ancient Egypt. Unfortunately, all injuries to the spinal cord were considered “a medical condition that cannot be healed”⁴². Throughout the 19th century, treatment for spinal cord injuries remained minimal, with manual extension and laminectomy to reduce compression as the main interventions⁴³.

As the turn of the century approached, several scientists at the time developed a better understanding of the pathological consequences of SCI. Charles Bell advocated that urine retention resulting in inflammation, infection, and ultimately renal failure was a cause of death following SCI. From this finding, it was soon determined that the severity of infection was directly proportional to survival time⁴³.

In 1898, Wilhelm Wagner developed the first successful and practical treatment of SCI. He described pathology, symptomatology, and treatment recommendations ranging from indications for surgery to the prevention of pressure sores⁴³. His published book became the standard reference for treating SCI throughout World War I, as the number of SCIs increased dramatically. Following the war and subsequent decrease in acutely injured SCI patients, the focus on rehabilitation for those chronically injured became more prevalent. By the 1920s, Donald Munro had developed the first effective SCI treatment center in Boston and was acknowledged by his colleagues as the “father of the treatment of paraplegia”. He was known for his holistic approach to treating patients with an emphasis on physiotherapy and mobilization through wheelchair use⁴³.

In 1943, Ludwig Guttman became the first director of the National Spinal Injuries Centre at Stoke Mandeville, where he implemented treatment protocols that became a model for other institutions to follow. He became known as the “founder of the modern treatment of spinal injuries” by combining the ideas previously mentioned and adapting his previous work on peripheral nerve injury to develop an integrated treatment program, including surgical techniques, aftercare, and rehabilitation ^{43,44}. He was such a strong advocate of physiotherapy in the form of sports that he organized the Stoke Mandeville Games, which would later influence the conception of the Paralympic Games ⁴⁵.

1.1.4 Current management and therapeutic strategies

Following a traumatic injury, the primary assessment at the scene prioritizes the ABCD approach: Airway, Breathing, Circulation, and Disability (neurologic status). When an SCI is initially suspected, immediate immobilization of the spine at the scene is recommended to prevent further injury ⁴⁶. Once stabilized, a clinical examination using the AIS scale, as described in section 1.1.2, should be performed to determine the level and severity of the injury, followed by computerized tomography (CT) imaging to further assess the injury and structural damage. Surgical decompression of the spinal cord is recommended within 24 hours after the initial SCI, which has been associated with improved neurologic outcomes ⁴⁷. The idea that “Time is Spine” highlights the importance of timely interventions acutely after injury will improve long-term outcomes ⁴⁸.

Spinal shock is a phenomenon in which there is an initial loss followed by a gradual return of reflexes caudal to the level of injury. Although the mechanism has not been fully elucidated, spinal shock can be described as a four-phase model: 1) areflexia/hyporeflexia 0 – 1 days post-injury, 2) initial return of reflexes 1 – 3 days post-injury, 3) early hyperreflexia 1 – 4 weeks post-injury, 4) late hyperreflexia 1 – 12 months post-injury ⁴⁹. Due to the progression of spinal shock, it is critical for clinicians and researchers to be aware of a spinal shock when assessing patients for completeness of injury and to enhance recovery while minimizing maladaptive responses.

As a result of injury to the spinal cord, patients may be unable to maintain adequate blood pressure to vital organs, including the CNS. This condition, known as neurogenic shock, is characterized by hypotension, bradycardia, and vasodilation due to unopposed parasympathetic vagal outflow, and can lead to death if not addressed immediately ⁵⁰. Evidence-based guidelines recommend the maintenance of a mean arterial pressure (MAP) of ≥ 85 -90 mmHg following acute spinal cord injury, a standard practice in the United States. Importantly, maintaining a MAP of ≥ 85 -90 mmHg has been shown to be an independent predictor of neurological improvement following spinal cord injury, as perfusion deficits resulting in ischemia can exacerbate the primary injury ⁵¹. A recent autopsy case from Japan demonstrated the importance of maintaining a MAP at ≥ 85 mmHg versus a systolic blood pressure of >90 mmHg following spinal cord injury. The findings described a fatal case of nonocclusive mesenteric ischemia (NOMI), where macroscopic and microscopic changes indicating necrosis and damage were evident in the intestinal tract, specifically at the ileal and ascending colon segments ⁵². This unfortunate

case emphasizes the call for international standardization of MAP maintenance following SCI.

Unfortunately, the importance of blood pressure maintenance does not end acutely after the injury. SCIs occurring at or above thoracic level 6 (T6) can result in autonomic dysreflexia, a life-threatening syndrome characterized by the loss of normal autonomic and cardiovascular control. This dysregulation results in episodic sympathetic hypertension due to noxious stimuli below the level of injury accompanied by parasympathetic-mediated bradycardia. Common triggers include bowel or bladder distention or irritation to the skin below the level of sensory function. If left untreated, severe complications, including debilitating headaches, seizures, and stroke, can occur⁵³. Fortunately, most episodes are mild and can be managed at home through proper bowel and bladder management, the removal of the noxious stimuli, and, if necessary, the use of antihypertensive drugs⁵⁴.

In addition to cardiovascular and blood pressure concerns, respiratory complications are the leading cause of death among SCI patients². Injuries occurring at the high cervical level can disrupt the descending bulbospinal pathways that are necessary for breathing and can cause paralysis to the diaphragm, the primary inspiratory muscle. Injuries below C5 can still result in compromised respiratory function due to weakness of secondary inspiratory muscles, including the intercostals and abdominal muscles. Vital capacity, or the maximum amount of air expelled following a maximum inhalation, is used to measure pulmonary function and determine the need for mechanical ventilation. Clinicians must also monitor the development of secretions, mucous plugs, atelectasis, and pneumonia. Mechanical ventilation increases the risk of these complications, and therefore weaning from mechanical ventilation should start as soon as possible⁵⁵.

Bowel and bladder dysfunction following SCI can lead to infection, induce autonomic dysreflexia, and significantly reduce the quality of life due to strict and time-consuming management protocols. Neurogenic bowel symptoms include slowed colonic transit, constipation, abdominal pain, and impaction^{56,57}. This dysfunction can also lead to pathological damage to the gastrointestinal tract⁵⁸⁻⁶⁰. Current research suggests that compromise of the tight junction proteins within the gastrointestinal wall can lead to bacterial translocation, systemic inflammation, and septicemia^{7,57,60}. Further, disruption to the luminal environment can cause an imbalance in the naturally occurring bacteria ecosystem that make up the gut microbiome and cause an increase in pathogenic bacteria. This disbalance, termed gut dysbiosis, has been shown in SCI patients, and its changes are injury-level and injury-severity dependent⁶¹⁻⁶⁴. Importantly, animal models have shown that this SCI-induced gut dysbiosis is detrimental to recovery following SCI^{7,65-67}. Unfortunately, the current management of neurogenic bowel is limited, although current research efforts aim to develop and improve evidence-based management strategies.

As previously described in section 1.1.3, a bladder infection following SCI can be serious and was once a leading cause of death⁴³. Currently, catheter placement and dependence are common among the SCI population suffering from neurogenic bladder dysfunction. Similar to mechanical ventilation, this puts them at risk for recurrent urinary tract infections (UTIs). Studies have previously shown that implementing prophylactic antibiotics does not reduce the rate of UTI and may increase a patient's risk of developing resistant bacteria⁶⁸. Overall, appropriate bowel and bladder education and management are of utmost importance to SCI individuals.

Due to the limited mobility following the injury, pressure sores are a common complication after SCI. This is a serious concern for SCI individuals as untreated pressure sores can lead to septicemia, the second leading cause of death in the SCI population ^{2,69}. Further, pressure ulcers can trigger autonomic dysreflexia ⁷⁰. The importance of treating and preventing pressure sores goes back to 1898 when Wilhelm Wagner published his practical treatment of SCI, as described in section 1.1.3. His recommendation of repositioning patients every 2 hours in the acute phase of injury is still recommended today, as well as moisture prevention and good nutrition. Unfortunately, even with prevention tactics, pressure sores are difficult to evade, and surgery may be necessary for non-healing ulcers.

1.1.5 Clinical trials and experimental approaches for SCI

Although there is currently no Food and Drug Administration (FDA) approved treatment for SCI, research efforts are well underway. A search on clinicaltrials.gov produces over 1500 studies for spinal cord injury, with 728 completed and 345 actively recruiting globally. These studies range from targeting sensory and motor function improvement, decreasing neuropathic pain and spasticity, and the maintenance and preservation of muscle and bone mass. Interventions such as pharmacologic treatments, cell-based therapies, and the use of technology have all been under investigation to achieve the common goal of curing SCI. To summarize these therapeutic approaches in the sections below, topics will be categorized as neuroprotection, neuroregeneration and plasticity, and neurorehabilitation.

1.1.5.1 Neuroprotection

Although there are many innovative and promising studies, this section will highlight several neuroprotective compounds that have reached phase III clinical trials. First, methylprednisolone sodium succinate (MPSS) is a glucocorticoid steroid that upregulates anti-inflammatory cytokine release and has been the only drug ever approved for treating acute SCI. A series of clinical trials by the National Acute Spinal Cord Injury Study (NASCIS) demonstrated significant motor recovery in patients at 6 weeks and 6 months post-injury ⁷¹⁻⁷³. However, these findings have been up for debate over the last few decades due to the increased risk of secondary complications, such as hyperglycemia and pneumonia ^{74,75}. The current recommendation for MPSS administration is a 24-hour infusion for adults who present with acute SCI within eight hours as a treatment option ⁷⁶. However, significant medical contraindications for the patient should be carefully considered ^{70,76}.

Minocycline is a tetracycline antibiotic that has been shown to reduce cell death and improve functional recovery after SCI in animal models by reducing axonal dieback and apoptosis of oligodendrocytes and microglia ⁷⁷⁻⁷⁹. A phase III clinical trial (ClinicalTrials.gov Identifier: NCT01828203) revealed that 7 days of intravenous minocycline treatment resulted in a greater motor recovery by six points compared to placebo. Although no difference was observed in thoracic-level injuries, an increase in motor recovery by 14 points was observed in patients with cervical-level injuries ⁸⁰.

Riluzole is an anti-epileptic drug that has shown promise as a neuroprotective drug in preclinical trials through the blockade of overactive sodium channels, prevention of glutamate excitotoxicity, and stimulation of brain-derived neurotrophic factor (BDNF) expression^{81,82}. Phase I/IIa clinical trial (ClinicalTrials.gov Identifier: NCT00876889) demonstrated significant neurological motor improvements with no serious adverse effects^{83,84}. These results led to a phase IIB/III multi-center randomized control trial (ClinicalTrials.gov Identifier: NCT01597518) that encompassed 17 sites in three countries⁸⁵. Unfortunately, as of April 19, 2021, this trial has been marked as “terminated,” citing enrollment challenges/slow enrollment as per the clinicaltrials.gov website.

Finally, highly relevant work to this dissertation is a phase III clinical trial investigating the effect of prebiotics for SCI patients with bowel and bladder dysfunction (ClinicalTrials.gov Identifier: NCT03987126). This study began recruiting in 2019 with primary outcomes investigating bowel motility and neurogenic bowel dysfunction score and secondary outcome measures assessing gut microbiome changes. This is a 12-week study actively recruiting patients that have had an SCI of at least 3 months. While there are currently no publications referencing the trial number, the primary completion date is June 1, 2023.

1.1.5.2 Neuroregeneration and plasticity

Neuroplasticity can be described as a functional or structural reorganization of the nervous system that encompasses the regeneration and sprouting of axons. For the purposes of this dissertation, plasticity will describe the number and strength of synaptic

connections, whereas regeneration and sprouting will refer to axonal outgrowth. In regard to the restoration of breathing following SCI, numerous studies have utilized a latent, spared pathway that can be activated following a lateral C2 hemisection model of SCI (LC2Hx; discussed in detail in section 1.2.3) through increasing respiratory drive as a mechanism to study plasticity^{86,87}. One well-described pathway that is able to mediate functional recovery of breathing is known as the crossed phrenic pathway (CPP)⁸⁷⁻⁸⁹. This pathway is typically latent, although it can be activated as a response to increased respiratory drive. The anatomy of the CPP is discussed in further detail in section 1.2.3⁹⁰⁻⁹².

Researchers have developed several techniques to increase respiratory drive and elicit this form of neuroplasticity. First, pharmacological treatments have been used to increase respiratory drive. Theophylline, a bronchodilator used to treat asthma, has previously been shown to activate the CPP to restore function by increasing respiratory drive following LC2Hx⁹³. Interestingly, chronic treatment of theophylline resulted in restored recovery that was persistent even after weaning from the drug⁹⁴. In addition to activating spared pathways, theophylline has been shown to improve the function of injured pathways through contusion studies⁹⁵. A contusion injury model is a more prevalent clinical representation as most SCIs are contusions versus transection injuries. Therefore, injured pathways that are present can potentially be utilized to mediate recovery.

Second, exposure to intermittent episodes of hypoxia, or low oxygen levels, has been shown to elicit a long-lasting respiratory motor output by activating the CPP. This phenomenon is known as long-term facilitation (LTF)⁹⁶⁻⁹⁸. The paradigm to induce LTF involves administering three 5-minute bouts of intermittent hypoxia (IH). This acute

intermittent hypoxia (AIH)-induced LTF is one of the most prominently studied models of respiratory plasticity, both in injured and uninjured animal models ^{99,100}. Mechanistically, AIH increases phrenic motor output resulting in LTF through increased serotonin release in proximity to the PMN. Elevated serotonin signaling on the post-synaptic phrenic motor neurons induces the synthesis of brain-derived neurotrophic factor (BDNF). BDNF then activates its high-affinity receptor, tropomyosin receptor kinase B (TrkB), and ultimately results in increased phosphorylation and trafficking of glutamate receptors ¹⁰¹⁻¹⁰⁴. Upregulation of glutamate receptors to the post-synaptic membrane allows for enhanced neuronal excitability. This form of plasticity can be used to enhance spared or latent pathways such as the CPP to enhance functional recovery of breathing and is used in preclinical models of SCI.

Third, previous work has demonstrated the removal of inhibitory substrates to promote regeneration. The regrowth of severed axons within the central nervous system is extremely limited due to inhibitory molecules and the glial scar ^{105,106}. In 1981, a seminal study by David and Aguayo showed that implementing a peripheral nerve graft can create a growth-permissive bridge allowing central nervous system axons to grow around the lesion and into the bridge ¹⁰⁷. This axonal growth was initially only permissive into the peripheral nerve bridge, with axons unable to return to the central nervous system environment. To overcome this obstacle, the enzyme chondroitinase-ABC (ChABC; previously described in section 1.1.1) has been used to degrade the inhibitory chondroitin sulfate proteoglycans (CSPGs) found within the glial scar. The use of ChABC has shown significant improvements in forelimb function and respiratory pathways ^{29,30,108-112}.

Lastly, stem cell transplantation studies have shown significant potential for regeneration and functional recovery following SCI ^{113,114}. Several cell types have been examined preclinically and in clinical trials of SCI, including neural stem cells, mesenchymal stem cells, oligodendrocyte precursor cells (OPCs), and autologous human Schwann cells (ahSCs) ¹¹⁵⁻¹¹⁹. Two promising studies have examined the transplantation of remyelinating cells. A Phase I/IIa clinical trial (ClinicalTrials.gov Identifier: NCT02302157) investigating the transplantation of OPCs has been completed ^{117,118}. These trials have shown to be safely administered to participants and well-tolerated for up to 10 years. These findings support further investigation to determine the efficacy of treating SCI. Another clinical trial (clinicalTrials.gov Identifier: NCT01739023) investigating the transplantation of ahSCs found similar results in that transplantation did not cause any significant adverse events and that it is feasible to continue with the recruitment of participants ¹¹⁹.

1.1.5.3 Neurorehabilitation

Physical rehabilitation following SCI can be difficult due to the loss of central control of motor function. Application of electrical currents to nerves and muscles during rehabilitation training, known as functional electrical stimulation (FES), uses the intact neuromuscular system to allow therapeutic exercise and functional recovery ¹²⁰. Although not yet recruiting, two new clinical trials will examine the use of FES to improve unaided cough (ClinicalTrials.gov Identifier: NCT05745298) and abdominal muscles for bowel management (ClinicalTrials.gov Identifier: NCT04307303). Electrical stimulation can also

be applied to the spinal cord. Although more invasive than FES, epidermal spinal cord stimulation aims to activate central circuits. This form of stimulation has been shown to improve urinary bladder control, voluntary upper limb control, trunk and leg motor function, and normalization of blood pressure ¹²¹⁻¹²⁴.

1.2 Neural control of breathing

Breathing is a necessary life function that allows for the exchange of oxygen and carbon dioxide through inhalation and expiration, respectively. This exchange of gases can be under conscious or unconscious control. Conscious control of breathing can be useful during times of stress to calm ourselves, while unconscious control of breathing is essential in maintaining proper levels of tissue oxygenation throughout our day-to-day lives. Unconsciously, the body can detect changes in oxygen and carbon dioxide levels and, in response, adjust breathing patterns as necessary. Because of this neural control of breathing, we are able to maintain proper ventilation while sleeping, adjust to physical exertion or altitude changes, and can achieve higher-order thinking instead of constantly focusing on breathing.

This rhythmic behavior is produced by the pre-Bötzinger Complex (preBötC) located in the ventrolateral medulla. This complex was first discovered and named in 1981 by Dr. Jack Feldman as he demonstrated that medullary slices containing these neurons were essential for the rhythmogenesis of inspiratory oscillations ^{[108][109][508]}. Disruption of this center has been shown to cause severe respiratory complications in both rat and goat models ^{[108][109][6,127][108]}. Axons from the preBötC cross midline to allow for bilateral synchronization

while also projecting to the other brainstem regions involved in the control of breathing, including the ventral respiratory columns that contain phrenic premotor neurons, retrotrapezoid nucleus, nucleus tractus solitarius (NTS), nucleus ambiguus, and regions of the raphe nucleus [REDACTED]-130[REDACTED]. The preBötC is a complex system that coordinates several nuclei while influencing and being influenced by emotions and cognition [REDACTED]

The preBötC projects to a sub-portion of the ventral respiratory columns known as the rostral ventral respiratory group (rVRG), located within the medulla. These premotor neurons further project caudally to provide glutamatergic input and the primary inspiratory drive to the phrenic motor nucleus (PMN) located in the ventral horn of spinal cord levels C3 – C6¹³²⁻¹³⁴. Anterograde and retrograde labeling studies have demonstrated that axons from the rVRG project bilaterally to the PMNs in the spinal cord¹³³⁻¹³⁶. Additionally, cervical interneurons also innervate PMN, although not to the extent of the descending supraspinal inputs¹³⁷.

In addition to glutamatergic input, the PMN receives serotonergic input from the raphe located in the midline of the caudal brainstem. Stimulation of the raphe obscurus has previously been shown to elicit excitation of phrenic motor neurons^{138,139}. This serotonergic input is often considered neuromodulatory as its production of neuronal excitability is induced through secondary messenger pathways following 5-HT_{2A} receptor activation on phrenic motor neurons^{101,140,141}. Previous studies have also demonstrated that serotonin is necessary and sufficient to induce respiratory plasticity that increases respiratory motor output¹⁰². Additionally, these serotonergic neurons in the raphe have chemosensitivity properties and are sensitive to hypercapnia and will increase firing rate in response¹⁴²⁻¹⁴⁵. Carotid bodies located on the bifurcation of the carotid arteries sense

low oxygen levels and send afferent signals to the NTS. The NTS then projects to the rostral ventrolateral medulla (RVLM), which sends signals to the ventral respiratory column to increase respiratory drive during hypoxia ¹⁴⁶. This is an important adaptation response in order to acclimate to changes in our environment.

The left and right PMN send projections into the periphery as a collection of axon bundles that make up the left and right phrenic nerve. The two phrenic nerves are crucial for inspiration as they provide the sole innervation to the diaphragm, the main inspiratory muscle. Contraction of the diaphragm pulls oxygen into the lungs due to the negative pressure environment it helps to create in the thoracic cavity and allows for the exchange of oxygen and carbon dioxide across the alveolar surface ¹⁴⁷. The post-inspiration phase describes the lengthening contraction of the diaphragm to allow increased time for alveolar gas exchange within the inflated lungs ¹⁴⁸. Finally, expiration is typically passive during eupnea, although expiratory muscles, including the internal intercostals and abdominal muscles, can become activated in response to exercise, speech, laughter, or crying ^{131,149}.

1.2.1 Respiratory Complications Following SCI

Almost 60% of all SCI cases occur at cervical levels, resulting in tetraplegia, or loss of function to all four limbs and the torso. Additionally, injuries at high cervical levels can disrupt descending axons from within the respiratory centers of the medulla that innervate the phrenic motor nucleus (PMN) located in C3-C6 of the spinal cord ^{150,151}. Loss of these descending inputs is particularly detrimental for those injured as the phrenic nerve originates from the PMN and goes on to innervate the diaphragm, the primary

muscle used for inspiration. Without these systems intact, patients are unable to breathe independently and require mechanical ventilation, which simultaneously can increase the risk of secondary infection and complications¹⁵²⁻¹⁵⁴. Although extensive work has been done to restore independent breathing after injury, few effective treatments are available, and the average life expectancy for persons with SCI has not improved in 40 years¹⁵⁵⁻¹⁵⁷.

1.2.2 Spontaneous recovery of breathing

Fortunately, spontaneous recovery of breathing is possible after cervical SCI (cSCI)¹⁵⁸. As most SCIs are incomplete, activation of spared pathways and strengthening of synapses, known as neuroplasticity, can generate spontaneous recovery¹⁵⁹⁻¹⁶². However, these outcomes are often suboptimal and highly variable among patients^{158,163}. Still, utilizing and enhancing spared pathways has proven to be an integral part of studying and developing interventions to restore breathing function. Inducing respiratory neuroplasticity can be elicited by administering intermittent exposures to lower oxygen levels, or hypoxia, resulting in an enhanced respiratory drive that remains elevated over time⁹⁸. This form of respiratory plasticity is termed long-term facilitation (LTF; covered in section 1.1.5.2).

1.2.3 The lateral C2 hemisection (LC2Hx) model of SCI

To study respiratory motor deficits following cervical SCI and the crossed phrenic pathway (CPP), the LC2Hx has been the model used for over a century by W.T. Porter in 1895 and is still common practice today^{87,164}. This type and level of injury completely

severs all ipsilateral descending inputs from the medulla to the PMN, resulting in ipsilateral hemidiaphragm paralysis. Functional recovery of the ipsilateral hemidiaphragm is possible through activating the latent, decussating tracts of the CPP physiologically or pharmacologically ^{86,93,99,101,164}. The bulbospinal projections that comprise the CPP descend contralaterally to the lesion and decussate at the level of the PMN, effectively bypassing the hemisection and allowing for restored function upon activation ⁹⁰ (Figure 2.1a). Breathing is altered but maintained through intact, spared pathways that allow for compensation and survival. Due to hemiparalysis, tidal volume is diminished. To compensate for this reduction, the respiratory rate increases. As minute ventilation is a function of respiratory rate multiplied by tidal volume, minute ventilation is unaffected ¹⁶⁵. Overall, the LC2Hx provides a consistent and reproducible model of SCI to study the utilization of spared pathways to restore breathing function after injury.

1.3 Gut Microbiome

The gut microbiome, or bacteria living within the gut, is composed of trillions of microorganisms. Although ties to the gut microbiome in health and disease are becoming more apparent, the idea that these organisms play a role in host physiological function is not new. As early as 340 A.D., Ge Hong, a Jin Dynasty scholar, described the use of a “yellow soup” composed of fecal matter from a healthy donor as a treatment for diarrhea. This treatment method is evidence of the first fecal matter transplant, a procedure in which stool from a healthy donor is transferred into the intestinal tract of a recipient to repopulate with healthy bacteria ¹⁶⁶.

By the 1860s, when diseases such as cholera were spreading throughout Europe, and an increase in surgical procedures were being performed and resulting in procedural infections, the role of microorganisms could not be ignored. Louis Pasteur, a father of germ theory, began to describe the role of these microorganisms. He, along with others, such as Robert Koch, began to describe four criteria that establish a causative role of bacteria in disease. Dr. Joseph Lister, a prominent surgeon at the time, also began to understand the impact of bacteria on procedure outcomes and became a pioneer of aseptic surgical techniques. Dr. Pasteur also had ideas that non-pathogenic microorganisms may play a role in healthy human physiology, a topic still studied today. Almost a century after these findings, Dr. Ben Eiseman performed the first recorded fecal matter transplants in four patients suffering from chronic *Clostridium difficile* infections. His idea was to reintroduce bacteria normally found in the colon in order to re-establish the balance of pathogenic and beneficial bacteria¹⁶⁷. These examples describe the beginnings of our understanding of the trillions of bacteria that reside in our intestines, termed the gut microbiome.

In addition to their large quantity, the gut microbiota encode over 3 million genes that produce metabolites, short-chain fatty acids, and neurotransmitters that all can interact with host physiology¹⁶⁸. In comparison, the human genome encodes just over 20,000 genes¹⁶⁸. To organize and study these bacteria, the gut microbiome is classified taxonomically. The composition at the phyla level of classification is predominately made up of Firmicutes, Bacteroidetes, Actinobacteria, Proteobacteria, and Verrucomicrobia¹⁶⁹. Of these, the Firmicutes and Bacteroidetes comprise 90% of the gut microbiota¹⁷⁰. The ratio of Firmicutes to Bacteroidetes has been associated with increased susceptibility to inflammation and obesity^{9,171-173}. Indeed, the composition of the gut microbiome has been

associated with both health and disease states ^{8,168,172,174,175}. A disruption to the microbiome resulting in an overall loss of beneficial bacteria and an abundance of pathogenic bacteria is known as gut dysbiosis. While the presence or absence of specific species of bacteria does not necessarily constitute a “healthy” gut microbiome but rather the diversity and richness of the population that allows for increased overall metabolic function ¹⁷⁶.

1.3.1 Gut-CNS Axis

The initial observations and findings described above have led to the expansion of the field of microbiology with the connection of the gut microbiome spanning several organ systems in both health and disease. One source of these connections is due to the imbalance of pathogenic and beneficial bacteria, which in turn, compromise tight junction proteins in the intestinal barrier. Dysregulation of the barrier leads to increased permeability and “leakage” of bacteria into the bloodstream, termed bacterial translocation, and causes harmful effects to the host. But these microorganisms can also communicate with major organs in a less direct and more mutualistic manner. The “Gut-Brain Axis,” or the bidirectional system of communication between the gut microbes and the brain, has become a prominent area of investigation in recent decades ⁸. Although the exact mechanisms of this communication pathway have not been fully elucidated, the process is described in two parts. First, the “top-down” approach describes the CNS control of the gut microbiome through signaling peptides, endocrine secretions, and the hypothalamic-pituitary-adrenal axis, through which cortisol is released and can regulate gut motility and integrity. Thus, both neural and hormonal exertions from the brain can influence the epithelial cells and enteric neurons that make up the intestines and the environment it

creates for the gut microbiota ¹⁷⁷. Second, the “bottom-up” approach encompasses several roles of the gut microbes, including direct neural activation, the endocrine release of serotonin, metabolic production of neuroactive molecules, and modulation of immune pathways ⁶. The “top-down” and “bottom-up” approaches are highly connected as changes in the luminal environment through decreased motility or mucosal secretions can alter populations of resident microbes within the gut. This can create an opportune environment that allows pathogenic bacteria to take over, or gut dysbiosis. Alterations in microbial populations can impact host levels of neurotransmitters and metabolites, including those necessary for plasticity ¹⁷⁸⁻¹⁸⁰.

1.3.2 Gut-CNS Axis and SCI

The effects of the gut microbiome have been studied extensively in various physiological models of health and disease, such as in stress, exercise, obesity, autism, schizophrenia, mood disorders, irritable bowel syndrome, autoimmune diseases, multiple sclerosis, stroke, Alzheimer’s disease, Parkinson’s disease, and Lou Gehrig’s disease ^{6,172,174,175,181-185}. More recently, trauma models are being evaluated, as traumatic brain injury has been confirmed to cause changes in the gut microbiota ¹⁸⁶. Furthermore, and of clinical importance, patients with traumatic injuries were found to have significant changes in gut microbial composition and relative abundance within the first 72 hours post-injury ¹⁸⁷. Models of traumatic brain injury have been used to establish and assess a type of feedback loop relationship between brain function and intestinal microbe composition. This process includes the effect of an injury on the gut microbe and, in turn, the subsequent role of the gut microbiome in the recovery process after injury ¹⁸⁸.

Spinal Cord Injury

With mounting evidence linking the gut microbiome and the brain, recent studies have begun to investigate the link between the gut microbiome and the distal portion of the CNS, the spinal cord. Kabatas et al. used a thoracic contusion model to demonstrate that spinal cord injury induces delayed gastric transit in the duodenum initially after injury but chronically in the stomach ⁵⁹. Anatomically, the thickness of gastrointestinal mucosal membranes was reduced after SCI. Further, Kiger et al. confirmed that SCI does indeed lead to gut dysbiosis and bacterial translocation, which in turn, result in poorer functional outcomes ⁷. Translationally, these results indicate an imbalance of bacterial composition that agree with human findings ^{61,63,64,189}. Investigation of the gut microbiome from patients with SCI involving either upper motor neuron or lower motor neuron bowel syndrome found that butyrate-producing enzymes are significantly reduced in SCI patients when compared to healthy controls ¹⁸⁹. These findings could perhaps call for a re-naming of the “Brain-Gut-Axis” to the “CNS-Gut Axis” ¹⁹⁰.

Inflammation

Inflammation following spinal cord injury also appears to have connections to the gut microbiome. Kigerl et al. found an increase in proinflammatory cytokines such as TNF-alpha, and IL-1beta to as early as 3 days post-SCI ⁷. O’Conner et al. described similar results with IL-12, MIP-2, and TNF-alpha levels increased, but at 4 weeks post-injury ⁶⁶. These cytokines decreased by 8 weeks post-injury, although IL1beta, IL-12, and MIP2

were found to be significantly correlated with beta diversity changes at this later time point. To begin to understand the underlying mechanisms of this SCI-induced inflammation, Meyers et al. investigated the role of PDE4B enzyme ⁶⁵. Gut dysbiosis and permeability following SCI activate the TLR4-TNFalpha-PDE4B axis. In turn, upregulation of PDERB exacerbates acute and chronic inflammation and obstructs recovery after SCI. Importantly, knockout of PDE4B prevented SCI-induced gut dysbiosis and bacterial translocation, indicating an essential role in the development of the inflammatory response post-SCI.

Secondary complications following SCI and gut dysbiosis include bacterial translocation and infection of distal organs. A 2013 Retrospective Nationwide Inpatient Sample (NIS) study found that SCI patients are more likely to develop acute respiratory distress syndrome (ARDS) or acute lung injury (ALI) than patients without SCI. Cervical, thoracic, and sacral level injuries were also more likely to result in patients' development of ARDS or ALI than lumbar fractures. Furthermore, and alarmingly, patients with SCI have a higher risk of developing ARDS/ALI and were more likely to die in hospital than those without ARDS/ALI ¹⁹¹. To further support these findings and describe a possible mechanistic link, Dickson et al. provide evidence that, in both animal models and humans with established ARDS, the lung microbiome is enriched with gut bacteria. This infection of bacteria from the gut to the lung is significantly correlated with alveolar TNF-alpha levels ¹⁹². This crosstalk between the gut and the lungs introduces another relationship described as the "Gut-Lung Axis" as the gut microbiome has been linked to lung homeostasis and inflammation, reviewed in Dang et al. 2019 ¹⁹³.

Neurotransmitters

Bacteria within the gut directly impact levels of major neurotransmitters in the host through both production and catabolism. Serotonin, as mentioned previously, plays a vital role in respiratory motor plasticity and recovery after spinal cord injury. Interestingly, the gut produces over 90% of the body's serotonin ¹⁹⁴. Although no bacteria have been identified to directly produce serotonin, Yano et al. were able to demonstrate that bacteria within the gut microbiome, in both mice and humans, promote colonic enterochromaffin cell synthesis of serotonin in order to supply the mucosa, lumen, and circulating platelets ¹⁷⁹. The role of this gut-synthesized serotonin does not have a clear role in the brain. However, patients with major depressive disorder were found to have altered gut microbial compositions compared to healthy controls, indicating the association of gut bacteria in psychiatric disorders and connections beyond the blood-brain barrier ¹⁸¹.

Furthermore, neurotrophic factors necessary for recovery after SCI also appear to be modulated by gut microbes. Bistoletti et al. found that fourteen days after antibiotic-induced gut dysbiosis, expression levels of BDNF and its high-affinity TrkB receptor are altered. However, these alterations appear to differ along the gut-brain axis. The enteric nervous system showed significant up-regulation of both BDNF and TrkB. Within the central nervous system, both BDNF and TrkB levels were decreased in the hippocampus and unchanged in the pre-frontal cortex ¹⁷⁸. Conversely, Bercik et al. describe increased BDNF expression in the hippocampus seven days after oral antibiotic disruption of the gut microbiome ¹⁸⁰. These findings suggest that gut bacteria may affect certain levels within the gut-brain axis differentially or even preferentially, but further examination is necessary.

Apolipoprotein E

Recently, the gut microbiome has been linked to the apolipoprotein E (APOE) gene. APOE genotype, specifically APOE4, is a strong genetic risk factor for Alzheimer's disease. In the APOE4-expressing mice, microbiomes were shown to have reduced butyrate-producing bacteria, short-chain fatty acid production, and mucin synthesis, which increases mucosal permeability ¹⁹⁵. These changes described are associated with an unhealthy gut microbiome.

Wang et al. describe a mechanistic link in how gut dysbiosis contributes to neuroinflammation and Alzheimer's disease. Largely, this link is described as alternations within the gut microbiome composition cause peripheral accumulation of phenylalanine and isoleucine, which stimulate the differentiation and proliferation of T helper (T1) cells. These T1 cells then activate M1 microglia and result in Alzheimer's-associated neuroinflammation. Furthermore, a sodium oligomannate drug, GV-971, was used to suppress or reverse gut dysbiosis and the cascading effects of phenylalanine and isoleucine accumulation, neuroinflammation, and cognitive impairment ¹⁹⁶.

The roles of genetics and gut dysbiosis in exacerbating disease states is becoming more understood. Work from our lab has also determined that APOE status can have a detrimental effect on respiratory recovery after SCI ⁵. By understanding the importance of factors such as genetics and the gut microbiome on the recovery process, we can begin to develop personalized medicine techniques and focus on novel therapeutic targets that aim to enhance functional restoration.

1.3.3 Gut-CNS Axis, SCI, and the restoration of breathing

Higher-level SCIs, especially those at the cervical level, can cause multiple organ system dysfunctions and disruption of the autonomic nervous system (ANS) ^{28,29}. Dysregulation of these systems, particularly immune organs regulated by the ANS, can contribute to systemic inflammation ^{30,31}, as indicated by elevated plasma levels of several pro-inflammatory cytokines in individuals with acute SCI ³². Gravely, inflammation and infection are particularly worrisome as septicemia and pneumonia are the leading causes of death in SCI patients¹. Additionally, systemic inflammation has been shown to have deleterious effects on synaptic plasticity within the CNS, as demonstrated in both hippocampal long-term potentiation ³³ and spinal cord LTF ^{34,35}. Notably, systemic inflammation undermines phrenic LTF through the serotonin-dependent pathway described in section 1.1.5.2. This impairment occurs downstream of serotonin receptor activation but upstream from BDNF/TrkB signaling ³⁶.

Since systemic inflammation negatively impacts plasticity, targeting immune organs after injury could improve chances for recovery. The ANS innervates major immune organs, including the spleen, lymph nodes, and bone marrow ³⁷, as well as the gastrointestinal (GI) system. In particular, the GI system is an intriguing target as it houses nearly 70% of the body's entire immune system, as it is the main route of contact with the external environment ³⁸. The immune system distributed throughout the GI tract is known as the gut-associated lymphoid tissue (GALT) ^{28,29}. Not only does the GALT surveillance the external environment, such as incoming food, bacteria, or pathogens, but it also tracks the trillions of commensal microbes residing within the intestinal that make up the gut microbiome ⁴⁰. Disruption of the sympathetic innervation to the GALT can alter the

sympathetic tone, gut motility, mucosal secretions, and epithelial permeability, initiating direct and indirect complications⁴¹. Direct changes to the epithelium through compromised tight junctions can result in permeability at the mucosal surface and result in bacterial translocation, or bacteria escaping the intestinal lumen into the periphery, which can stimulate systemic inflammation⁴². Indirectly, changes in the luminal environment through decreased motility or mucosal secretions can alter populations of resident microbes within the gut. This can create an opportune environment that allows pathogenic bacteria to take over, known as gut dysbiosis. Alterations in microbial populations can impact host levels of neurotransmitters and metabolites, including those necessary for plasticity^{43,44,45}. Both human and animal studies have confirmed that microbial diversity is significantly altered within the first 72 hours post-injury, with levels of beneficial bacteria specifically reduced^{46,47}. Although gut dysbiosis can impair recovery and contribute to central and peripheral inflammation, treatment of a dysbiotic microbiome has proven to be effective in improving functional outcomes^{48,49,50,51,52}.

Data from our lab indicates that gut dysbiosis after SCI is dynamic and improves over time. The most significant change in bacterial diversity occurs one-day post-injury and returns to baseline levels approximately two months post-injury. This finding is consistent with breathing recovery times seen in the literature. Acutely after injury, spontaneous phrenic motor recovery and phrenic LTF are absent but improve by two months post-injury⁹⁹. Similarly, interventions given at acute time points elicit only marginal recovery of diaphragmatic activity⁵³, but when given at later time points, respiratory function is robustly restored⁵⁴. Taken together, it is my central hypothesis that

gut dysbiosis occurring acutely after injury exacerbates systemic inflammation, which in turn, inhibits functional recovery of breathing.

By understanding the extent to which gut dysbiosis contributes to inflammation and impaired functional recovery of breathing, we can administer treatments that target gut dysbiosis. These treatments could then be used in combination⁸ with other interventions used to restore breathing function in order to achieve their full potential and effectiveness at more acute time points. Facilitating functional recovery and independent breathing at earlier time points could allow for earlier weaning times from mechanical ventilation, reducing the risk of infection and rehospitalization. Ultimately, by taking a holistic approach and accounting for ancillary organ systems that may undermine recovery, this research aims to aid SCI patients to be in the best possible state for optimal recovery.

CHAPTER 2. TARGETING THE MICROBIOME TO IMPROVE GUT HEALTH AND BREATHING AFTER SPINAL CORD INJURY

2.1 Introduction

Spinal cord injury (SCI) is a devastating condition characterized by debilitating motor and sensory function, as well as internal organ pathology and dysfunction. This internal organ dysfunction, particularly gastrointestinal (GI) complications, and neurogenic bowel, can reduce the quality of life of individuals with an SCI and potentially hinder recovery following injury. The gut microbiome impacts a variety of central nervous system functions and has been linked to a number of health and disease states. An imbalance of the gut microbiome (i.e., gut dysbiosis) contributes to a number and variety of neurological disorders and may be a factor influencing the recovery and repair process after SCI. Here we examine the impact of high cervical SCI on the gut microbiome and find that there is a transient gut dysbiosis immediately after injury but persistent gut pathology. However, probiotic treatment leads to improved gut health and respiratory motor function measured through whole-body plethysmography. Concurrent with these improvements was a systemic decrease in the cytokine tumor necrosis factor- α and an increase in neurite sprouting and regenerative potential of neurons. Collectively, the results of these experiments present evidence that the gut microbiome is a critically important therapeutic target to improve visceral organ health and motor recovery after SCI.

The gut-central nervous system (CNS) axis is a bi-directional pathway where alterations or disruptions in the normal fauna and flora of the gut, i.e. gut dysbiosis, can lead to disruptions in CNS function, and conversely, CNS disease can lead to dysbiosis. As a result of this unique relationship, gut dysbiosis has been linked to a variety of neurological disorders, including depression, amyotrophic lateral sclerosis, and cognitive

decline or impairment^{183,184,197}. In this study, we investigated how injury at the cervical level of the spinal cord can lead to gut dysbiosis, which can potentially further lead to greater CNS dysfunction and impaired functional recovery (Figure 1 a; Schematic).

2.2 Materials and Methods

2.2.1 Animals and Housing

All experiments were approved by the Institutional Animal Care and Use Committee at the University of Kentucky. Adult female Sprague Dawley rats from Envigo were used in all experiments and allowed to acclimate for at least one week prior to beginning experimental procedures. Animals were co-housed in a 12-hour light/dark cycle with standard chow and water available *ad libitum*. Animals housed together remained with their cage mate throughout the entirety of the experiment and were in the same experimental group to avoid coprophagic cross-colonization. For all experiments, animals were randomized into the specified groups using an online random number generator.

2.2.1.1 Groups

The first set of experiments included three cohorts of animals that were separated into three groups: (1) LC2Hx (n = 16), (2) surgical sham (n = 12), or (3) drug control (naïve + surgical drugs; n = 8). Animals in the third group received all surgical drugs, including isoflurane anesthesia, and post-surgical care (same as groups one and two) but did not

receive any incisions. Group 3 was a necessary control to include because anesthesia and opioids have been shown to impact the gut microbiome ^{198,199}.

The second set of experiments included three cohorts of animals that all received a LC2Hx and were separated into two treatment groups in which they received one of the following types of oral gavage: (1) fecal matter transplant (FMT; n = 12) or (2) vehicle FMT (control; n = 12).

The third set of experiments included two cohorts of animals that all received a LC2Hx and were separated into four treatment groups in which they received one of the following types of oral gavage: (1) vehicle (n = 5), (2) low dose probiotics (n = 6), (3) mid dose probiotics (n = 6), or (4) high dose probiotics (n = 5).

2.2.2 Fecal Matter Transplant

Fecal samples used for the FMT were collected from young (approximately 3 months old), healthy donor animals using an aseptic technique. Immediately after fecal sample collection, samples were pooled and processed to make the FMT slurry solution. Fresh fecal samples were diluted to a 1:10 concentration in sterile PBS (10%), L-cystine HCL (0.05%), glycerol (20%), and sterile water (60%) and filtered with a 100 μ m filter to remove fiber content ⁶⁷. Vehicle-treated animals received all components of the filtered dilution solution without fecal content. The FMT or vehicle solution was administered via oral gavage for three consecutive days beginning on the day of injury ⁶⁷, and then twice each week until the endpoint at 28 days post-injury ¹⁸³. Each animal received a total of nine oral gavage doses with each dose consisting of 500 μ L of the assigned solution.

2.2.3 Probiotics

The probiotic Visbiome (Lot no. 65026 and 65847) was diluted into the following concentrations: (1) vehicle = sterile water only, (2) low dose = 15 mg (2.7 billion bacteria) in 1 ml sterile water^{200,201}, (3) mid dose = 130 mg (24 billion bacteria) 1 ml sterile water^{202,203}, or (4) high = 260 mg (48 billion bacteria) 1 ml sterile water. The assigned concentration of Visbiome was delivered via oral gavage beginning the day of the injury and continued once daily until the endpoint at 14 days post-injury. Each animal received a total of oral gavage doses with each dose consisting of 500 μ L of the assigned solution.

2.2.4 Left C2 Hemisection (LC2Hx)

Adult female Sprague Dawley rats were anesthetized with isoflurane gas. Once an appropriate plane of anesthesia was met, animals were prepared for surgery by shaving and sterilizing the surgical site with alternating 70% ethanol and betadine swabs. Ophthalmic ointment was applied to the eyes to prevent drying throughout the procedure. While in the prone position, an incision was made between the ears and extend approximately two inches caudally. The underlying musculature was bluntly dissected and retracted to expose the process of the C2 lamina. The final layer of musculature was then cut and cleared away from the bone so that the intervertebral space between C1 and C2 could be visualized. A C2 laminectomy was performed by cutting the lamina in this space on the left and right sides of the C2 spinous process and extending caudally until the dorsal aspect of the C2 vertebrae was removed and the spinal cord was exposed. Micro-scissors were used to perform a durotomy and a 27-gauge hypodermic needle was bent at a 45-degree angle and

used to perform the left C2 hemisection (LC2Hx). Briefly, anatomical landmarks were used to determine midline at the C2 level at which the needle was inserted through the spinal cord until the ventral aspect of bone was reached and then dragged laterally to the animal's left until completely severing the cord. Three passes were made to ensure complete disruption of pathways on the left side. Finally, all three layers of musculature previously dissected were sutured individually (3-0 absorbable suture) and the skin was closed with surgical staples. All animals received buprenorphine (0.05mg/kg; immediately and 12 hours post-surgery) and carprofen (5mg/kg; immediately, 12-, and 24 hours post-surgery) subcutaneously. Surgical animals were monitored twice daily for the four days post-injury with subcutaneous saline given as needed. Animals recovered for one week on a heated rack separated from naïve animals and remained on a standard 12-hour light/dark cycle with food and water accessible *ad libitum* prior to returning to standard housing. Welfare and weights were checked weekly throughout the entire experiment.

2.2.5 Whole Body Plethysmography

Whole Body Plethysmography (WBP) (DSI, Buxco FinePointe) was used to assess ventilatory patterns in awake, unanesthetized rats before and after LC2Hx. At the designated timepoints pre- and post-injury, animals were placed into individual DSI whole body plethysmography chambers and breathing measurements were recorded every two seconds for the duration of approximately one hour. At the beginning of each experiment, an acclimation period of 20-minutes under normoxic conditions (21% O₂) was used to minimize atypical respiratory patterns while initially exploring the chamber (i.e., sniffing). Immediately after, a 30-minute baseline recording was taken under normoxic conditions

(21% O₂), followed by a 10-minute hypoxic challenge (11% O₂), and finally a 10-minute post-hypoxia recording under normoxic conditions (21% O₂). From the recordings, we examined respiratory rate (breaths/min), tidal volume (mL/breath/g), and minute ventilation (mL/min/g). Food and water were restricted while breathing measurements were taken. At the conclusion of the experiment, animals were returned to their home cages where food and water were accessible *ad libitum*.

2.2.6 Diaphragmatic Electromyogram (DiaEMG)

Animals were anesthetized with isoflurane gas using the SomnoSuite low-flow anesthesia system (Kent Scientific). Once an appropriate level of anesthesia was met, animals were transferred into a faraday cage and switched to a nose cone for continued delivery of approximately 2.4% isoflurane throughout the procedure. Animals were placed in the supine position, and a laparotomy was performed. Upon visualization of the phrenic nerve on the diaphragm, bipolar needle electrodes were inserted bilaterally into the dorsolateral quadrant of the costal hemidiaphragm. Electrodes were placed in close proximity to the phrenic nerve while being cautious to avoid piercing the nerve. Bipolar electrodes were connected to an amplifier and data acquisition system (BMA-400 Four-channel Bioamplifier, CWE, Inc., Ardmore, PA, USA; CED 1401 with Spike2 Data Analysis Computer Interface, CED, Cambridge, UK) to record and analyze the electromyogram (EMG) signal. Following electrode insertion, the faraday cage was closed, and a 10-minute baseline recording was measured. Immediately following the baseline recording, three 15-second nasal occlusions were performed to assess each animal's maximal respiratory output. Sufficient time between nasal occlusions was allowed for burst

amplitude to return to approximately pre-occlusion levels. At the conclusion of the EMG recording, animals were given ketamine/xylazine intraperitoneally while being weaned off isoflurane and transitioned to lung health experiments.

2.2.7 16S rRNA Sequencing

Fecal samples were collected from study animals using an aseptic technique pre- and at various timepoints post-LC2Hx in order to assess the gut microbiome. Samples were immediately stored at -80°C until all samples were collected for further processing. The bacterial 16S rRNA gene was then isolated from the fecal samples using DNeasy PowerSoil Pro Kit (Ref #47014 and 47016; Lot #169034368 and 17203302). DNA from each sample was diluted to a concentration ranging between 1-50ng/μL and mailed to Argonne National Laboratory for sequencing.

Read processing: 16SV4 was amplified using 515F-806R primers. Fastq files were demultiplexed using qiime2 demux emp-paired function. Raw data were processed with qiime2. Briefly, reads were denoised with dada trimming nucleotides based on quality plots (trim reads when the average quality <30- see code for details). Unique reads were clustered to 99% identity using the silva-138-99-seqs-515-806 database (ASV99% or OTUs). Chimeras were removed using vsearch uchime-denovo function. Samples had an average of 29,245 reads (Table 1). ASVs with <50 reads total abundance were removed since they were present in <2 samples and will not significantly contribute to the analysis. ASVs were classified using the feature-classifier classify-sklearn function with the silva-138-99-515-806-nb-classifier. When taxonomic classification was not available at lower

levels, the immediately following taxonomic level classification was used. Filtered ASV 99% table (referred to as OTUs in the figures) was subsampled to analyze 15,000 reads per sample. Two samples with an unusually low number of reads were removed.

Table 2.1 Summary of 16S sequencing reads processing.

	Number (mean)	% of reads
Raw input (91 samples)	29245.0889	88.55
Denoised dada	25398.6111	86.77
ASV 100% (total)	2305	NA
ASV 99% (total)	1707	NA
ASV 99% (per individual)		
ASV 99% non-chim	1,393	NA
ASV 99% non-chim (per individual)		
ASV 99% non-chm filtered (>50 reads, >n=2; per individual)	896	NA
ASV 99% non-chm filtered (>50 reads, >n=2; per individual)	896	NA
ASV 99% non-chm filtered rarefied (15,000 reads; 89/91 samples)	896	NA
Taxonomic levels (Family)from ASV99% non-chm filtered rarefied	48	NA

Read processing: OTU abundance matrix was analyzed using vegan, and labdsv packages in R. Principal coordinate analysis was performed on rarefied reads and log10 normalized reads at the OTU and family taxonomic level. Simper analyses were performed to identify OTUs that explain most of the variation in the ordination space.

Statistical analysis: Statistical analysis of group separation in the ordination space was performed calling Permanova with the Adonis function in R. Mixed-effect time series statistical analysis of clusters and OTUs abundance was done using prism.

2.2.8 Sectioning and Staining

2.2.8.1 CNS

Following euthanasia at the designated times post-injury, the skull and spinal column were removed and drop-fixed in 4% paraformaldehyde (PFA) for 48 hours at 4°C. The brainstem and cervical spinal cord were then dissected from the skull and spinal column and placed in fresh 4% PFA for an additional 24 hours at 4° and then cryoprotected in 30% sucrose at 4°C until sectioning. The injury was used as the epicenter to create three 4mm sections (brainstem, C1/2, and C3/4 levels). Tissue sections were then embedded in Optimal Cutting Temperature embedding media (OCT, Sakura Tissue-TEK), and cryosections were taken at 30µm (Leica cryostat) and placed directly onto gelatin-coated slides (Thermo Fischer Scientific) and stored at -20°C.

2.2.8.1.1 *CRESYL VIOLET*

Slides were placed in CitriSolv solution prior to serially rehydrating the tissue in decreasing concentrations of ethanol. Slides were then rinsed in distilled water, stained with 0.5% Cresyl Violet solution (Sigma Cat #C5042), rinsed in distilled water, dehydrated in the reverse order of ethanol concentrations used, and placed in CistroSolv. Coverslips were then applied using permount (Electron Microscopy Sciences Cat #17986-01). Slides were imaged on a Keyence BZ-X810 microscope (Keyence Corporation of America, Itasca, IL, USA) using bright field illumination at 2x.

2.2.8.1.2 *IMMUNOHISTOCHEMISTRY (IHC)*

Frozen sections were thawed to room temperature (approximately 20°C) and placed in Heat Induced Epitope Retrieval at 85°C for 15 minutes. Next, slides were permeabilized with 0.4% TritonX-100 in 1xPBS for 15 minutes prior to blocking in a solution of 3% normal goat serum, 0.2% TritonX-100 in 1xPBS for 60 minutes at room temperature. Slides were then incubated in 5-HT primary antibody diluted to 1:2000 (rabbit, ImmunoStar Cat #20080; Lot #1650001) and NeuN primary antibody diluted to 1:5000 (mouse, ImmunoStar Cat #MCA-1B7; Lot #) at 4°C overnight. Next, slides were washed with 1xPBS before incubating in goat anti-rabbit AlexaFluor 594 (Life Technologies Ref #A11037; Lot #1777945) and goat anti-mouse IgG AlexaFluor 488 (Life Technologies Ref #A11046; Lot #) for 120 minutes at room temperature. Finally, slides received a final wash in 1xPBS and were mounted with Fluoromount-G (SouthernBiotech Cat #0100-01). Slides were imaged on a Keyence BZ-X810.

2.2.8.2 Gut Tissue (Swiss Roll)

Following euthanasia at the designated times post-injury, the laparotomy incision made for the diaEMG recording was expanded distally to fully visualize the abdominal cavity. The stomach and cecum were then identified as markers for the beginning and end of the small intestine. The small intestine was then removed and divided into thirds, with the final third known as the ileum. The ileum was then flushed with 1xPBS and rolled into a swiss roll configuration for sectioning as previously described^{204,205}. In brief, the ileum was cut longitudinally along the mesentery attachment to expose the lumen. A 1ml syringe plunger was used to roll the ileum from the distal to the proximal end in the formation of the swiss roll. The tissue was then placed in 4% PFA at 4°C for 24 hours and then moved to 70% EtOH until paraffin embedding and sectioning at a thickness of 5µm. Slides were stained with hematoxylin and eosin (H&E) and Alcian blue for histological assessment and summation of goblet cells respectively. To assess intestinal injury, the Chiu/Park scoring system was employed and all evaluators were blinded to injury or treatment. The Chiu/Park score ranges on a scale of 0 – 5 (0 = normal mucosa; 1 = subepithelial space at the villous tip; 2 = extension of subepithelial space with moderate lifting; 3 – massive lifting down the sides of villi, some denuded tips; 4 = denuded villi, dilated capillaries; 5 = disintegration of lamina propria)²⁰⁶.

Additionally, slides underwent MALDI imaging. A Waters Synapt G2Si mass spectrometer (Waters Corporation, Milford, MA) equipped with an Nd:YAG UV laser with a spot size of 50µm was used to detect released N-glycans. A total of 300 laser spots per pixel at X and Y coordinates were collected at a raster size of 100µm. Data acquisition,

spectrums were uploaded to High-Definition Imaging (HDI) Software (Waters Corporation) for mass range analysis from 750 to 4000m/z. HDI generated glycan and glycogen images were obtained.

2.2.9 Systemic Inflammation

Blood was collected via the lateral tail vein at the designated timepoints pre- and post-injury. Serum levels of IFN- γ , IL-1 β , IL-4, IL-5, IL-6, IL-10, IL-13, KC/GRO, TNF- α were assayed using the Meso Scale Discovery (MSD) V-PLEX Proinflammatory Panel 2 Rat Kit (Lot #K002026; Catalog #K15059D-1; Rockville, Maryland 20850-3173).

2.2.10 Lung Health

Rats were anesthetized by intraperitoneal injection of xylazine and ketamine. After a tracheotomy, the rats were connected to the flexiVent system. The computer-controlled small animal instrument ventilated the rats with a tidal volume of 10 ml/kg at a frequency of 90 breaths/minute. Following two snapshots, two total lung capacity maneuvers, and two more snapshots on the flexiVent, we performed a pressure-volume loop perturbation in each individual subject for three acceptable recorded measurements, of which an average was calculated for compliance, resistance, and inspiratory capacity.

2.2.11 Open Field Chamber

At the designated timepoints pre- and post-injury, rats were placed in SuperFlex Open Field System chambers (16x16 inches; Omnitech Electronics Inc., Columbus, OH, USA) for five minutes and allowed to explore freely while lateral and horizontal movements were recorded. Total distance, vertical activity count, vertical time, and center time were measured using Fusion Software v6.5 and analyzed using GraphPad Prism v9.5.0.

2.2.12 Dorsal Root Ganglia (DRG) Outgrowth

DRGs were harvested at 28 DPI for FMT-treated animals, and 14 DPI for probiotic-treated animals. After excising the spinal column from the animal, the dorsal aspect of the vertebral column was removed to expose the spinal cord and the DRGs. DRGs were removed from the surrounding bone using fine forceps. Projections from the DRGs were removed using microscissors. DRGs of FMT-treated animals were harvested from the entire cord, while DRGs of probiotic-treated animals were harvested from only the cervical level, except for one probiotic-treated animal in which the DRGs were removed from the thoracic level. DRGs were placed in collagenase/dispase enzymes (2000U/mL collagenase: 50U/mL dispase) overnight to digest and dissociate. Dissociated DRGs were cultured on either a 6-well plate (FMT) or a 24-well plate (probiotics) with Neurobasal A Complete Media (Neurobasal A media, B27, Pen/Strep, GlutaMAX). The DRGs of each individual animal were plated in 6 separate wells. Media was changed to media plus anti-mitotic agents Fudr (4mM) and Pen/Strep (100uM) one-day post-plating. Cells were allowed to grow for 5 days (FMT) or 3 days (PBX) total. Cells were then fixed with 4%

paraformaldehyde. Of note, one 6-well plate of probiotic-treated cells underwent a media change one day late, inconsistent with the protocol utilized for all other cell culture used in this experiment. Thus, data from this group of cells were excluded from analysis after a statistical comparison of total outgrowth, and the number of projections revealed non-insignificant differences with respect to the rest of the cells, which underwent the scheduled media changes as intended. To perform immunohistochemistry, cells were stained with primary antibody Beta-III Tubulin, then secondary antibody goat anti-mouse IgG Alexa 594.

DRGs were imaged using a Keyence BZ-X810 Fluorescence Microscope. Each of 6 wells per individual animal was imaged four times, for a total of 24 images per animal. Image locations were chosen randomly. Random subsets of FMT and probiotic DRG images were quantified. Every cell exhibiting viability in each image was quantified. Cells were considered viable if there was evidence of a projection originating from the soma. ImageJ software with the NeuronJ plug-in was used to quantify total neurite outgrowth. The total number of projections from the soma was quantified by counting the total primary projections originating directly from the soma.

2.2.13 Statistical Analysis

Table 2.2. Summary of Statistical Analyses

Experiment 1: LC2Hx + Gut Microbiome Studies	
Outcome Measure	Statistical Tests
Gut Microbiome	Alpha diversity, Beta diversity, F:B ratio,
Gut Pathology	Unpaired t-test; Mann-Whitney test
Gut MALDI	Unpaired t-test
DiaEMG	Unpaired t-test

Experiment 2: FMT Studies	
Outcome Measure	Statistical Tests
Gut Pathology	Unpaired t-test; Mann-Whitney test
Gut MALDI	Unpaired t-test
DiaEMG	Unpaired t-test
WBP	Two-way ANOVA RM with Bonferonni post hoc
Serum Inflammation	Two-way ANOVA RM with Bonferonni post hoc
Lung Health	Welches t-test + ID outliers
DRG Outgrowth	Unpaired t-test

Table 2.3. Summary of Statistical Analyses (continued)

Experiment 3: Probiotic Studies	
Outcome Measure	Statistical Tests
Gut Pathology	One-way ANOVA with Dunnett's post hoc; Kruskal-Wallis test
Gut MALDI	One-way ANOVA with Tukey's post hoc
DiaEMG	One-way ANOVA with Tukey's post hoc
CNS Injury Confirmation	One-way ANOVA with Tukey's post hoc
WBP	Two-way ANOVA RM with Tukey's post hoc
Serum Inflammation	Two-way ANOVA RM with Tukey's post hoc
Lung Health	One-way ANOVA with Tukey's post hoc
Open Field	Two-way ANOVA RM with Tukey's post hoc
DRG Outgrowth	One-way ANOVA Tukey's post hoc

2.3 Results

2.3.1 Cervical SCI leads to acute gut dysbiosis and gastrointestinal tract pathology.

Nearly 60% of all SCI cases are at the cervical level. To model this type of injury, we employed a well-characterized left C2 hemisection (LC2Hx) model of SCI performed in the rat leading to the functionally defined decrease in diaphragm activity and altered ventilatory patterns to investigate the extent to which there is gut dysbiosis (Figure 2.1 a-b) ^{2,87}. In Experiment 1 (Figure 2.1 c), adult female Sprague Dawley rats were separated into three experimental groups: 1) LC2Hx, 2) surgical sham (all surgical procedures and drugs minus lesion), and 3) drug control (no surgical procedure but with anesthetic

intervention and post-surgical drugs) (Figure 2.1 c; Experimental design). Due to the impact of anesthesia and opioid-based analgesics on gut function and the gut microbiome, a surgical drug group was a necessary control^{198,199}. Animals were co-housed throughout the experiment, and cage mates were in the same experimental group to prevent bacterial transfer via coprophagia.

Electromyography (EMG) of the diaphragm ipsilateral to the injury was significantly lower in LC2Hx animals compared to surgical sham and drug control animals (Figure 2.1 b; One-way ANOVA with Tukey's posthoc LC2Hx/drug control $p = 0.0161$; LC2Hx/surgical sham $p < 0.0001$). To assess the impact of a LC2Hx on the gut microbiome, fecal samples were collected pre-injury (i.e., 0 days post injury (dpi)) and on days 1, 3, 7, 14, 21, 28, 58, and 84 dpi and were prepared for 16S rRNA sequencing and the hypervariable region V4 was amplified using the 515F-806R primers. Following 16S rRNA sequencing, we performed principal component analysis on the Bray Curtis distances of normalized operational taxonomic units rarefied reads. There was a significant separation of surgical sham and LC2Hx samples in the ordination space at the operational taxonomic unit level (Figure 2.2 a; permanova $p = 0.001$). Indeed, 16S rRNA analysis of fecal samples before and following this injury demonstrated a rapid and robust change in the gut microbiome. This was most evident by the significant increase in the Firmicutes to Bacteroidetes (F:B) ratio one-day post-injury in LC2Hx but not drug control or surgical sham animals (Figure 2.2 b; ; $p < 0.05$). At the phylum level, the Firmicutes and Bacteroidetes bacteria constitute 90% of the gut microbiome phylogenetic composition^{170,207}. An increase in the F:B ratio has been used previously to describe gut dysbiosis, or an imbalance of pathogenic and beneficial bacteria⁹. A high F:B ratio has been associated

with increased susceptibility to inflammation and obesity^{9,171-173}. The presence of a high F:B ratio following SCI has also been shown previously in thoracic-level mice models⁷. However, this finding has been inconsistent among other preclinical models of SCI^{7,65,208}.

Although the F:B ratio returned toward pre-injury levels by three days post-injury, histological evaluation of the gastrointestinal (GI) tract revealed profound gut pathology evidenced by subepithelial blebbing and disruption of the epithelial lining following LC2Hx (Figure 2.2 c – marked by black arrows). Neurogenic shock and autonomic nervous system impairment following SCI can cause hypoperfusion of visceral organs, inducing inflammation and pathological changes^{52,209}. Subepithelial blebs found at the tips of villi, called Gruenhagen spaces^{210,211}, are an indication of ischemia within the intestine and can eventually lead to disruption and disintegration of the epithelial lining in prolonged ischemic occurrences²¹². This hypoperfusion and loss of epithelium can induce further mucosal atrophy through necrosis and apoptosis of crypt cells. Further, crypt destruction can result in decreased villi length as these cells provide stem cells that develop and populate the villi²¹³. We observed no change in villi length in L2CHx animals (Figure 2.2 d; unpaired t-test; $p < 0.058$). Blinded evaluation of the tissue using the Chiu/Park scoring system of GI tract pathology revealed greater levels of pathology and intestinal injury in SCI animals (Figure 2.2 d; Mann-Whitney test $p > 0.999$). The Chiu/Park scoring grades the degree of intestinal mucosal injury on a scale of 0 – 5, with 0 indicating normal mucosal lining and 5 indicating disintegration of the lamina propria²⁰⁶.

Utilizing matrix-assisted laser desorption ionization (MALDI) imaging, we found there to be increased levels of glycogen in the ileal tissue of LC2Hx animals compared to the surgical sham, although this increase was not significant (Figure 2.2 e-f; unpaired t-

test, $p = 0.20$). Glycogen is a storage macromolecule that can influence bacterial survival during times of extreme stress²¹⁴. Glycogen stores allow for protein N-glycosylation in the brain, and dysregulation is known to drive pathogenesis in multiple diseases^{215,216}. Additionally, glycosylation is a hallmark of intestinal mucins, or glycoproteins, that act as the first line of defense to the intestinal epithelium against pathogens and luminal microbiota²¹⁷. Interestingly, microbiota have been found to regulate host protein glycosylation has been linked to intestinal health and disease²¹⁸. This relationship further emphasizes the importance of maintaining a healthy gut microbiome. Moreover, mucins are synthesized by goblet cells, most abundantly populated within the crypts of the small intestine. A reduction in these cells and the barrier they produce may lead to increased permeability, bacterial translocation, and systemic inflammation. Taken together, the increase in the F:B ratio immediately following LC2Hx, the reduction of goblet cells, and the increase in glycogen we observed may be a compensatory response to upregulate mucin production and repair the intestinal barrier or impairment.

These findings expand upon previous observations of the ileum at 24 hours post-injury at the thoracic level (T7/8 transection), where the proliferation of submucosal lymphatic tissue and widening of mucosal epithelial cell interspaces were apparent⁶⁰. Our findings are also consistent with previous findings in low thoracic injuries (T10/11 contusion), where decreased mucosal layer thickness and persistent atrophy began at 48 hours post-injury and were evident until 4 weeks post-injury⁵⁹. A separate T10 contusion study found similar results in the jejunum at 3dpi, with evidence of decreased villi height, increased crypt depth, and increased subepithelial space at the tip of villi²¹⁹. Our results are the first to show that the high cervical LC2Hx model can provide meaningful insights

into the serious problem of bowel and GI tract disease and pathology after SCI. Indeed, gastrointestinal complications following SCI are a major factor impacting the quality of life and account for 11% of rehospitalizations in the first year post-SCI ^{220,221}. Furthermore, individuals with injuries occurring at the cervical level are more likely to experience constipation and abdominal bloating and are more likely to be hospitalized compared to lower-level injuries ^{222,223}. Moreover, gastrointestinal dysfunction can compromise intestinal barrier function, allow for bacterial translocation in which intestinal bacteria translocate into the bloodstream, and contribute to systemic inflammation and multiple organ dysfunction syndrome (MODS), further impacting recovery and quality of life of SCI individuals ²²⁴.

2.3.2 Targeting gut dysbiosis improves ventilatory function and gut health.

Considering the finding that there was an immediate gut dysbiosis and persistent GI tract pathology after SCI, we aimed to restore pre-injury levels and microbiome balances through oral gavage of fecal matter from young, uninjured animals or probiotics. Indeed, previous studies demonstrated that treating neurotrauma-induced gut dysbiosis leads to improved locomotor recovery, smaller lesion sizes, and prevention of anxiety-like behavior ^{7,67}. However, the impact of treating gut dysbiosis following LC2Hx on breathing function, GI tract injury, and its long-term effects remain unexplored. We aimed to answer these questions and hypothesized that the dynamic changes in the gut microbiome immediately post-LC2Hx impede functional recovery of breathing in the acute to the sub-acute phase of SCI. Further, treatment of the resulting gut dysbiosis will improve gut health and allow for a more profound recovery of breathing at acute time points post-injury.

Animals received fecal matter transplants (FMT) for three consecutive days beginning the day of injury, followed by bi-weekly gavage until the predetermined endpoint. This gavage regimen combines two prior reports of FMT studies in rats (Schmidt et al., 2020, Kelly et al., 2016) ^{67,183}. FMT from young, uninjured animals into animals with LCHx led to marginal improvements in tidal volume in the first cohort of animals (Figure 2.3 a; $n = 4/\text{group}$ Two-way ANOVA $p = 0.2666$). To differentiate whether this change was due to peripheral lung mechanics or central respiratory pathways, we assessed lung mechanics using the flexiVent system. There was a trend towards increased inspiratory capacity in FMT-treated animals, which may indicate that the FMT treatment mitigated atelectasis, or partial lung collapse (Figure 2.3 b; Welch's t-test; inspiratory capacity $p = 0.0585$). Additional measures of lung health, such as compliance, resistance, and total live cells, did not differ between groups suggesting the overall lung mechanic findings did not account for the increase in tidal volume. Therefore, these findings suggest that the change in tidal volume may be driven centrally rather than by peripheral lung mechanic compensation. However, when all cohorts were completed ($n = 12/\text{group}$), this observation of improved tidal volume disappeared, and there were no statistically significant differences between groups in whole-body plethysmography (WBP) or diaphragmatic EMG (diaEMG) measurements (Figure 2.4 a and b). Inspiratory capacity remained elevated, and total live cells found in the bronchioalveolar lavage fluid were reduced with FMT treatment suggesting a reduction in inflammation and atelectasis, although compliance and resistance remain unchanged between groups (Figure 2.3 c; Welch's t-test; inspiratory capacity $p = 0.1122$, total live cells $p = 0.3086$).

As FMT led to mixed and inconsistent improvements, we initiated an alternative strategy of using a standardized probiotic treatment to mitigate gut dysbiosis based on previous findings (Kigerl et al., 2016). Indeed, Kigerl et al. reported functional motor recovery following thoracic SCI in mice when dosed with probiotics daily. Therefore, we implemented a daily probiotic regimen. The regimen consisted of a low, mid, and high dose. The gavage volume was maintained at 0.5 ml, but the bacterial concentration increased from 2.7×10^9 , to 24×10^9 , to 48×10^9 bacteria/dose in our rat LC2Hx model. In WBP studies and under normoxic conditions (21% O₂), animals treated with high-dose probiotics showed the expected reduction in tidal volume but were able to increase their respiratory at 7 dpi compared to the vehicle-treated group (Figure 2.4 c. Two-way RM ANOVA with Tukey's posthoc; frequency vehicle/high $p = 0.0210$; tidal volume vehicle/high $p = 0.0074$). Animals in the low and mid-dose groups were not able to produce this elevated respiratory rate. Minute ventilation was maintained at 7 dpi and 14 dpi due to the compensatory increase in frequency in the high-dose group (Figure 2.4 c; Two-way RM ANOVA with Tukey's posthoc; vehicle/high 7dpi $p = 0.1221$; vehicle/high 14 dpi $p = 0.1712$).

Alternatively, when challenged under hypoxic conditions (11% O₂), minute ventilation for all three probiotic doses (low-, mid-, and high-dose) was increased at 7dpi when compared to vehicle-treated animals with the mid-dose group mounting the highest response compared to vehicle-treated (Figure 2.5 a; Two-way RM ANOVA with Tukey's posthoc vehicle/mid 7dpi $p = 0.1218$). Examinations of lung health studies indicated no statistically significant differences in lung compliance, resistance, or total live cell counts (Figure 2.5 b.). The inspiratory capacity was significantly different; however, posthoc

analysis revealed no significant differences between groups (Figure 2.5 b; One-way ANOVA inspiratory capacity $p = 0.0385$, Dunnett's posthoc vehicle/low $p = 0.4146$, vehicle/mid $p = 0.9894$, vehicle/high $p = 0.2111$). Interestingly, when we evaluated diaphragm EMG, the animals in the low-dose group were able to produce the largest burst amplitude ipsilateral to the injury compared to all other groups (Figure 2.4 d; One-way ANOVA with Tukey's posthoc low/vehicle $p = 0.2624$; low/mid $p = 0.0855$; low/high = 0.0984). Importantly, there were no differences in injury severity between groups based on spared tissue analysis. This indicates that these improvements in respiratory function were not due to a less severe injury in any particular group (Figure 2.6 a – b. One-way ANOVA $p = 0.9411$). While probiotic treatment improved respiratory motor function, we did not observe changes in overall locomotor function demonstrated by the open field test (Figure 2.7). These findings suggest that probiotic treatment following cervical spinal cord injury may improve respiratory recovery through compensatory mechanisms by increasing the respiratory rate and amplitude of the diaphragmatic output.

In addition to improvements in ventilatory function, treatment of gut dysbiosis following SCI also led to improved gut pathology within the ileal tissue of the small intestine. FMT treatment produced marginal improvement in gut pathology. Less gaping between villi was evident with FMT treatment, an indication of a healthier physiological state as these projections are important for the absorption of nutrients by increasing the surface area of the small intestine. There were minimal increases in villi length and crypt depth, and better Chiu/Park scoring indicating pathological improvements following FMT treatment compared to sham-treated animals (Figure 2.8 a – d; unpaired t-test; b. villi length $p = 0.2807$; c. crypt depth $p = 0.4801$; d. mean of vehicle = 2.227; mean of FMT = 1.958).

Of note, the endpoint for the FMT study was 28 dpi in comparison to animals in comparison to animals in Experiment 1, as well as animals in Experiment 3 (i.e., probiotic treatment), which both had an endpoint of 14 dpi. Because we observed the initial improvement in total volume by 14 dpi (Figure 2.3 a) but no changes in gut pathology by 28 dpi in Experiment 2 (Figure 2.4 a – d), we used the 14 dpi timepoint for Experiment 3. The extra two weeks in Experiment 2 may have allowed more healing and repair making it difficult to detect differences with FMT treatment. Probiotic treatment resulted in increases in villi length in a dose-dependent manner, although these differences were not statistically significant, while there were no differences in crypt depth (Figure 2.8 e – g. One-way ANOVA; villi length $p = 0.1817$; crypt depth $p = 0.8036$). Additionally, we observed a reduction in the severity of pathological damage indicated by the Chiu/Park score with all doses of probiotic treatment compared to vehicle-treated, although this reduction was not significant (Figure 2.8 h; Kruskal-Wallis test $p = 0.3865$; mean of vehicle = 2.200; mean of low = 1.833; mean of mid = 1.750; mean of high = 1.200). Overall, these findings suggest that treatment of gut dysbiosis acutely after SCI improves gut pathology and potentially improves gut function.

2.3.3 Probiotic Treatment after SCI reduces the systemic inflammatory response and increases the sprouting and regeneration potential of neurons.

To begin to investigate the mechanism of these functional and pathological improvements, we obtained serum samples throughout the experiment to assess systemic inflammation. We observed a decrease in TNF-alpha at all time points in both FMT and probiotic-treated animals compared to vehicle-treated. This reduction was significant at 28 dpi in FMT-treated animals (Figure 2.9 a; Two-way RM ANOVA with Bonferroni posthoc

28 dpi $p = 0.0062$) and at 3 dpi in all probiotic-treated animals, regardless of dose level (Figure 2.9 b; Two-way RM ANOVA with Tukey's posthoc 3dpi vehicle/low $p = 0.0316$, vehicle/mid $p = 0.0152$, vehicle/high $p = 0.013$). Additionally, there was an overall effect of FMT treatment on IL-6 serum levels with FMT treated animals having lower IL-6 compared to vehicle-treated (Figure 2.9 a; Two-way RM ANOVA treatment $p = 0.0459$). These findings are consistent with clinical observations. The pro-inflammatory cytokine IL-6 was found to be elevated in patients at 48 hours post-injury but decreased by 7 days post-injury²²⁵. Conversely, an alternate study revealed that this increase is persistent as levels of IL-6, as well as TNF-alpha, are significantly elevated levels in SCI patients in the post-acute (2-52 weeks post-injury) and chronic (>52 weeks post-injury) phases of recovery compared to healthy controls²²⁶. Importantly for the recovery of breathing, systemic inflammation has been shown to impair respiratory plasticity²²⁷. Therefore, the reduction in systemic inflammation following treatment with probiotics may play an important role in the improved minute ventilation observed in figure 2.4 c.

We assessed if FMT or probiotic treatment could alter neuronal growth and sprouting characteristics⁴. To do this, we harvested dorsal root ganglion neurons from the animals in Experiments 2 and 3. Sholl analysis was used to determine the longest axon length and the total number of crossings or branching of axons. The summation of axon length (total outgrowth) and the total number of projections from the soma were also quantified. There were trends of increased total axon outgrowth, number of crossings, and axon length in FMT-treated animals, although these changes were not statistically significant (Figures 2.10 a and b; unpaired t-test; total outgrowth $p = 0.3477$; total number of crossings $p = 0.2996$; longest axon length $p = 0.1362$). There was no difference in the

number of projections from the soma in FMT versus vehicle-treated animals (Figures 2.10 b; unpaired t-test; number of projections from soma $p = 0.9683$). Probiotic treatment significantly improved the number of primary projections from the soma, with the high-dose probiotic group producing the greatest number of projections compared to all other groups (Figure 2.10 a and c; One-way ANOVA with Tukey's post hoc vehicle/high $p < 0.001$; low/high $p = 0.0002$; mid/high $p = 0.0067$). There was also a trend of increased total neurite outgrowth, and longest axon length in DRGs treated with high-dose probiotics in comparison to all other groups. Alternately, the mid-dose probiotic group produced the largest total number of crossings (Figure 2.10 c). These findings indicate that treatment of gut dysbiosis with FMT or probiotics allowed for probiotics to increase neurite outgrowth potential, longer axon projections, neurite branching ability, and increased sprouting of primary projections from the DRG soma. All of these are potential mechanisms of plasticity and recovery either centrally or in the innervation of the GI tract.

Given the enhanced potential to increase primary projections in DRGs in probiotic-treated animals, we next examined the extent of serotonergic sprouting below the level of injury as a potential mechanism for improved respiratory function. Serotonin is critical in activating silent spinal pathways that are important for recovery. We did not observe statistically significant differences in serotonin levels at the C4 ventral horn of animals treated with probiotics versus vehicle at 14 dpi (Figure 2.11 a – b). Because we observed a significant increase in respiratory rate following high-dose probiotic treatment at 7 dpi, examination of serotonergic levels in the brainstem at this more acute time point may be more revealing of a potential mechanism.

2.4 Discussion

Collectively, our experiments present compelling evidence that treating SCI-induced gut dysbiosis improves functional and pathological outcomes. We determined that this dysbiosis is transient, and most severe immediately post-injury. Interestingly, previous studies have determined that interventions for respiratory recovery, including administration of intermittent hypoxia and chondroitinase ABC (ChABC), are more efficacious at chronic time points post-injury^{30,99,108}. The immediate dysbiosis we observed may be a factor that undermines the effectiveness of early treatment strategies. Understanding the role of the gut-CNS axis and its influence on recovery mechanisms may improve the success of interventions at more acute time points following SCI.

Whole-body plethysmography studies indicate that probiotic treatment improves respiratory rate and overall minute ventilation following cervical SCI. As over half of SCI cases occur at the cervical level, which can impair descending respiratory drive pathways, any improvements in breathing function are of critical importance. Additionally, we found that treatment of gut dysbiosis with probiotics also led to improvements in the pathology of ileal tissue following SCI, demonstrated by an increase in villi length and improvements in the Chiu/Park score. Gastrointestinal complications can severely impact an SCI individual's quality of life, especially those with high-level injuries resulting in tetraplegia. Moreover, 11% of hospitalizations in the SCI population are due to GI complications⁵⁷. Compromise of gut barrier function can lead to bacterial translocation (leaky gut) and potentially life-threatening septicemia, which is sadly a leading cause of death following SCI. These realities demonstrate the importance of maintaining gut health following SCI for overall well-being and potentially enhancing recovery. This work further emphasizes the importance of personalized and precision medicine through a holistic approach. Studies

from our lab have previously demonstrated that genetic background, particularly apolipoprotein E (APOE) genotype, influences respiratory motor plasticity potential ⁵. APOE status has also been robustly associated with distinct microbiome profiles ¹⁷⁵. Future work evaluating the impact of genotype-associated microbiota composition in injury models may reveal important factors that enhance recovery potential.

Mechanistically, the improvement in respiratory function may be attributed to the reduction in systemic inflammation following the treatment of gut dysbiosis. FMT treatment reduced the systemic IL-6 level following LC2Hx. Additionally, both FMT and probiotic treatment reduced systemic TNF-alpha levels at all time points post-injury compared to vehicle-treated animals. This reduction in systemic proinflammatory cytokine levels may contribute to the observed respiratory recovery, as previous studies have demonstrated that systemic inflammation can impair respiratory plasticity ²²⁷. Additionally, FMT and probiotic treatment improved the regenerative potential of neurons. The ability for plasticity and regeneration of axons – either centrally or peripherally - is of utmost importance for SCI recovery. Several mechanisms to improve regenerative capacity have been employed, including enhancing the expression of neurotrophic factors, inhibition of PTEN, administration of intermittent hypoxia, and application of ChABC to digest inhibitory molecules within the glial scar ^{30,108,228-232}. We now show that treatment of gut dysbiosis can also enhance the regenerative capacity of neurons and can potentially be used in conjunction with these other interventions. Overall, these findings provide evidence that treatment of gut dysbiosis following SCI is a critical therapeutic target for recovery at a holistic level.

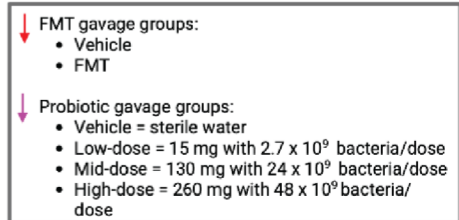
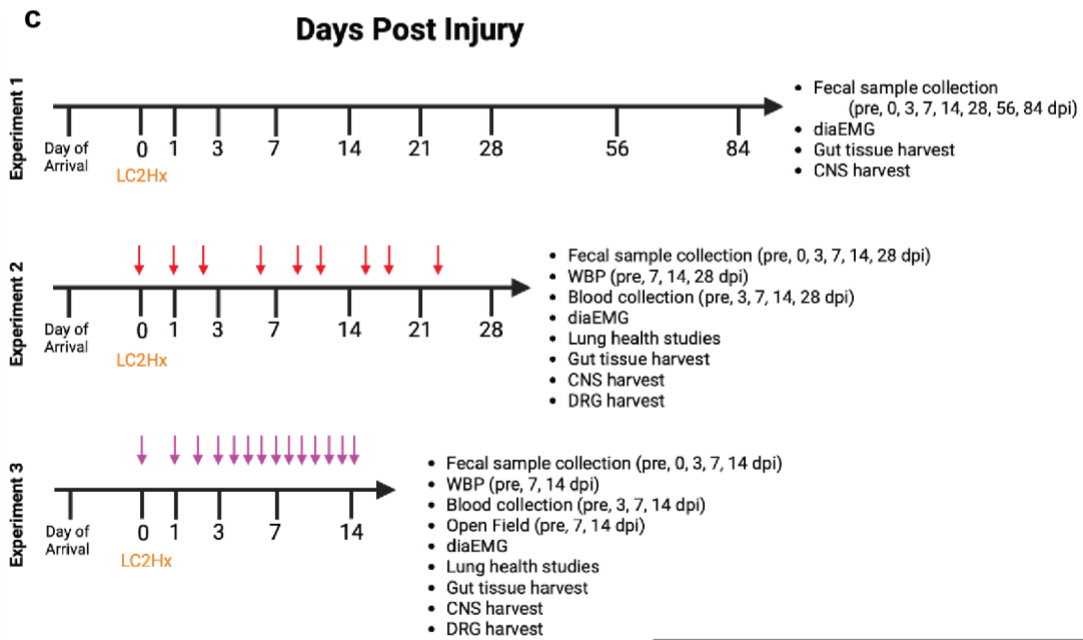
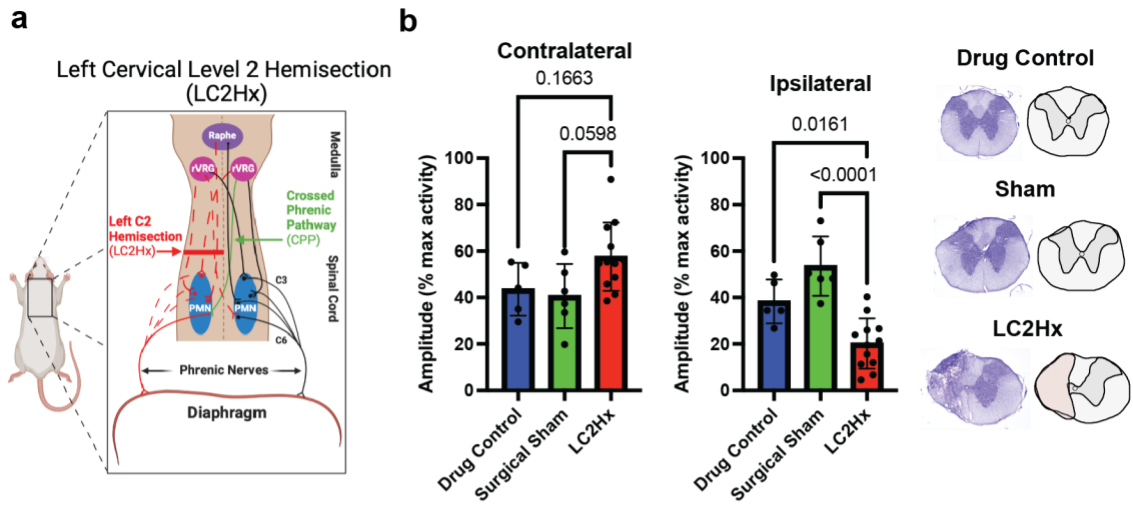


Figure 2.1 Injury model and experimental design.

a, Schematic representation of the LC2Hx model disrupting the respiratory pathway. **b**, Quantification of diaphragm burst amplitude as a percent maximum activity contralateral and ipsilateral to the LC2Hx and histological images indicating the injury severity for each group (drug control = blue, sham = green, LC2Hx = red). As expected, the LC2hx produced a significant decrease in the burst amplitude on the ipsilateral side of the lesion (One-way ANOVA $p < 0.0001$). **c**. Experimental design; Experiment 1: Evaluating gut dysbiosis following LC2Hx, groups: drug control (n = 5), surgical sham (n = 6), LC2hx (n = 12); Experiment 2: Fecal matter transplant (FMT) treatment following LC2Hx, groups: vehicle (FMT slurry without fecal component, n = 12) or FMT-treated (n = 12), three consecutive gavages beginning day of surgery followed by biweekly gavage until endpoint; Experiment 3: Probiotic treatment following LC2Hx, groups: vehicle (sterile water, n = 5)), low-dose probiotic = 15 mg with 2.7×10^9 bacteria/dose (n = 6), mid-dose probiotic = 24×10^9 bacteria/dose (n = 6), high-dose probiotic = 24×10^9 bacteria/dose (n = 5) gavage daily beginning day of injury.

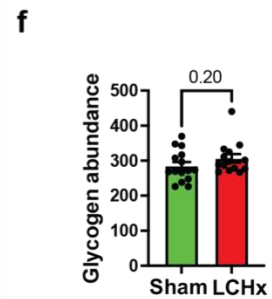
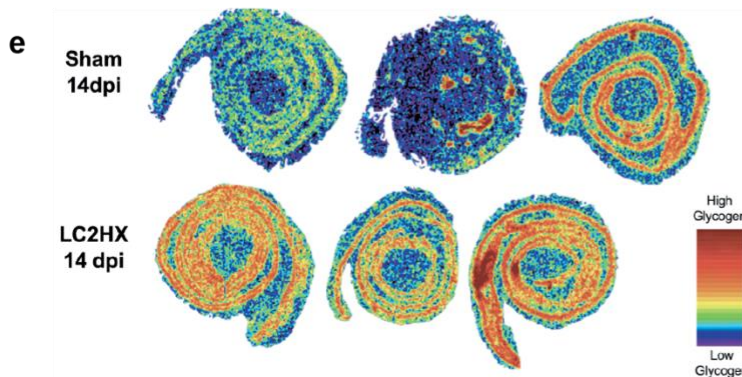
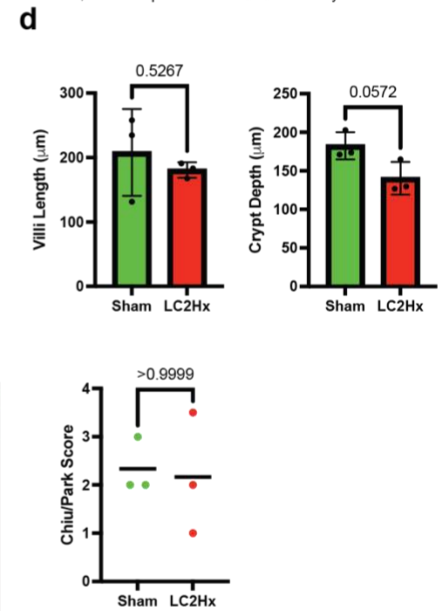
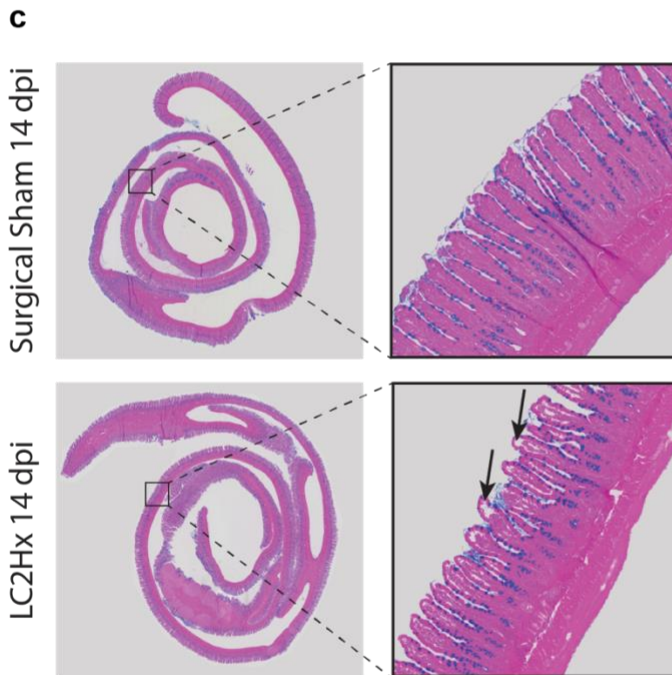
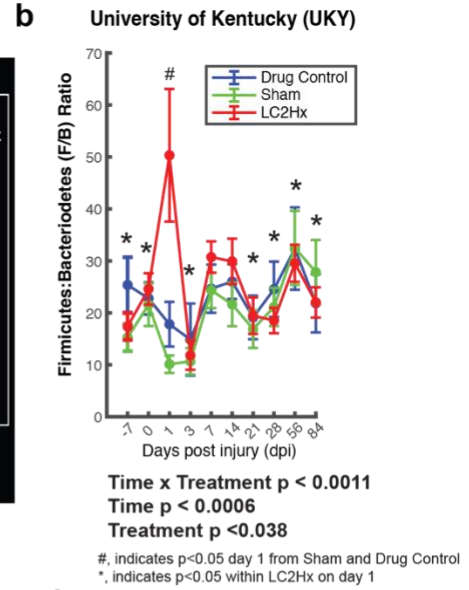
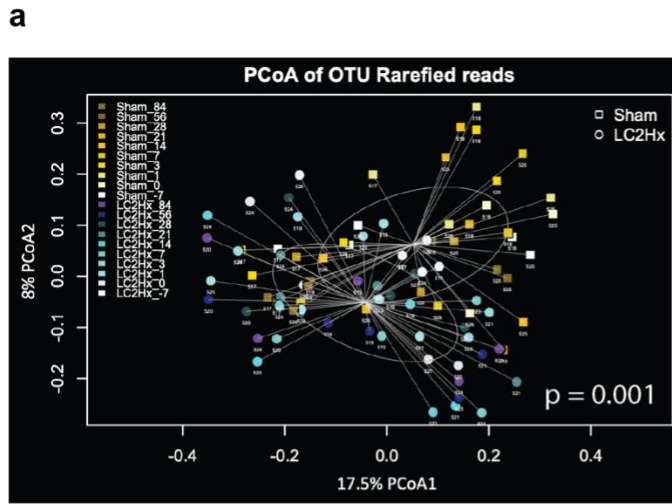


Figure 2.2 Cervical SCI leads to acute dysbiosis and GI tract pathology.

a, Principal coordinate analysis (PCoA) on Bray Curtis distances of normalized operational taxonomic units (OTUs) rarefied reads colored by day post-injury in surgical sham (square) or LC2Hx (circle) (permnova $p = 0.0001$). **b**, 16S rRNA sequencing data revealed a significant increase in the Firmicutes:Bacteroidetes ratio at 1 dpi in the LC2hx group (Two-way RM ANOVA $p < 0.0011$). **c - d**, Histological representations of ileal tissue pathology at 14 dpi revealed no change in villi length, although there was a strong trend in the reduction of crypt depth (unpaired t-test; villi length $p > 0.52$; crypt depth $p < 0.058$). The Chiu/Park scoring system was used to determine injury severity and revealed no differences between groups (Mann-Whitney test $p > 0.999$). **e - f**, MADLI imaging revealed that LC2hx leads to metabolic dysregulation of glycogen in the ileum at 14 dpi. Bars represent mean \pm SD. Bolded text indicates a p-value < 0.05 .

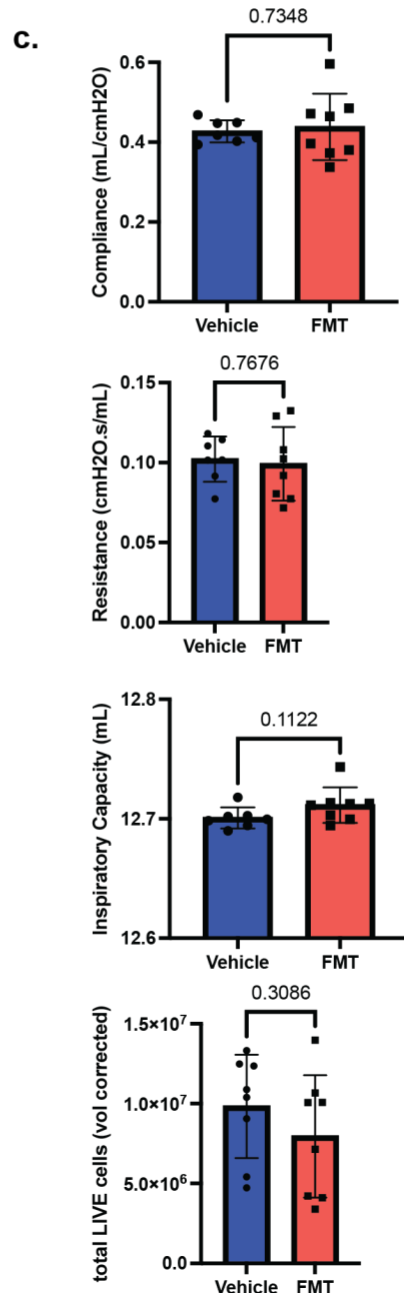
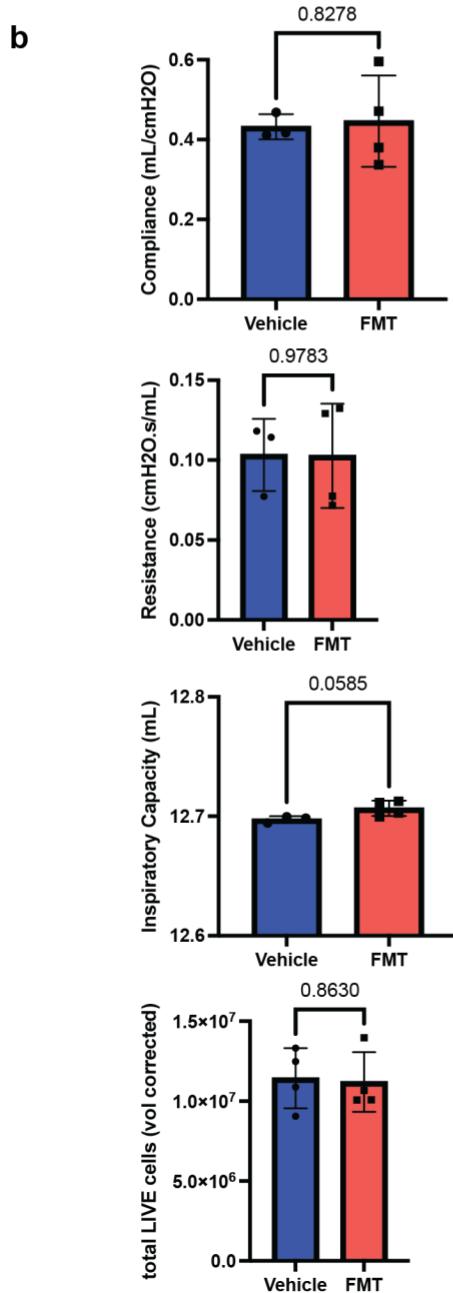
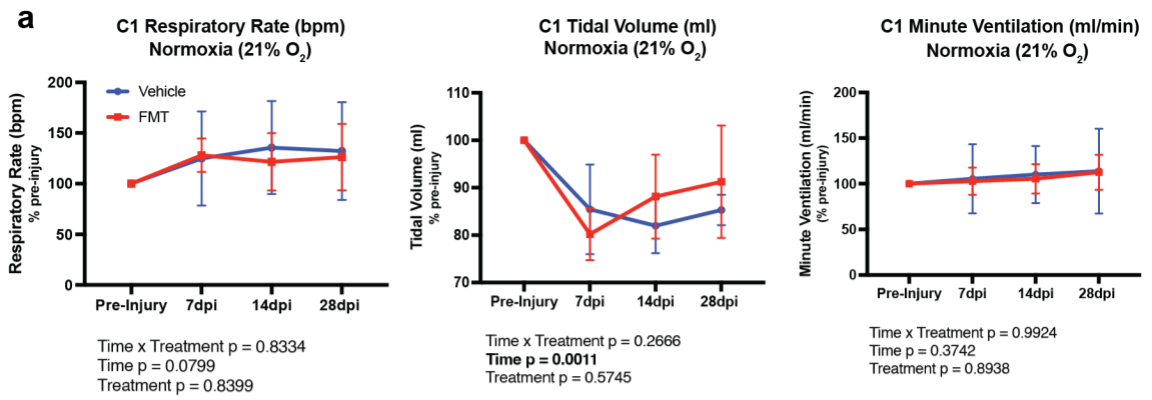
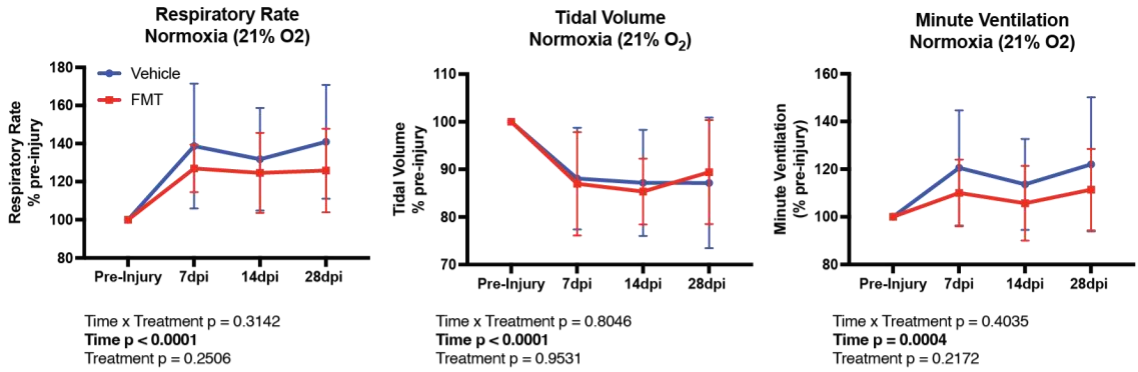


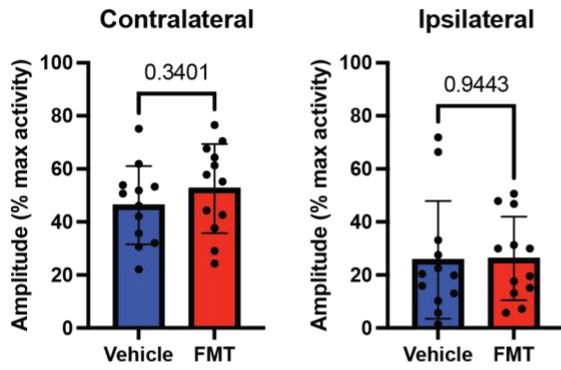
Figure 2.3. FMT treatment does not improve ventilatory function following LC2Hx.

a, Quantification of WBP measurements (respiratory rate, tidal volume, and minute ventilation) in cohort 1 (n = 4 animals/group) following LC2Hx and treatment with vehicle (blue) or FMT (red) revealed marginal differences between groups, although there appeared to some improvement in the tidal volume of FMT-treated animals at 14 and 28 dpi. (Two-way ANOVA treatment p = 0.5745). **b**, Lung health measurements (compliance, resistance, inspiratory capacity, and total live cell counts) in cohort 1 (n = 4 animals/group) revealed no significant differences between groups (Welch's t-test compliance p = 0.8278, resistance p = 0.9783, inspiratory capacity p = 0.0585, total live cell counts p = 0.8630). **c**, Lung health measurements (compliance, resistance, inspiratory capacity, and total live cell counts) in cohorts 1 and 2 (n = 8 animals/group) revealed no significant differences between groups (Welch's t-test compliance p = 0.7348, resistance p = 0.7676, inspiratory capacity p = 0.1122, total live cell counts p = 0.3086). Bars represent mean \pm SD. Bolded text indicates a p-value < 0.05.

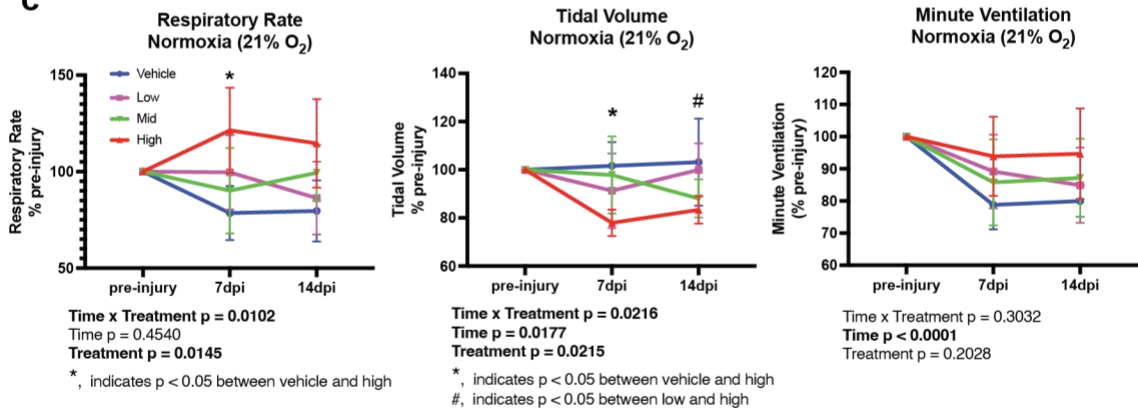
a



b



c



d

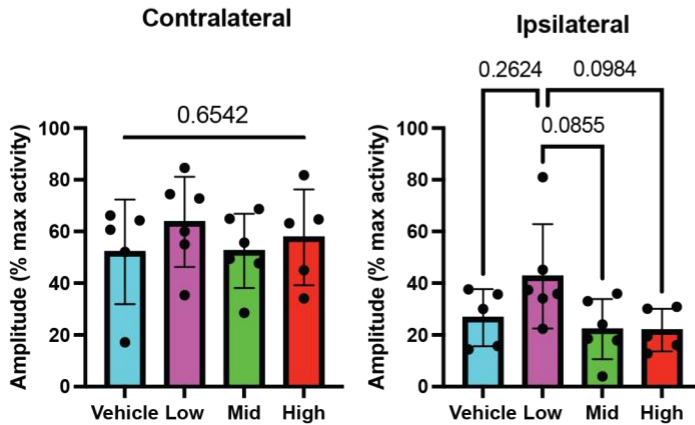


Figure 2.4. High-dose probiotic treatment mitigates decline in respiratory rate following SCI.

a, Quantification of WBP measurements (respiratory rate, tidal volume, and minute ventilation) and **b**, diaEMG studies following LC2Hx and treatment with vehicle (blue) or FMT (red) revealed marginal differences between groups. **c – d**, Quantification of WBP and diaEMG studies following LC2Hx and treatment with vehicle (blue), low-dose (purple), mid-dose (green), or high-dose (red) probiotics. **c**, Treatment with probiotics following LC2Hx revealed a significant increase in the respiratory rate in the high-dose probiotics versus vehicle-treated animals at 7 dpi (Two-way RM ANOVA with Tukey's posthoc $p = 0.0340$). Conversely, there was a significant decrease in tidal volume in the high-dose probiotic versus vehicle-treated animals at 7 and high-dose versus low-dose probiotic-treated animals at 14 dpi (Two-way RM ANOVA with Tukey's posthoc high/vehicle 7 dpi $p = 0.0121$ and high/low 14 dpi $p = 0.0496$) Although not significantly different, all probiotic treated animals were able to maintain a higher minute ventilation than vehicle-treated animals at all time points post-injury. **d**, diaEMG studies revealed no significant differences between any treatment groups in the contralateral or ipsilateral diaphragm following LC2Hx, although the low-dose probiotic treated group was able to mount a greater burst amplitude compared to all other groups (One-way ANOVA with Tukey's posthoc low/vehicle $p = 0.2624$, low/mid $p = 0.0855$, low/high $p = 0.0984$). Bars represent mean \pm SD. Bolded text indicates a p -value < 0.05 .

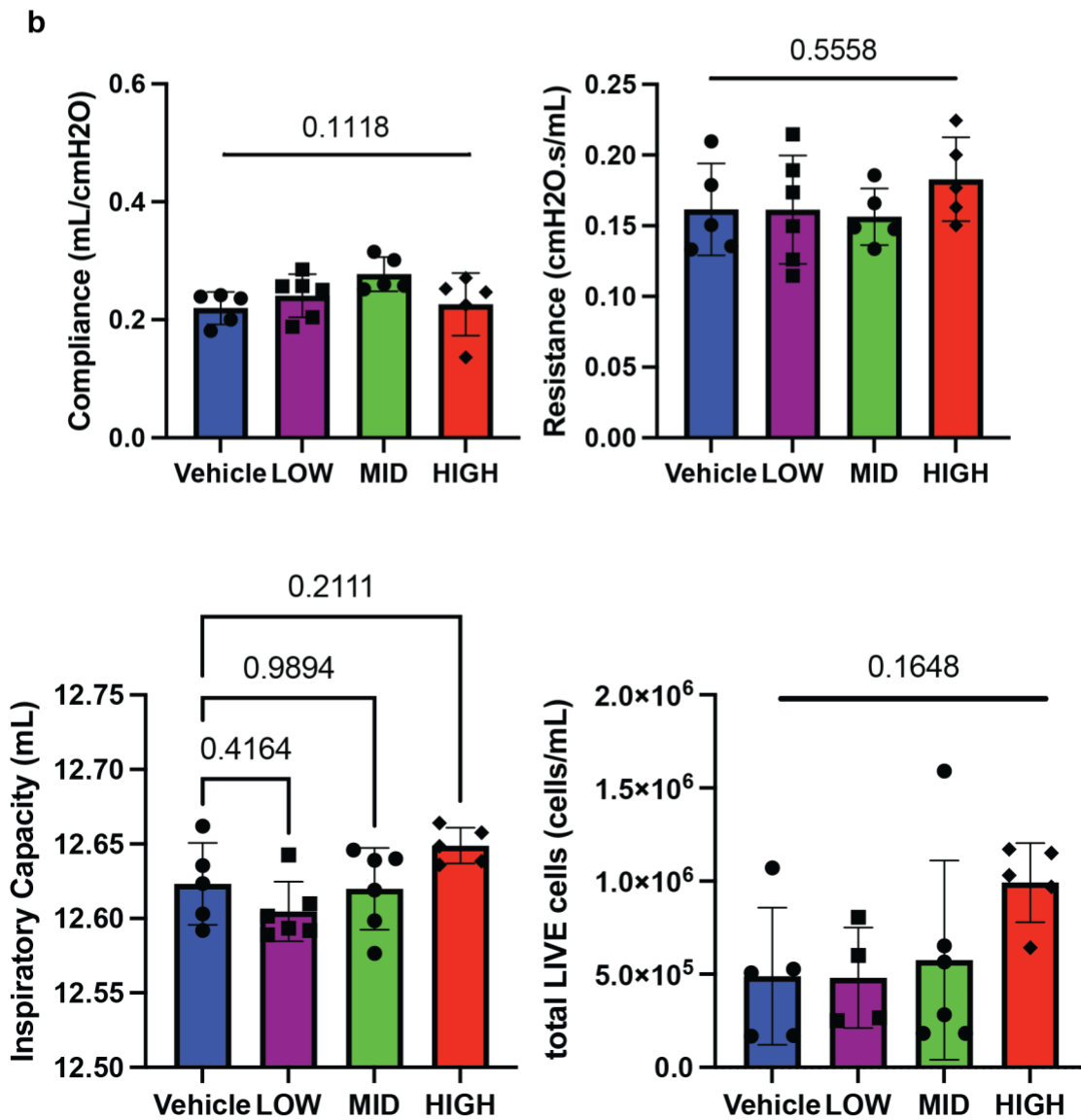
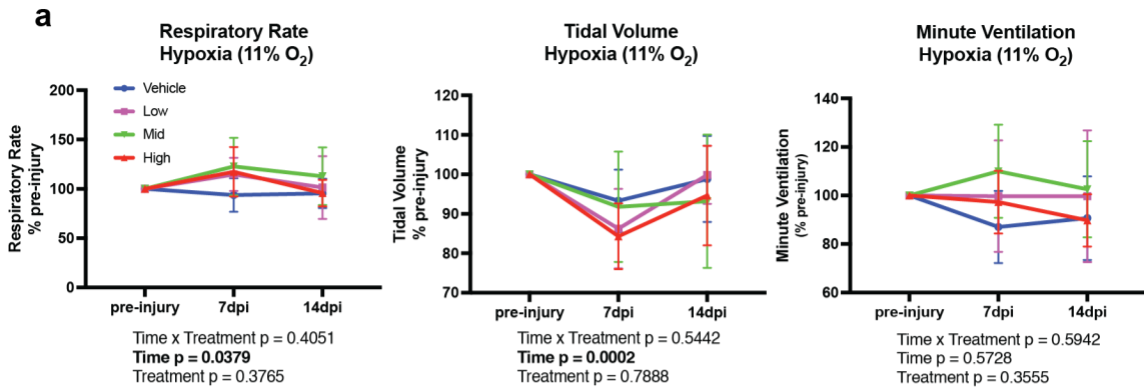


Figure 2.5. Hypoxic whole-body plethysmography and lung mechanic measurements following SCI and probiotic treatment.

a, Quantification of WBP measurement (respiratory rate, tidal volume, and minute ventilation) under hypoxic conditions (11% oxygen) in vehicle (blue), low-dose (purple), mid-dose (green), or high-dose (red) probiotic animals pre-injury, 7, and 14 days post-LC2Hx revealed marginal differences between groups. There appeared to some improvement in the minute ventilation of probiotic-treated animals at 7 dpi, as all probiotic-treated groups produced an increases minute ventilation compared to vehicle, although this increase was not statistically significant. (Two-way ANOVA treatment $p = 0.3555$). **b**, Lung health measurements revealed no significant differences in compliance, resistance, inspiratory capacity, or total live cell counts (One-way ANOVA compliance $p = 0.1118$, resistance $p = 0.5558$, total live cell counts $p = 0.1648$). Inspiratory capacity differed between groups, although there was no significant difference in posthoc comparisons (One-way ANOVA inspiratory capacity $p = 0.0385$, Dunnett's posthoc vehicle/low $p = 0.4146$, vehicle/mid $p = 0.9894$, vehicle/high $p = 0.2111$). Bars represent mean \pm SD. Bolded text indicates a p -value < 0.05 .

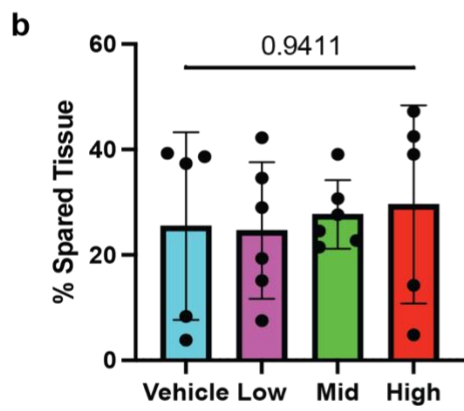
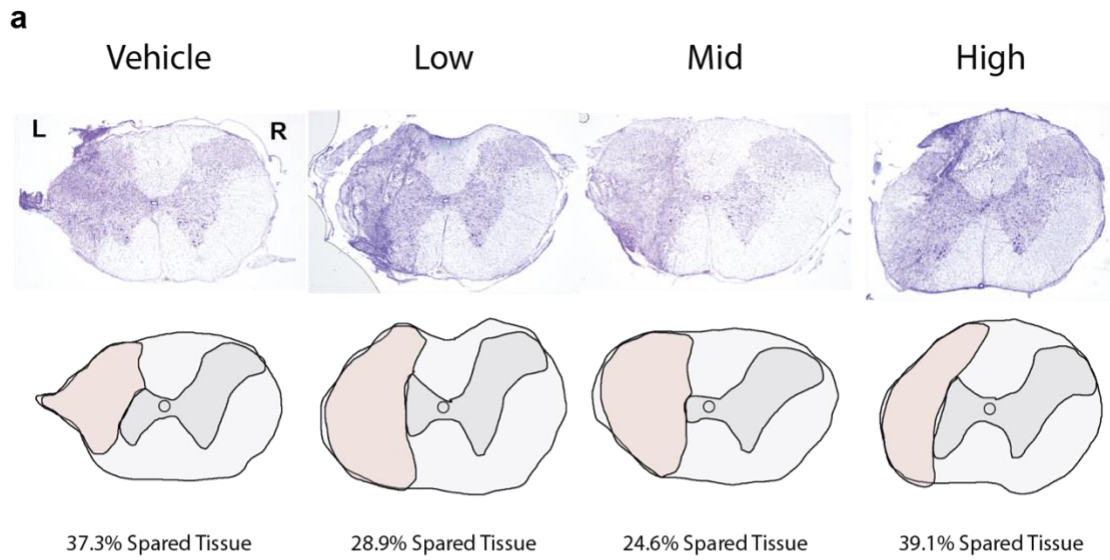
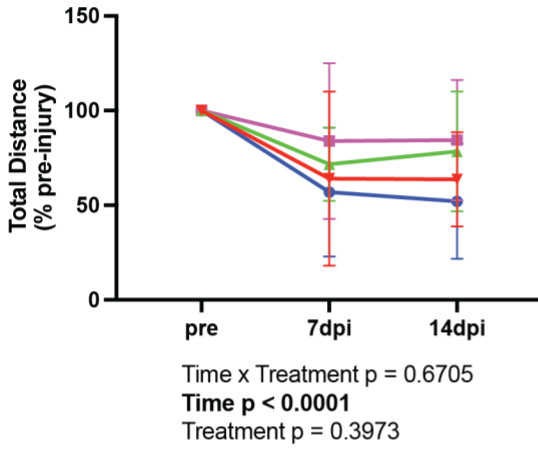


Figure 2.6 Confirmation of LC2Hx in Experiment 3: Probiotic treatment following LC2Hx.

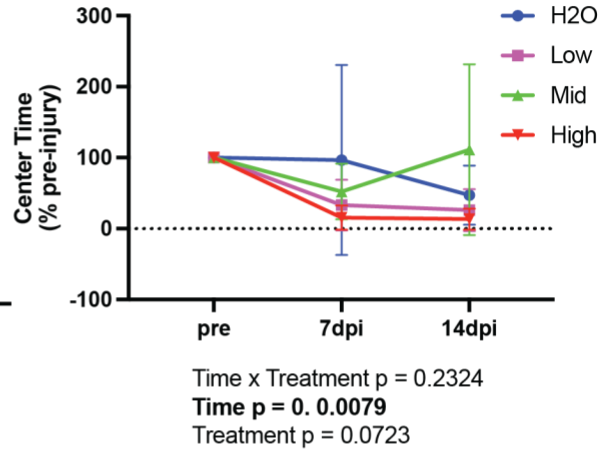
a, Representative images of cresyl violet staining at the level of injury (spinal level C2) in vehicle, low-dose, mid-dose, and high-dose probiotic-treated animals 14 days post-LC2Hx.

b, Quantification of spared tissue indicated no significant differences between groups (vehicle = blue, low = purple, mid = green, high = red) at the level of injury, demonstrating that all animals were equally injured (One-way ANOVA $p = 0.9411$). Therefore, improvements observed in outcome measures are not attributed to a less severe injury. Bars represent mean \pm SD.

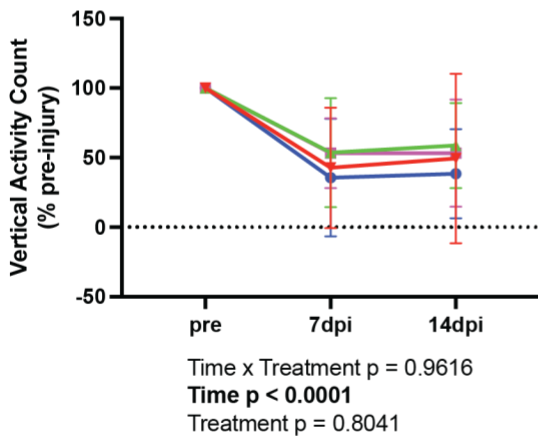
a



b



c



d

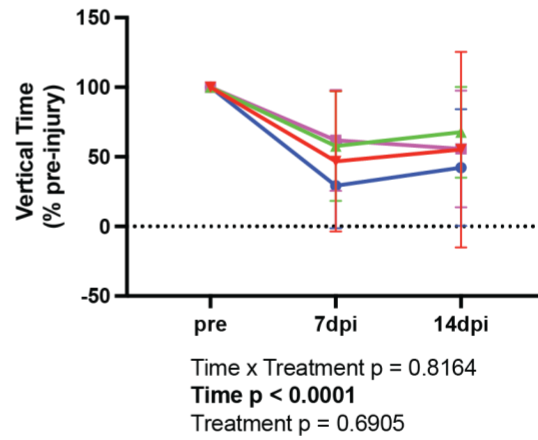


Figure 2.7 Probiotics treatment does not affect locomotor activity following LC2Hx.

Evaluation of locomotion was assessed in activity chambers pre-injury and at 7 and 14 dpi.

a, All probiotic-treated groups demonstrated an increase in total distance traveled at both time points post-injury, although this trend was not statistically significant (Two-way ANOVA treatment $p = 0.3973$). **b**, Center time was higher in vehicle-treated animals at 7 dpi compared to all probiotic groups, although not significantly (Two-way ANOVA treatment $p = 0.0723$). Bonferroni post hoc analysis revealed no significant differences between groups at any time point. **c – d**, There were no significant differences between groups in **c**, vertical activity count, or **d**, vertical time (Two-way ANOVA vertical activity count $p = 9616$, vertical time $p = 8164$). As expected, there was a time effect in all measurements, as all animals were injured. Bars represent mean \pm SD. Bolded text indicates a p -value < 0.05 .

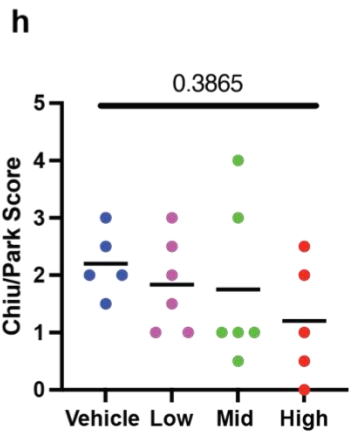
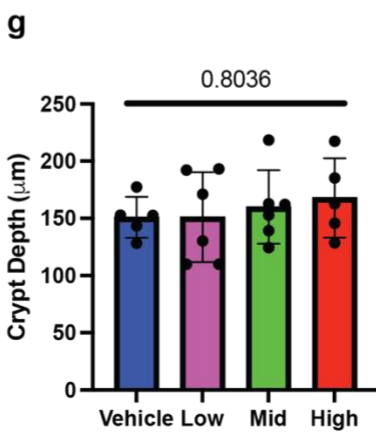
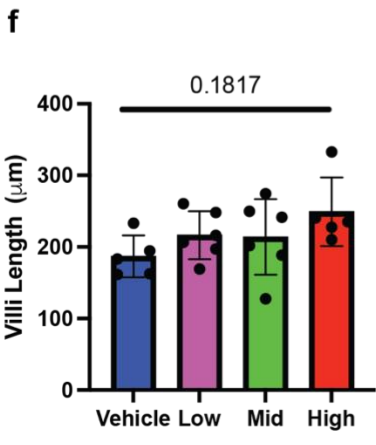
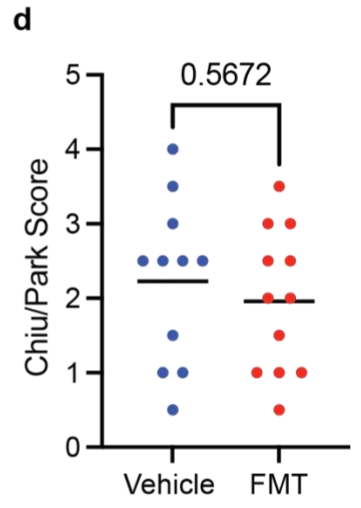
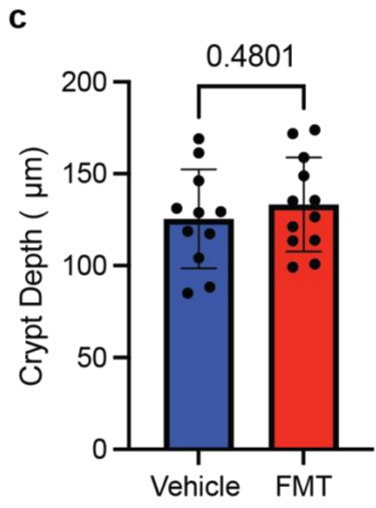
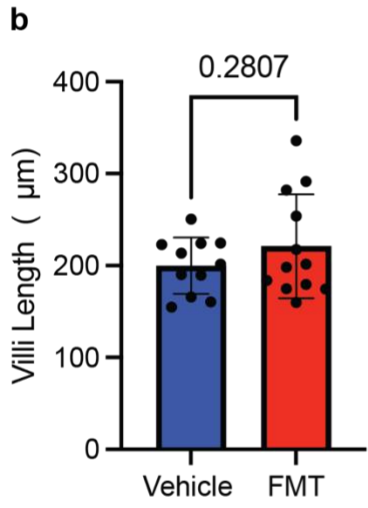
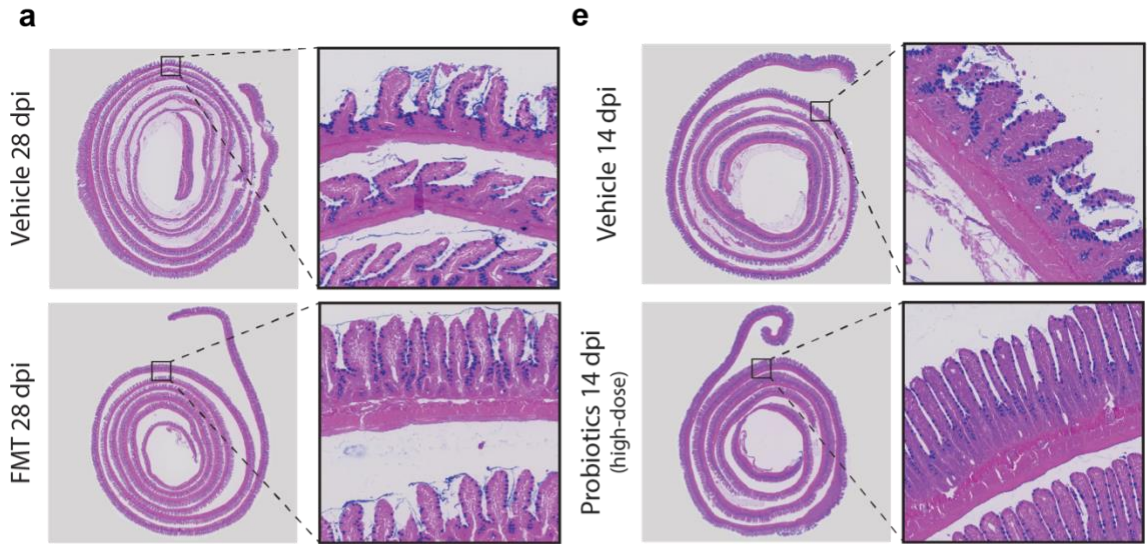


Figure 2.8 Targeting gut dysbiosis improves gut health.

a, Representative histological images of ileal tissue stained with alcian blue in vehicle (blue) and FMT-treated (red) animals at 28 days post-LC2Hx at 2x (left) and 5x (right - enlarged window). **b – d**, Quantification of **b**, villi length (unpaired t-test $p = 0.2807$), **c**, crypt depth (unpaired t-test $p = 0.4801$), and injury severity represented by the **d**, Chiu/Park score (Mann-Whitney test $p = 0.5672$; mean of vehicle = 2.227; mean of FMT = 1.958) revealed no significant changes in the vehicle versus FMT-treated animals at 28 days post-LC2Hx. **e**, Representative histological images of ileal tissue stained with alcian blue in vehicle and high-dose probiotic-treated animals at 14 days post-LC2Hx at 2x (left) and 5x (right - enlarged window). **f – h**, Quantification of ileal histology at 14 days post-LC2Hx in vehicle (blue), low-dose (purple), mid-dose (green), or high-dose (red) probiotic-treated animals. **f**, Quantification of villi length revealed a trend of increased length as the probiotic dose increased compared to vehicle, although these differences were not significant (One-way ANOVA with Dunnett's posthoc $p = 0.1817$; vehicle/low $p = 0.5316$; vehicle/mid $p = 0.5906$; vehicle/high $p = 0.0791$). **g**, Quantification of crypt depth revealed no significant difference between groups (One-way ANOVA with Dunnett's posthoc $p = 0.8036$; vehicle/low $p > 0.999$; vehicle/mid $p = 0.9362$; vehicle/high $p = 0.7399$). **h**, Quantification of the Chiu/Park score, a measurement of injury severity, revealed no significant differences, although there was a trend of a decreasing score with the increase in probiotic dose compared to vehicle (Kruskal-Wallis test $p = 0.3865$; mean of vehicle = 2.200; mean of low = 1.833; mean of mid = 1.750; mean of high = 1.200). This finding and the increase in villi length with an increased probiotic dose indicate a healthier gut pathology with high-

dose probiotic treatment compared to vehicle. Bars represent mean \pm SD. Bolded text indicates a p-value < 0.05 .

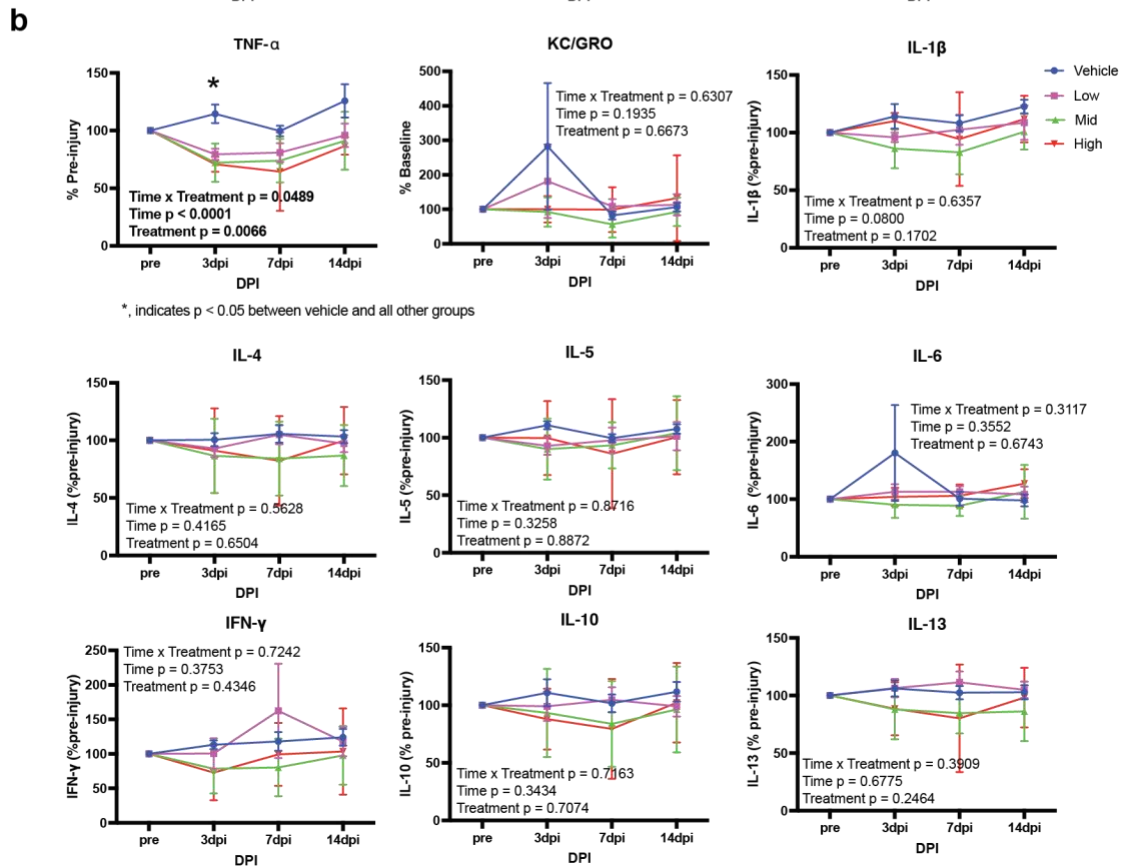
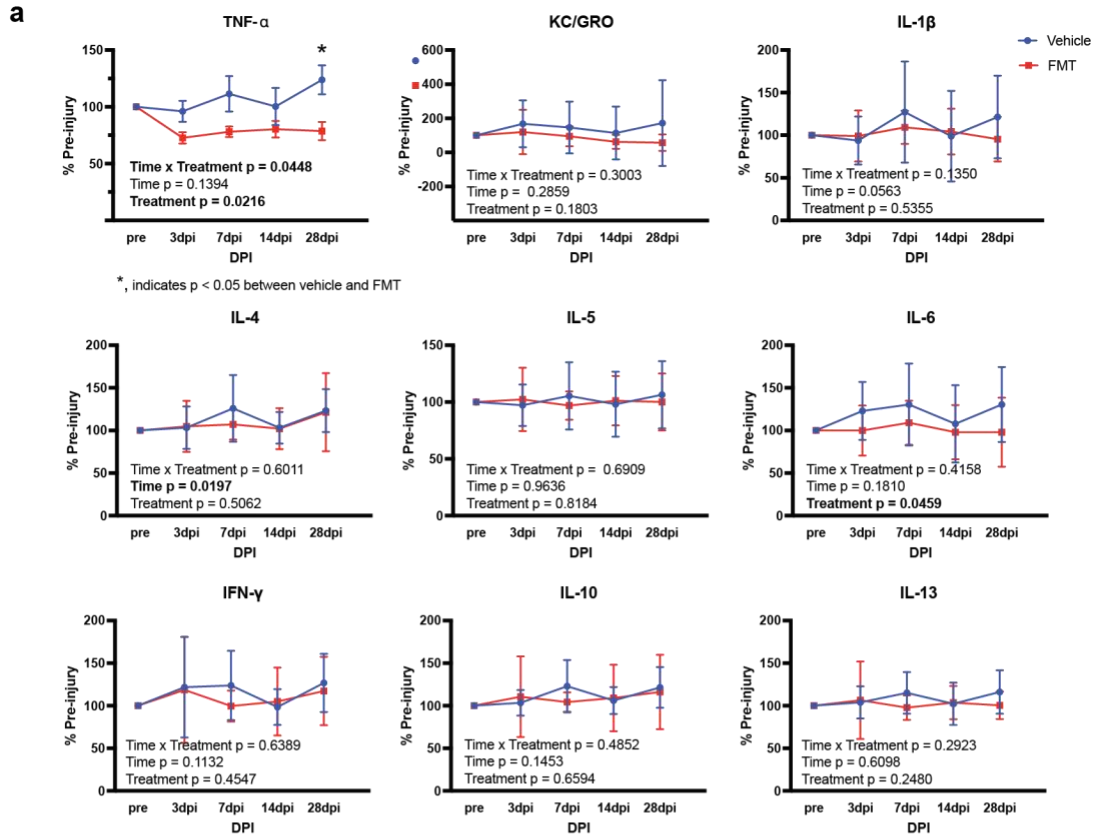
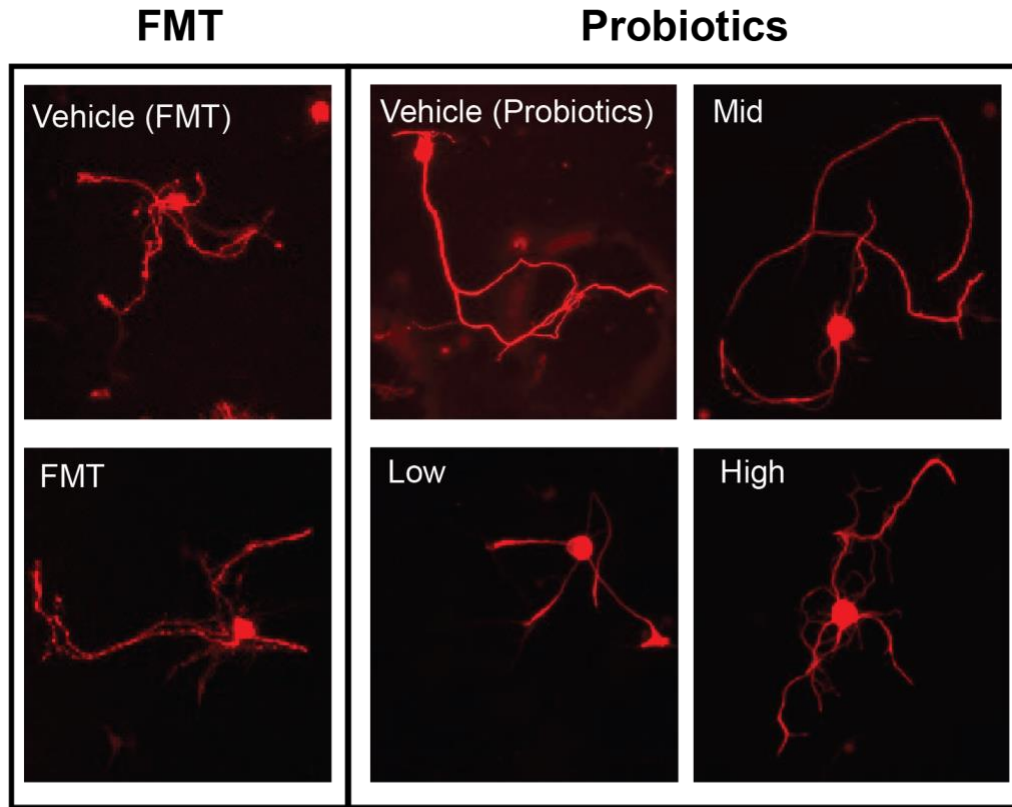


Figure 2.9 Treating gut dysbiosis reduces the systemic inflammatory response.

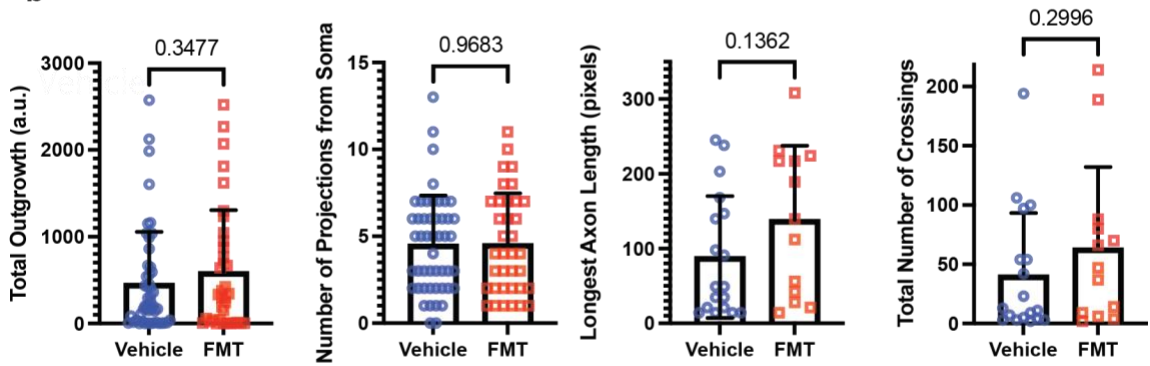
a, Quantification of proinflammatory cytokines in the serum vehicle (blue) and FMT-treated (red) animals pre-injury and at 3, 7, 14, and 28 days post-LC2Hx. Of the nine cytokines tested, TNF-alpha and IL-6 both revealed treatment effects and decreased at all time points post-injury (Two-way ANOVA TNF-alpha $p = 0.0216$ and IL-6 $p = 0.0459$). Bonferroni's posthoc analysis revealed that this decrease was significant in TNF-alpha levels in FMT-treated compared to vehicle-treated animals at 28 dpi ($p = 0.0062$).

b, Quantification of proinflammatory cytokines in the serum of vehicle (blue), low-dose (purple), mid-dose (green), or high-dose (red) probiotic animals pre-injury and at 3, 7, and 14 days post-LC2Hx. TNF-alpha revealed a treatment effect and was decreased in all probiotic treated animals compared to vehicle-treated at all timepoints. (Two-way ANOVA TNF-alpha $p = 0.0066$). Tukey's posthoc analysis revealed this decrease to be significant at 3dpi in all probiotic-treated groups compared to vehicle (vehicle/low $p = 0.0316$, vehicle/mid $p = 0.0152$, vehicle/high $p = 0.0139$). Bars represent mean \pm SD. Bolded text indicates a p -value < 0.05 .

a



b



c

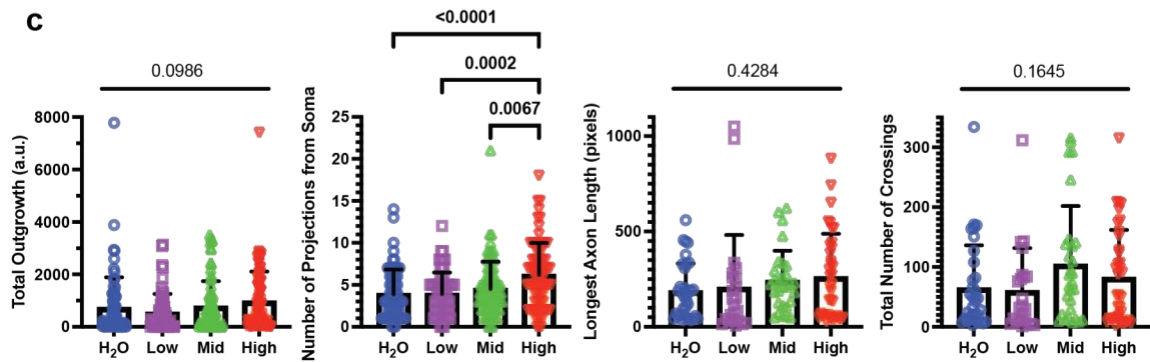


Figure 2.10 Probiotic treatment following SCI increases the sprouting and regenerative potential of neurons.

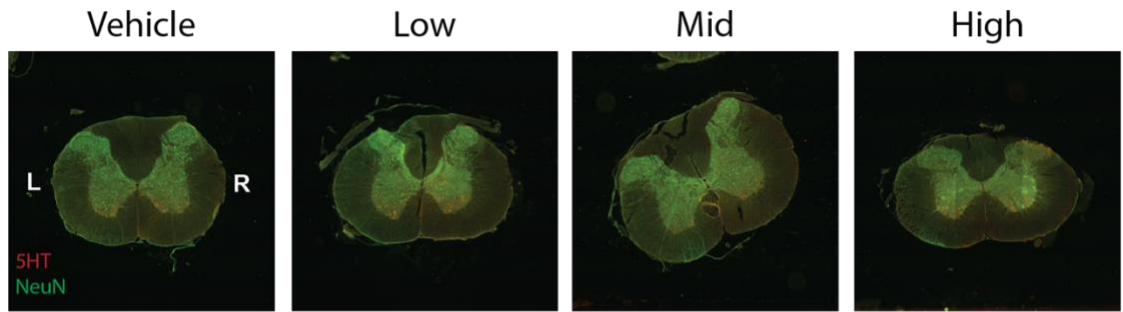
a, Representative images for DRGs treated with vehicle (blue) or FMT (red) (Experiment 2) and vehicle (blue), low- (purple), mid- (green) , or high-dose (red) probiotics (Experiment 3).

b, Mean \pm SD of total neurite outgrowth of DRGs *in vitro* measured for *in vivo* FMT versus vehicle-treated animals. There was no significant difference in total outgrowth (p-value = 0.3477). Mean \pm SD of the total number of primary projections growing from DRG soma *in vitro* for FMT versus vehicle-treated animals. There was no significant difference in the total number of primary projections growing from the DRG soma (p-value = 0.9683). Mean \pm SD of the length of the longest measured axon extending from the DRG. The length of the longest axon was increased in DRGs from FMT-treated animals (0.1362). Mean \pm SD of the total number of neurite crossings of the concentric rings in a Scholl analysis of DRGs *in vitro* for animals treated with FMT or vehicle *in vivo*. The total number of crossings was increased in animals treated with FMT (p-value = 0.2996), thus indicating that total neurite branching was increased in animals treated with FMT

c, Probiotic treatment did not cause a significant difference in the total neurite outgrowth of DRGs in comparison to vehicle-treated (p-value = 0.0986), although there was a trend towards increased total neurite outgrowth of DRGs from animals treated with high-dose versus low-dose probiotics (p-value = 0.0644, difference = 4.452 \pm 1.792). The total number of projections of high-dose probiotics was significantly increased compared to vehicle (2.290 ± 0.5143 ; p-value < 0.0001****), low-dose probiotics (2.262 ± 0.5351 ; p-value = 0.0002***), and mid-dose probiotics (1.650 ± 0.5056 ; p-value = 0.0067**).

The length of the longest axon increased as the concentration of the probiotic treatment increased (p-value = 0.4284). The total number of crossings increased for the DRGs of animals treated with the mid and high concentrations of probiotics (p-value = 0.1645), thus indicating that total neurite branching was increased by the mid and high probiotic concentrations. Bars represent mean \pm SD. Bolded text indicates a p-value < 0.05.

a



b

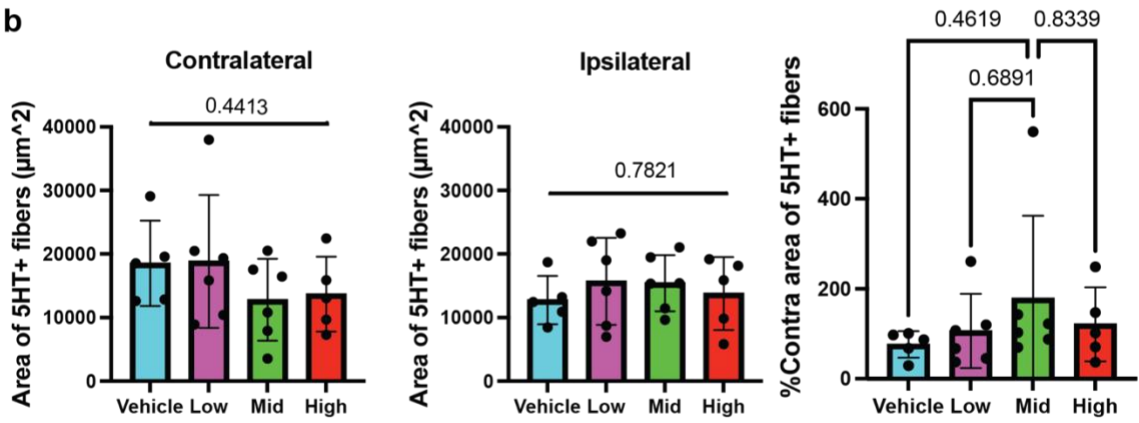


Figure 2.11 Probiotics treatment does not alter serotonin levels at the level of the phrenic motor nucleus.

a, Representative images of 5-HT (serotonin) staining at the level of the phrenic motor nucleus (spinal level C4) in vehicle, low-dose, mid-dose and, high-dose probiotic-treated animals 14 days post-LC2Hx (5-HT is in red, NeuN is in green). **b**, Quantification of 5-HT staining indicated no significant differences between groups (vehicle = blue, low = purple, mid = green, high = red) at the level of C4 on the contralateral or ipsilateral side of injury (One-way ANOVA contralateral $p = 0.4413$, ipsilateral $p = 0.7821$). Evaluation of the ipsilateral side as a percentage of the contralateral side indicated that all probiotic groups had more serotonin than vehicle-treated, although this trend was not statistically significant (One-way ANOVA $p = 0.6941$). Bars represent mean \pm SD.

CHAPTER 3. INTERINSTITUTIONAL COMPARISONS OF THE GUT MICROBIOME FOLLOWING CERVICAL SPINAL CORD INJURY

3.1 Introduction

Spinal cord injuries (SCI) are heterogeneous and cause unique pathological changes between patients due to the level and severity of the damage. This variability makes studying SCI especially challenging. To study mechanisms of recovery, scientists have developed injury models that are consistent and reproducible in the effort to find a cure. The lateral C2 hemisection (LC2Hx) model has been used for over a century and employed widely by laboratories investigating strategies for respiratory recovery following cervical SCI⁸⁷. This model results in paralysis of the ipsilateral hemidiaphragm, although various physiological and pharmacological techniques have been developed to increase respiratory drive and activate spared pathways that allow for recovery of function on the side of paralysis. This spared pathway is known as the crossed phrenic pathway^{89,91,92,101}. Interestingly, results using this consistent and reproducible model still vary. Several reasons for disparities between studies have been explored, including age, sex, the strain of rodents, circadian rhythm, and genetic predisposition^{3,5,99,233,234}. We aimed to build off these studies and investigate the impact of the gut microbiome following LC2Hx at different institutions. Indeed, the site of the research institution and the environment in which the research animals are can alter the gut microbiome, although how these changes impact recovery following SCI has not been explored²³⁵. We used the LC2Hx model in female Sprague-Dawley retired breeders to determine whether the gut microbiome established at two separate research institutions plays a role in respiratory recovery. Investigating these differences is important for clinical translation. As the human

population of SCI is highly variable, factors that could potentially impact outcomes must be explored.

3.2 Methods

3.2.1 Animals and Housing

All experiments were approved by the Institutional Animal Care and Use Committee at the University of Kentucky or Drexel University. Adult female Sprague Dawley rats from Envigo were used in all experiments and allowed to acclimate for at least one week prior to beginning experimental procedures. Animals were co-housed in a 12-hour light/dark cycle with standard chow and water available *ad libitum*. Animals housed together remained with their cage mate throughout the entirety of the experiment and were in the same experimental group to avoid coprophagic cross-colonization. For all experiments, animals were randomized into the specified groups using an online random number generator.

3.2.2 Left C2 Hemisection (LC2Hx)

3.2.2.1 University of Kentucky

Adult female Sprague Dawley rats were anesthetized with isoflurane gas. Once an appropriate plane of anesthesia was met, animals were prepared for surgery by shaving and sterilizing the surgical site with alternating 70% ethanol and betadine swabs. Ophthalmic ointment was applied to the eyes to prevent drying throughout the procedure. While in the

prone position, an incision was made between the ears and extend approximately two inches caudally. The underlying musculature was bluntly dissected and retracted to expose the process of the C2 lamina. The final layer of musculature was then cut and cleared away from the bone so that the intervertebral space between C1 and C2 could be visualized. A C2 laminectomy was performed by cutting the lamina in this space on the left and right sides of the C2 spinous process and extending caudally until the dorsal aspect of the C2 vertebrae was removed and the spinal cord was exposed. Micro-scissors were used to perform a durotomy and a 27-gauge hypodermic needle was bent at a 45-degree angle and used to perform the left C2 hemisection (LC2Hx). Briefly, anatomical landmarks were used to determine midline at the C2 level at which needle was inserted through the spinal cord until the ventral aspect of bone was reached and then dragged laterally to the animal's left until completely severing the cord. Three passes were made to ensure complete disruption of pathways on the left side. Finally, all three layers of musculature previously dissected were sutured individually (3-0 absorbable suture) and the skin was closed with surgical staples. All animals received buprenorphine (0.05mg/kg; immediately and 12-hours post-surgery) and carprofen (5mg/kg; immediately, 12-, and 24-hours post-surgery) subcutaneously. Surgical animals were monitored twice daily for the four days post-injury with subcutaneous saline given as needed. Animals recovered for one week on a heated rack separated from naïve animals and remained on a standard 12-hour light/dark cycle with food and water accessible *ad libitum* prior to returning to standard housing. Welfare and weights were checked weekly throughout the entire experiment.

3.2.2.2 Drexel University

Adult female Sprague Dawley rats were anesthetized with Ketamine (100 mg/kg) and Xylazine (10 mg/kg). Once an appropriate plane of anesthesia was met, animals were prepared for surgery by shaving and sterilizing the surgical site with alternating 70% ethanol and betadine swabs. Ophthalmic ointment was applied to the eyes to prevent drying throughout the procedure. While in the prone position, an incision was made with a #15 scalpel between the ears and extend approximately two inches caudally. The underlying musculature was bluntly dissected and retracted to expose the process of the C2 lamina. The final layer of musculature was then cut and cleared away from the bone so that the intervertebral space between C1 and C2 could be visualized. A C2 laminectomy was performed by cutting off the C2 spinous process and then removing the lamina with a rongeur tool, beginning caudally and extending rostrally until C2 until the dorsal aspect of the C2 vertebrae was removed, and the spinal cord was exposed. A #11 scalpel was used to perform a durotomy. The left C2 dorsal root was then visualized and the #11 scalpel was used to perform the left C2 hemisection (LC2Hx) just caudal to the left C2 dorsal root. Briefly, anatomical landmarks were used to determine the midline at the C2 level at which scalpel was inserted through the spinal cord until the ventral aspect of bone was reached and then dragged laterally to the animal's left until completely severing the cord. Three passes were made to ensure complete disruption of pathways on the left side. Finally, the dura was sutured and all three layers of musculature previously dissected were sutured (4-0 absorbable suture) and the skin was closed with surgical staples. All animals received 0.1 ml anti-sedean, 5 ml lactated ringers, 0.2 ml Extended-release buprenorphine subcutaneously. Surgical animals were monitored thrice daily for the four days post-injury

and given 1 ml nutritional at each check. Additionally, 5 ml of lactated ringers was administered subcutaneously twice daily. Animals recovered for one week separated from naïve animals and remained on a standard 12-hour light/dark cycle with food and water accessible *ad libitum* prior to returning to standard housing. Welfare and weights were checked weekly throughout the entire experiment.

3.2.3 16S rRNA Sequencing

Fecal samples were collected from study animals using an aseptic technique pre- and at various time points post-LC2Hx in order to assess the gut microbiome. Samples were immediately stored at -80°C until all samples were collected for further processing. Samples from Drexel University were mailed overnight on dry ice to the University of Kentucky after all samples were collected for further processing. The bacterial 16S rRNA gene was then isolated from the fecal samples using DNeasy PowerSoil Pro Kit (Ref # 47016; Lot # 17203302). DNA from each sample was diluted to a concentration ranging between 1-50ng/μL and mailed to Argonne National Laboratory for sequencing.

Read processing: 16SV4 was amplified using 515F-806R primers. Fastq files were demultiplexed using qiime2 demux emp-paired function. Samples from rats that were 10.5 months old (total of 91). The naïve group was removed due to the small size, which will never be statistically significant, and it added noise to the analysis. Raw data were processed with qiime2. Briefly, reads were denoised with dada trimming nucleotides based on quality plots (trim reads when the average quality <30- see code for details). Unique reads were clustered to 99% identity using the silva-138-99-seqs-515-806 database

(ASV99% or OTUs). Chimeras were removed using `vsearch uchime-denovo` function. Samples had an average of 29,245 reads (Table 1). ASVs with <50 reads total abundance were removed since they were present in <2 samples and will not significantly contribute to the analysis. ASVs were classified using the feature-classifier `classify-sklearn` function with the `silva-138-99-515-806-nb-classifier`. When taxonomic classification was not available at lower levels, the immediately following taxonomic level classification was used. Filtered ASV 99% table (referred to as OTUs in the figures) was subsampled to analyze 15,000 reads per sample. Two samples with an unusually low number of reads were removed.

Read processing: OTU abundance matrix was analyzed using `vegan`, and `labdsv` packages in R. Principal coordinate analysis was performed on rarefied reads and log₁₀ normalized reads at the OTU and family taxonomic level. Simper analyses were performed to identify OTUs that explain most of the variation in the ordination space.

Statistical analysis: Statistical analysis of group separation in the ordination space was performed calling Permanova with the `Adonis` function in R. Mixed-effect time series statistical analysis of clusters and OTUs abundance was done using `prism`.

3.2.4 Sectioning and Staining

Following euthanasia at the designated times post-injury, the skull and spinal column were removed and drop-fixed in 4% paraformaldehyde (PFA) for 48 hours at 4°C. The brainstem and cervical spinal cord were then dissected from the skull and spinal column and placed in fresh 4% PFA for an additional 24 hours at 4° and then cryoprotected

in 30% sucrose at 4°C until sectioning. The injury was used as the epicenter to create three 4mm sections (brainstem, C1/2, and C3/4 levels). Tissue sections were then embedded in Optimal Cutting Temperature embedding media (OCT, Sakura Tissue-TEK) and cryosections were taken at 30µm (Leica cryostat) and placed directly onto gelatin-coated slides (Thermo Fischer Scientific) and stored at -20°C.

3.2.4.1 Cresyl Violet

Slides were placed in CitriSolv solution prior to serially rehydrating the tissue in decreasing concentrations of ethanol. Slides were then rinsed in distilled water, stained with 0.5% Cresyl Violet solution (Sigma Cat #C5042), rinsed in distilled water, dehydrated in the reverse order of ethanol concentrations used, and placed in CistroSolv. Coverslips were then applied using permount (Electron Microscopy Sciences Cat #17986-01). Slides were imaged on a Keyence BZ-X810 microscope (Keyence Corporation of America, Itasca, IL, USA) using bright field illumination at 2x.

3.3 Results

3.3.1 Institution-specific gut microbiome profiles following cervical SCI.

To assess the impact of cervical spinal cord injury on the gut microbiome at separate research institutions acutely and out to chronic time points, fecal samples were collected at pre- (-7 and 0 dpi) and post-injury (1, 3, 7, 14, 21, 28, and 84 dpi). 16S rRNA sequencing analysis of these fecal samples revealed a rapid and robust increase in the

Firmicutes to Bacteroidetes ratio (F:B) one-day post-injury in animals from the University of Kentucky. At the phylum level, the Firmicutes and Bacteroidetes bacteria constitute 90% of the gut microbiome phylogenetic composition^{170,207}. An increase in the F:B ratio has been used previously to describe gut dysbiosis, or an imbalance of pathogenic and beneficial bacteria⁹. Interestingly, this increase was not observed in animals from Drexel University, as the F:B ratio remained relatively unchanged at all time points (Figure 3.1b).

Additionally, the relative abundance of bacteria at the phylum level revealed several differences between the two research institutions. Samples from the University of Kentucky also appeared to have elevated levels of Actinobacteria pre-injury (0 dpi) compared to Drexel University (Figure 3.1a). Further, the relative abundance of Actinobacteria increased in animals from the University of Kentucky at 1, 14, 21, 28, and 84 dpi. While the Firmicutes and Bacteroidetes make up 90% of the relative abundance of the gut microbiome, Proteobacteria, Verrucomicrobiota, and Actinobacteria make up the remaining 10%¹⁷⁰. Although Actinobacteria represent a small percentage of the gut microbiome, this group of bacteria has been associated with the maintenance of gut health, and species such as Bifidobacteria and Lactobacilli are commonly used in probiotics to promote gut health²³⁶. The increase in Actinobacteria may have been a compensatory mechanism due to the decrease in the F:B ratio observed in animals from the University of Kentucky.

Drexel University appeared to have a higher relative abundance of Verrucomicrobiota, especially at the pre-injury (0 dpi) and 3 dpi time points (Figure 3.1a). Verrucomicrobiota are mucin-degrading bacteria that promote gut health and are involved in glucose homeostasis²³⁷. The increased levels of Verrucomicrobiota pre-injury in

animals from Drexel University may have allowed for a healthier gut barrier that aided in preventing the increase in the F:B ratio observed in animals from the University of Kentucky.

The beta diversity, or the difference between samples, between the two institutions was distinctly separated at 0 (pre-injury), 3, and 84 dpi. Interestingly, although separate, the two groups followed a similar shift at 3 dpi before returning to their respective pre-injury levels by 84 dpi (Figure 3.1c). While the bacterial communities may have differed between the institutions, the injury may have caused a similar shift in the overall composition of the gut microbiome. Overall, these differences suggest that the environment plays a prominent role in the constitution of the gut microbiome before and after SCI.

3.3.2 Inter-institutional variables impact the gut microbiome.

Previous work from our lab has established that surgical sham and drug control naïve animals did not exhibit an increase in the F:B ratio observed in LC2Hx animals (Figure 2.1c from Section 2.3.1). To confirm that all animals in this study were injured with the same level of severity, we examined the extent of the injury in the cervical spinal cord. Cresyl violet stained histological sections revealed no significant difference in the amount of spared tissue, indicating the injury severity was similar between institutions (Figures 3.2a and b; unpaired t-test $p = 0.3469$). Importantly, the spinal cord histology did reveal a discrepancy in the level of injury. Drexel University appears to be injured at cervical level 3 (C3), whereas the University of Kentucky injuries are at cervical level 2 (C2) (Figures 3.2a and c).

To further investigate the variables that potentially influence the institution-specific gut microbiomes, we tracked institutional differences. Table 3.1 summarizes the differences in housing, surgical procedure, and post-surgical care. Of note, the bedding, food, and water type are all unique to each institution which could account for the differences in the gut microbiome observed pre-injury. Additionally, differences were also observed throughout the surgical procedure, including anesthetic drugs, post-surgical drugs, and post-surgical food and bedding. These environmental differences likely contribute to the distinct gut microbiome profiles observed pre- and post-SCI.

3.4 Discussion

SCI is a life-changing, devastating injury that is made especially difficult to study due to its heterogeneous nature. While research efforts have developed promising treatment strategies, translation of these findings to clinical use has proven to be difficult. Understanding potential barriers and factors that prevent this translation is critical. Here, we investigate how environmental differences influence the gut microbiome following the widely used LC2Hx model of injury. The environment can strongly influence the gut microbiome²³⁸. Here, for the first time, we demonstrate that environmental differences influencing the composition of the gut microbiome also produce distinctive microbiome profiles following SCI.

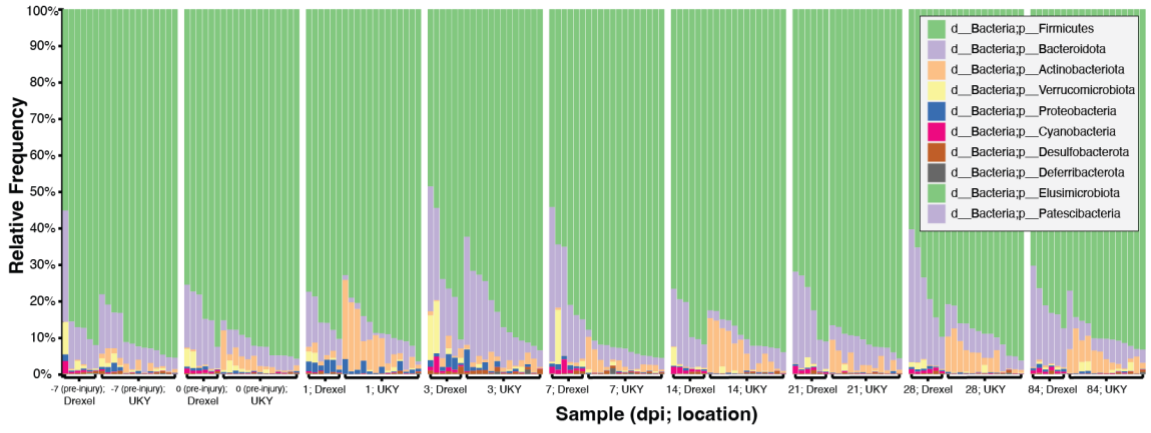
We observed an increase in the F:B ratio, an indication of gut dysbiosis, in animals from the University of Kentucky that was not observed in animals that received the same injury at Drexel University. Additionally, each institution displayed unique gut

microbiome profiles before and after injury. These findings reveal a need for further investigation of microbial compositions that are best suited for recovery. This could allow for novel therapeutic targets that can enhance functional restoration following SCI.

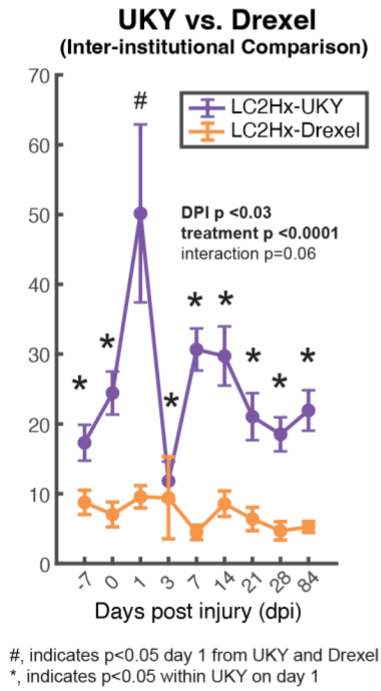
While the injury in these studies was determined to be varied, the overall damage to the spinal cord was comparable. Previously, it has been demonstrated that an incomplete lesion can produce the same effects as a complete LC2Hx ²³⁹. Additionally, the level of injury was found to be an independent factor of gut dysbiosis in patients with SCI ⁶². This study evaluated paraplegic versus tetraplegic patients and not specific levels of injury. It is unlikely that a C2 versus a C3 level with similar injury severity would significantly alter the gut microbiome in different ways. The cervical level does not have direct innervation pathways to the gut. The injury to the cervical spinal cord and the subsequent overall impairments to the animal as a whole may be the cause of the observed microbiome changes. Previous work from our lab has determined that drug control (naive animals that received all surgical drugs but no injury) and surgical sham animals did not exhibit gut dysbiosis observed in animals that received a LC2Hx (Section 2.3.1, Figure 2.2) Therefore, environmental factors listed in Table 3.1 are more likely the cause for the differences observed. While the hemisection model of SCI is easily reproducible, the variables around the injury must be considered. Several aspects of the surgical procedure and animal care that contribute to differences in the gut microbiome could not be matched at each institution due to existing animal facilities and laboratory protocols. The variances observed between two institutions using the same injury model highlight the importance of variables that can impact outcomes and potential recovery. These differences observed in the preclinical setting highlight potential targets that must be considered when studying

SCI. Further examining and understanding the role of these differences and how they impact the gut microbiome, overall health, and recovery potential following SCI may allow for improved outcomes and translation of experimental therapeutics to clinical use.

a



b



c

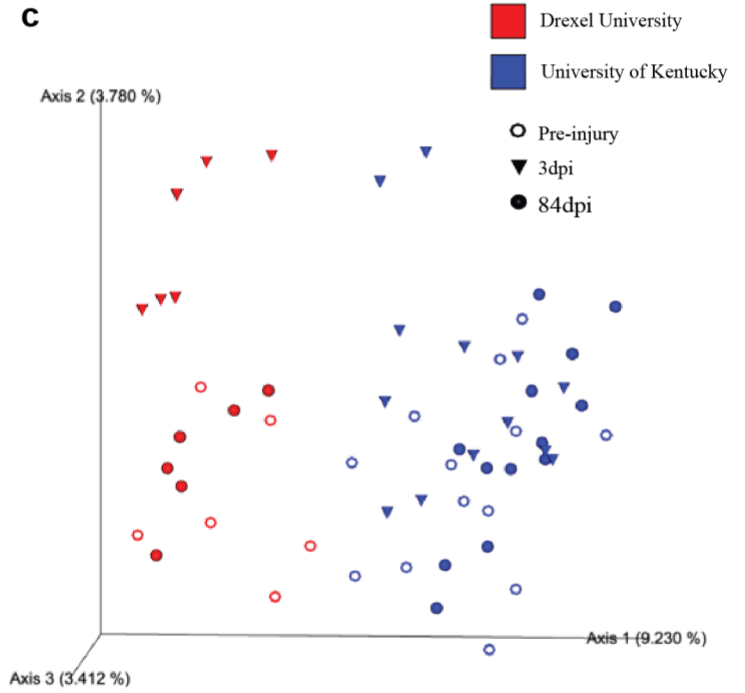
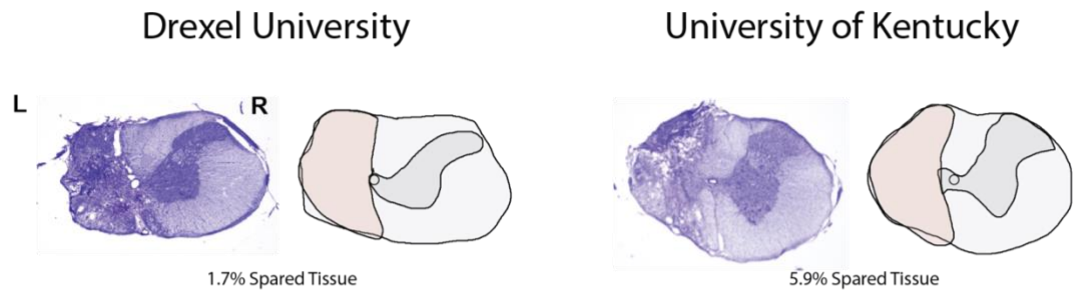


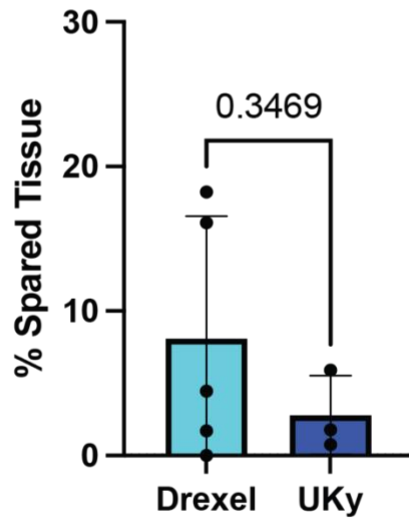
Figure 3.1 The gut microbiome has distinct profiles between institutions and following cervical spinal cord injury.

a, Comparison of the relative abundance of bacteria that comprise the gut microbiome at the phylum level between animals that received a cervical spinal cord injury at Drexel University or the University of Kentucky pre-injury (-7 and 0 dpi) and post-injury (1, 3, 7, 14, 21, 28, 84 dpi). **b**, 16S rRNA sequencing data revealed a significant increase in the Firmicutes:Bacteroidetes ratio at 1 dpi in the University of Kentucky group compared to all other time points and at 1 dpi compared to Drexel University (Two-way RM ANOVA $p < 0.0011$.) **c**, Bray Curtis dissimilarity measurement revealed that Drexel University (red) and the University of Kentucky (blue) cervical SCI animals were distinctly different pre-injury (rings) and at 3 (filled triangles) and 84 dpi (filled rings), although these differences followed a similar trend post-injury. Bars represent mean \pm SD. Bolded text indicates a p -value < 0.05 .

a



b



c

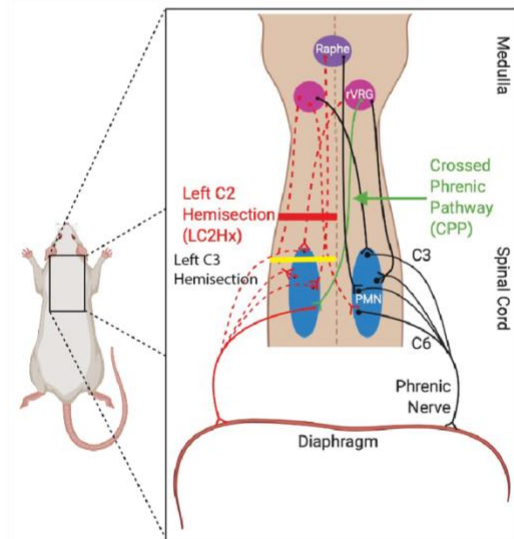


Figure 3.2 Interinstitutional confirmation of injury

a, Representative images of cresyl violet staining at the level of injury in Drexel University and University of Kentucky animals 84 dpi. Confirmation of injury revealed a slight difference in the level of injury between institutions. While the University of Kentucky performed the hemisection at the spinal level C2, it appears that Drexel University performed the hemisection at the spinal level C3. **b**, Quantification of spared tissue at the level of injury indicated no significant differences between injured groups, demonstrating that all animals were equally injured (Drexel University = light blue, University of Kentucky = dark blue; unpaired t-test $p = 0.3469$). **c**, Schematic representation of the level of injury performed by the University of Kentucky (red = LC2Hx) and Drexel University (yellow = LC2Hx). Bars represent mean \pm SD.

Table 3.1. Interinstitutional differences using the LC2Hx model.

Variables	University of Kentucky	Drexel University
Animal - strain	Sprague-dawley	Sprague-dawley
Animal - sex	Female	Female
Animal - age	Retired breeders (9 months to 1 year)	Retired breeders (9 months to 1 year)
Animal - company	Envigo	Envigo
Time of arrival to time of surgery	7 days	7 days
Surgery	LC2Hx	LC2/3Hx
Housing (animals/cage)	double	triple
Pre-injury bedding	P.J. Murphy Coarse SaniChip	Bed-o'cobs 1/4"
Post-injury bedding	Rolled pellets	Bed-o'cobs 1/4"
Duration on post-injury bedding	1 week	n/a same bedding
Staple removal	10 dpi + isoflurane	14 dpi (no isoflurane)
Chew bars	wooden chew bars	Manzanita sticks
Enrichment	enviro-dry (when on regular bedding)	Kraft paper tubes
Anesthesia	Isoflurane	Xylazine [20mg/ml] SQ; Ketamine [100mg/ml] IP
Post-surgical drugs	Carprofen [1.5 mg/ml] 1ml x3; Buprenorphine [0.3mg/mL] 1ml x2; Sterile saline 5ml + prn	Buprenorphine ER [0.3mg/ml] 0.2 ml; Antisedan 0.1 ml; Lactated ringers 5 ml
Antibiotics	Topical anitibiotic ointment (TAO) and newskin prn	Topical anitibiotic ointment (TAO) prn
Food	2018 Teklad Global 18% Protein Rodent Diet	PicoLab Rodet Diet 20
Water	Reverse osmosis (RO) water	Tap
Aftercare	newskin prn	
Light cycle	12:12	12:12
Nutrical	if not ambulating	yes, post-surgery
Treats	fruit loops	plain cheerios

CHAPTER 4. DISCUSSION

SCI is a devastating, life-altering condition that not only has acute repercussions but lifelong consequences. While many factors can influence the recovery process, the impact of the gut microbiome has yet to be fully explored. In recent years, the influence of the gut microbiome has been associated with a range of diseases and disorders as the role of the gut-CNS-axis has become more apparent ^{6,172,182,188,193,240-242}. Bi-directional relationships between the gut microbiome and other organ systems are also becoming more evident, further emphasizing the importance of the gut microbiome to overall health and well-being ^{193,243-246}.

Regarding SCI, previous studies have explored the treatment of SCI-induced gut dysbiosis and have revealed improved locomotor recovery of the hindlimbs, as well as improved emotional affect ^{7,67}. We aimed to build off these studies and investigate the role of the gut microbiome in the recovery of respiration following LC2Hx. While there is no direct innervation of the gut from the cervical level of the spinal cord, cervical SCI can disrupt the autonomic nervous system and cause psychological and physical stress. Each of these complications can impact the gut microbiome. In turn, the gut microbiome can influence systemic inflammation and serotonin levels ^{179,182}.

As described in section 1.3.3, inflammation is detrimental to respiratory plasticity ²²⁷. The gastrointestinal system is the first line of defense from our external environment as we ingest nourishment and sustenance. The microbiota within the gut play an essential role in maintaining the intestinal barrier. Dysbiosis can compromise the tight junction proteins within this barrier, leading to gut permeability, bacterial translocation, and, ultimately, systemic inflammation ²⁴⁷.

Additionally, serotonin is necessary and sufficient to induce this form of plasticity¹⁰². Approximately 95% of the body's serotonin is located in the gut²⁴⁸. Additionally, tryptophan, the precursor to serotonin, is an essential amino acid that must be acquired through the diet. Studies in humans with irritable bowel syndrome and emotional distress have demonstrated the gut microbiome may impact the regulation of serotonin¹⁸⁵.

We hypothesized that the well-established LC2Hx model used to study the recovery of breathing would induce gut dysbiosis. Additionally, this dysbiosis would impair respiratory recovery through mechanisms of increased systemic inflammation and reduced serotonin availability (Figure 4.1). These experiments were vital in expanding our knowledge and understanding of the gut microbiome in connection with SCI as well as determining possible mechanisms for improving functional recovery after injury.

4.1 Major Finding #1: Targeting gut dysbiosis following SCI improves functional and pathological outcomes.

We reveal for the first time that LC2Hx induces gut dysbiosis immediately after the injury that was not observed in surgical sham or drug control animals. This finding was demonstrated by the increase in the Firmicutes-to-Bacteroidetes (F:B) ratio at 1 dpi (Figure 2.2 b). Although this was a rapid, acute occurrence, this change in the gut microbiome may have had lasting effects as gut pathology and metabolic dysregulation were evident at 14 dpi. These findings demonstrate the critical role of the gut microbiome in maintaining the intestinal barrier.

To improve this SCI-induced gut dysbiosis, animals were treated with an FMT or probiotics. FMT-treated animals exhibited limited respiratory recovery potential and regenerative ability of axons, although gut pathology and systemic inflammation were marginally improved (Figures 2.4, 2.5, 2.9, 2.10). Previous studies examining the effect of FMT treatment following cervical SCI also did not observe an improvement in motor function⁶⁷. Alternatively, probiotic treatment following SCI at a lower thoracic level resulted in improved locomotor function of the hindlimbs⁷. Based on these findings and because probiotics have a more consistent composition than FMT, we transitioned to the use of probiotics. Probiotic treatment resulted in improved respiratory recovery, demonstrated by an increase in respiratory rate that allowed for compensation in minute ventilation. Additionally, there was an increased ipsilateral hemidiaphragm amplitude in low-dose probiotic-treated animals (Figure 2.4).

To determine potential mechanisms for this recovery, immunohistology studies were performed and revealed that there was no increase in serotonin labeling at the level of the phrenic motor nucleus (Figure 2.11). Examination of the brainstem serotonin levels may be more informative as frequency is controlled at this level. Additionally, the probiotic treatment improved gut pathology and evidenced by an increase in villi length and a reduction of the Chiu/Park score (Figure 2.8). Potential effects for this improvement can be demonstrated by the decrease in systemic proinflammatory cytokine levels (Figure 2.9). In turn, this reduced inflammation may have allowed for the regeneration and sprouting of axons. TNF-alpha plays an important role in synaptic plasticity through the upregulation of AMPA receptors and strengthening of excitatory synapse^{249,250}. However, it also is historically considered pro-inflammatory with aberrant production associated with sepsis

²⁵¹. Maintaining levels of TNF-alpha following SCI, as demonstrated in figure 2.9, may allow for improved recovery. Additionally, the proinflammatory cytokine IL-6 is elevated in cerebrospinal fluid in a severity-dependent fashion following SCI ³⁵. We demonstrate that treating gut dysbiosis through FMT following cervical SCI reduces IL-6 levels in the serum compared to vehicle-treated animals. Finally, treatment of the SCI-induced gut dysbiosis with probiotics improved the regenerative capacity of DRGs, marked by the increased number of projections from the soma (Figure 2.10).

Histological assessments of the injury were evaluated to confirm that these improvements were due to treating the gut microbiome rather than variations in injury severity or level (Figure 2.6). Moreover, activity chamber outcomes revealed there were no differences in locomotion in any group (Figure 2.7). Taken together, these outcomes demonstrate that our findings of improved respiratory function are a result of treating gut dysbiosis following SCI rather than variations in injury severity. Overall, our findings demonstrate that treatment of the gut microbiome with probiotics may play a significant role in the functional recovery of respiration following SCI.

4.2 Major finding #2: Cervical SCI induces distinct gut microbiome profiles at separate institutions and potentially influences outcomes.

We examined the gut microbiome composition of animals receiving a LC2Hx at two separate institutions. 16S rRNA sequencing revealed differences between the microbiomes of the two institutions when observing the relative abundance of microbes at the phylum level. Actinobacteria was more abundant in fecal samples from the University of Kentucky compared to Drexel University at almost all time points. Actinobacteria play an important

role in gut barrier homeostasis and provide enzymes necessary for the degradation and metabolism of substances introduced through the diet ²³⁶. Conversely, Drexel University had a higher relative abundance of Verrucomicrobiota pre-injury (0 dpi) and acutely post-injury (3dpi) (Figure 3.1a). The phylum Verrucomicrobiota is thought to promote gut health as it is a mucin-degrading bacterial community that maintains homeostasis of mucin levels in the intestines ²³⁷.

Additionally, a significant increase in the Firmicutes:Bacterioidetes (F:B) ratio at 1 dpi in animals from the University of Kentucky but not Drexel University (Figure 3.1 b). Interestingly, analysis of beta diversity revealed that the two institutions remained distinctly different, although followed a similar dynamic pattern by shifting at 3 dpi but returning to pre-injury levels by 84 dpi (Figure 3.1 c).

While injury severity was similar between animals, the level of injury slightly differed, with animals from Drexel University receiving a slightly lower hemisection at C3 rather than C2 (Figure 3.2a - c). This discrepancy may influence the differences observed in the gut microbiome profiles, although the overall connections to gut from the cervical region of the spinal cord do not significantly differ. Previous studies at examining a cervical level 5 contusion demonstrated similar changes in the gut microbiome as the LC2Hx at the University of Kentucky ⁶⁷. Therefore, one cervical spinal level variation of injury is not believed to contribute to robust differences in the gut microbiome. Several other factors between the institutions may play a role in these observed differences. Due to pre-existing animal facilities and laboratory protocols, several variables were not able to be matched between the institutions. These factors are detailed in Table 3.1 and highlight a selection

of differences that can influence the gut microbiome and may account for variability in results between labs.

4.3 Methodological Considerations and Limitations

To fully analyze our results, we must consider potential limitations to this work. Sex differences were not investigated throughout this work, as only female rats were examined. Previous studies on the gut microbiome and SCI, separately, have determined that sex can influence the differentiation of outcomes^{3,10}. Additionally, retired breeders were used in the initial and FMT studies. The aging gut microbiome has been shown to drive detrimental changes in the gut-brain axis²⁵². To mitigate this variable in our subsequent probiotic studies, we used young, healthy animals (180 – 220 grams, approximately three months old). Our FMT study involved the transfer between young, healthy animals to older animals. This was an important experimental design element as the average age of persons with an SCI has increased from 29 years in the 1970s to 43 years in 2015². However, overall results revealed marginal improvements. Moreover, in the preparation of the FMT, fecal samples were pooled from co-housed young, healthy donor animals⁶⁷. Transplantation from a single donor and not pooling samples may have produced more significant results, as evidenced by previous studies^{174,253}. Finally, due to the length of time of the LC2Hx surgical procedure, several cohorts were needed to fulfill the number of animals needed for each group. Time of year, location, shipping, and colony can all influence the gut microbiome. 16S rRNA studies may have been influenced by the use of separate cohorts. Therefore, they were examined separately prior to combining. Overall,

numerous factors can influence the gut microbiome. While controlling for specific and relevant variables to a study is necessary, controlling for all factors influencing the gut microbiome is nearly impossible and unrealistic for clinical translation purposes.

4.4 Future Directions

While the findings from this dissertation reveal the improvements in respiratory recovery following the treatment of SCI-induced gut dysbiosis, several questions remain unanswered. Future studies should further investigate potential mechanisms that mediate this recovery, including serotonin quantification at the level of the brainstem. Additionally, tryptophan, the precursor to serotonin, is an essential amino acid that must be acquired from the diet. As the gut houses 95% of the body's serotonin, depletion studies of tryptophan and serotonin from the gut could provide insight into the connection between the gut microbiome and respiratory recovery, as serotonin is necessary and sufficient to produce spinal respiratory plasticity^{102,254,255}. Recently, genetically engineered probiotics have been developed to modulate the gut microbiome and produce GABA in models of multiple sclerosis²⁵⁶. If gut levels of tryptophan and/or serotonin are found to modulate respiratory recovery, this advancement of genetically engineering probiotics could provide a novel therapeutic mechanism.

To further assess the link between gut dysbiosis and respiratory plasticity, FMT studies that take fecal samples from LC2Hx animals and transplant them to naïve animals could elucidate components of this relationship. Additionally, germ-free studies with animals void of microorganisms may also shed light on the role of the gut microbiome in the

recovery process following CNS trauma. Investigating respiratory recovery from germ-free animals, as well as germ-free animals that have had their gut microbiomes repopulated with an FMT from healthy versus LC2Hx animals could further elucidate the importance of the gut microbiome following neurotrauma. Interestingly, studies in germ-free mice have demonstrated that the gut microbiome regulates CNS microglia maturation and function ²⁵⁷. Dysregulation of microglia due to gut dysbiosis may be a mechanism of impaired recovery and poorer efficacy of therapeutics that are administered at acute time points post-SCI.

While we observed improvement in respiratory recovery following SCI, examination of the diaphragm muscle following treatment of gut dysbiosis may elucidate potential mechanisms for this observed recovery. Previous studies have determined that gut dysbiosis impairs skeletal muscle adaptation to exercise ²⁴⁴. As the diaphragm is a skeletal muscle and the main muscle used for inspiration, investigating how the gut microbiome influences its function, especially under conditions to increase the respiratory drive for recovery, may reveal critical mechanisms for optimal muscle health and recovery.

In our studies, we used probiotics, or beneficial bacteria often found in foods such as yogurt, to treat gut dysbiosis. While we observed improved respiratory recovery and gut pathology with this treatment following SCI, prophylactic measures to prevent the severity of gut dysbiosis may allow for improved recovery. Administration of prebiotics or compounds that stimulate the growth of beneficial bacteria in the gut, prior to traumatic brain injury revealed improved outcomes ²⁵⁸. While it is impossible to predict the occurrence of neurotrauma, these findings highlight the importance of maintaining a healthy gut microbiome prior to injury. This could be especially critical for those at high

risk for neurotrauma, such as military personnel and athletes. Pretreating with prebiotics may prevent the gut dysbiosis we observed following SCI and may mitigate the reduce the need for probiotic treatment after the injury.

Finally, further exploration of inter-institutional differences, including the role of the gut microbiome, could reveal significant differences that account for varying outcomes between laboratories. This could not only lead to a calling for standardization between laboratories but may also elucidate key differences that can be beneficial for successful clinical translation.

4.5 Conclusion

The work described throughout this dissertation is the first to investigate the connection between gut-CNS-axis and respiratory recovery following SCI. Overall, our data demonstrate that the gut microbiome is an important mediator in the recovery process following SCI. These findings may have profound implications clinically, as gastrointestinal complications are a persistent problem and decrease the quality of life for SCI individuals. Therapeutically targeting the gut microbiome following SCI may improve pathology and overall function of the gut and, in turn, improve the recovery process and overall health by reducing systemic inflammation. This allows for a more permissive environment for axonal outgrowth and, ultimately, recovery potential. Additionally, many factors can influence the gut microbiome and potential outcomes following SCI. We demonstrate that separate institutions using the same SCI model produce distinctive gut microbiome profiles following injury. Ultimately, these diverse

profiles could impact recovery by promoting pro- or anti-inflammatory states. Taken together, the major findings elucidated throughout this work highlight the importance of the gut microbiome in the recovery process and provide a novel therapeutic target to enhance functional outcomes following SCI.

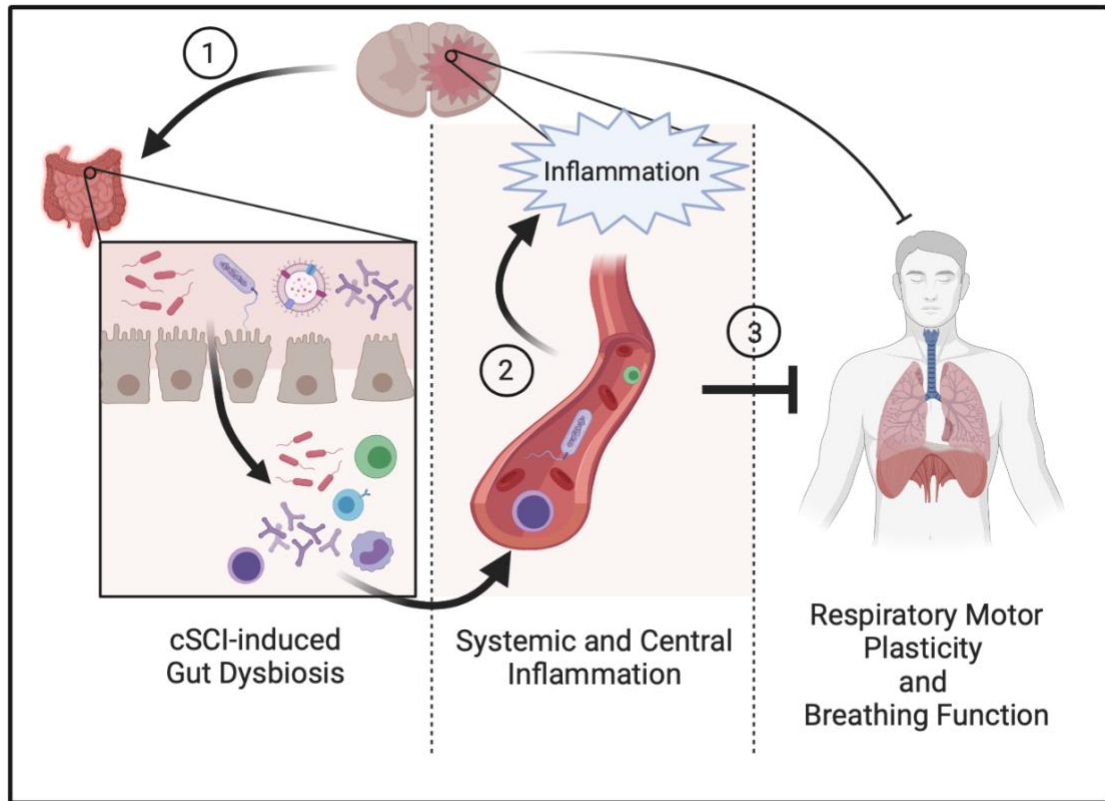


Figure 4.1 Schematic summary of the proposed mechanism of gut dysbiosis impeding the functional recovery of breathing.

1) Cervical SCI induces gut dysbiosis. 2) This dysbiosis compromises the tight junction proteins of the gut wall leading to bacterial translocation and ultimately exacerbating systemic and central inflammation. 3) Inflammation impedes respiratory motor plasticity and functional recovery of breathing.

APPENDIX

List of Abbreviations

ahSC = autologous human Schwann cells

AIH = Acute intermittent hypoxia

ANS = Autonomic nervous system

ASIA = American Spinal Injury Association

AIS = ASIA Impairment Scale

APOE = Apolipoprotein E

BDNF = Brain-derived neurotrophic factor

ChABC = Chondroitinase ABC

CNS = Central nervous system

CSF = Cerebral spinal fluid

CSPG = Chondroitin sulfate proteoglycan

CPP = Crossed phrenic pathway

ECM = Extracellular matrix

FES = Functional electrical stimulation

GI = Gastrointestinal

GALT = Gut-associated lymphoid tissue

GFAP = glial fibrillary acidic protein

HMGB1 = High-Motility Group Box 1

IL = Interleukin

LC2Hx = Left cervical level 2 hemisection

LTF = Long-term facilitation

MAP = Mean arterial pressure

MCP-1 = Monocyte chemotactic protein

MRI = Magnetic resonance imaging

NOMI = Nonocclusive mesenteric ischemia

NTS = Nucleus tractus solitarius

OPC = Oligodendrocyte precursor cells

PMN = Phrenic motor nucleus

PNN = Perineuronal net

preBötC = pre-Bötzinger Complex

rVRG = Rostral ventral respiratory group

SCI = Spinal cord injury

TrkB = tropomyosin receptor kinase B

REFERENCES

- 1 Organization, W. H. *Spinal Cord Injury*, <<https://www.who.int/news-room/fact-sheets/detail/spinal-cord-injury>> (2013).
- 2 National Spinal Cord Injury Statistical Center. *Traumatic Spinal Cord Injury Facts and Figures at a Glance*, <<https://www.nscisc.uab.edu/public/Facts%20and%20Figures%202022%20-%20English%20Final.pdf>> (2022).
- 3 Doperalski, N. J., Sandhu, M. S., Bavis, R. W., Reier, P. J. & Fuller, D. D. Ventilation and phrenic output following high cervical spinal hemisection in male vs. female rats. *Respir Physiol Neurobiol* **162**, 160-167 (2008). <https://doi.org/10.1016/j.resp.2008.06.005>
- 4 Omura, T. *et al.* Robust Axonal Regeneration Occurs in the Injured CAST/Ei Mouse CNS. *Neuron* **86**, 1215-1227 (2015). <https://doi.org/10.1016/j.neuron.2015.05.005>
- 5 Strattan, L. E. *et al.* Novel Influences of Sex and APOE Genotype on Spinal Plasticity and Recovery of Function after Spinal Cord Injury. *eNeuro* **8** (2021). <https://doi.org/10.1523/ENEURO.0464-20.2021>
- 6 Wang, Y. & Kasper, L. H. The role of microbiome in central nervous system disorders. *Brain Behav Immun* **38**, 1-12 (2014). <https://doi.org/10.1016/j.bbi.2013.12.015>
- 7 Kigerl, K. A. *et al.* Gut dysbiosis impairs recovery after spinal cord injury. *J Exp Med* **213**, 2603-2620 (2016). <https://doi.org/10.1084/jem.20151345>
- 8 Dinan, T. G. & Cryan, J. F. The Microbiome-Gut-Brain Axis in Health and Disease. *Gastroenterol Clin North Am* **46**, 77-89 (2017). <https://doi.org/10.1016/j.gtc.2016.09.007>
- 9 Spychala, M. S. *et al.* Age-related changes in the gut microbiota influence systemic inflammation and stroke outcome. *Ann Neurol* **84**, 23-36 (2018). <https://doi.org/10.1002/ana.25250>
- 10 Sisk-Hackworth, L., Kelley, S. T. & Thackray, V. G. Sex, puberty, and the gut microbiome. *Reproduction* **165**, R61-R74 (2023). <https://doi.org/10.1530/REP-22-0303>
- 11 Rowland, J. W., Hawryluk, G. W., Kwon, B. & Fehlings, M. G. Current status of acute spinal cord injury pathophysiology and emerging therapies: promise on the horizon. *Neurosurg Focus* **25**, E2 (2008). <https://doi.org/10.3171/FOC.2008.25.11.E2>
- 12 Tator, C. H. & Fehlings, M. G. Review of the secondary injury theory of acute spinal cord trauma with emphasis on vascular mechanisms. *J Neurosurg* **75**, 15-26 (1991). <https://doi.org/10.3171/jns.1991.75.1.0015>
- 13 Alizadeh, A., Dyck, S. M. & Karimi-Abdolrezaee, S. Traumatic Spinal Cord Injury: An Overview of Pathophysiology, Models and Acute Injury Mechanisms. *Front Neurol* **10**, 282 (2019). <https://doi.org/10.3389/fneur.2019.00282>
- 14 Allen, A. R. Surgery of experimental lesion of spinal cord equivalent to crush injury of fracture dislocation of spinal column. *JAMA* **57:878–80** (1911).

- 15 Jones, T. B., McDaniel, E. E. & Popovich, P. G. Inflammatory-mediated injury and repair in the traumatically injured spinal cord. *Curr Pharm Des* **11**, 1223-1236 (2005). <https://doi.org/10.2174/1381612053507468>
- 16 Fitch, M. T. & Silver, J. CNS injury, glial scars, and inflammation: Inhibitory extracellular matrices and regeneration failure. *Exp Neurol* **209**, 294-301 (2008). <https://doi.org/10.1016/j.expneurol.2007.05.014>
- 17 Jones, T. B., Hart, R. P. & Popovich, P. G. Molecular control of physiological and pathological T-cell recruitment after mouse spinal cord injury. *J Neurosci* **25**, 6576-6583 (2005). <https://doi.org/10.1523/JNEUROSCI.0305-05.2005>
- 18 Beck, K. D. *et al.* Quantitative analysis of cellular inflammation after traumatic spinal cord injury: evidence for a multiphasic inflammatory response in the acute to chronic environment. *Brain* **133**, 433-447 (2010). <https://doi.org/10.1093/brain/awp322>
- 19 Kigerl, K. A. *et al.* Identification of two distinct macrophage subsets with divergent effects causing either neurotoxicity or regeneration in the injured mouse spinal cord. *J Neurosci* **29**, 13435-13444 (2009). <https://doi.org/10.1523/JNEUROSCI.3257-09.2009>
- 20 Kroner, A. *et al.* TNF and increased intracellular iron alter macrophage polarization to a detrimental M1 phenotype in the injured spinal cord. *Neuron* **83**, 1098-1116 (2014). <https://doi.org/10.1016/j.neuron.2014.07.027>
- 21 Morganti, J. M., Riparip, L. K. & Rosi, S. Call Off the Dog(ma): M1/M2 Polarization Is Concurrent following Traumatic Brain Injury. *PLoS One* **11**, e0148001 (2016). <https://doi.org/10.1371/journal.pone.0148001>
- 22 Popovich, P. G., Stuckman, S., Gienapp, I. E. & Whitacre, C. C. Alterations in immune cell phenotype and function after experimental spinal cord injury. *J Neurotrauma* **18**, 957-966 (2001). <https://doi.org/10.1089/089771501750451866>
- 23 Donnelly, D. J. & Popovich, P. G. Inflammation and its role in neuroprotection, axonal regeneration and functional recovery after spinal cord injury. *Exp Neurol* **209**, 378-388 (2008). <https://doi.org/10.1016/j.expneurol.2007.06.009>
- 24 Silver, J. The glial scar is more than just astrocytes. *Exp Neurol* **286**, 147-149 (2016). <https://doi.org/10.1016/j.expneurol.2016.06.018>
- 25 Adams, K. L. & Gallo, V. The diversity and disparity of the glial scar. *Nat Neurosci* **21**, 9-15 (2018). <https://doi.org/10.1038/s41593-017-0033-9>
- 26 Tran, A. P., Warren, P. M. & Silver, J. The Biology of Regeneration Failure and Success After Spinal Cord Injury. *Physiol Rev* **98**, 881-917 (2018). <https://doi.org/10.1152/physrev.00017.2017>
- 27 Zhu, Y., Soderblom, C., Trojanowsky, M., Lee, D. H. & Lee, J. K. Fibronectin Matrix Assembly after Spinal Cord Injury. *J Neurotrauma* **32**, 1158-1167 (2015). <https://doi.org/10.1089/neu.2014.3703>
- 28 Hynds, D. L. & Snow, D. M. Neurite outgrowth inhibition by chondroitin sulfate proteoglycan: stalling/stopping exceeds turning in human neuroblastoma growth cones. *Exp Neurol* **160**, 244-255 (1999). <https://doi.org/10.1006/exnr.1999.7212>
- 29 Bradbury, E. J. *et al.* Chondroitinase ABC promotes functional recovery after spinal cord injury. *Nature* **416**, 636-640 (2002). <https://doi.org/10.1038/416636a>

- 30 Alilain, W. J., Horn, K. P., Hu, H., Dick, T. E. & Silver, J. Functional regeneration of respiratory pathways after spinal cord injury. *Nature* **475**, 196-200 (2011). <https://doi.org/10.1038/nature10199>
- 31 Society, A. S. I. A. I. S. C.
- 32 Maynard, F. M., Jr. *et al.* International Standards for Neurological and Functional Classification of Spinal Cord Injury. American Spinal Injury Association. *Spinal Cord* **35**, 266-274 (1997). <https://doi.org/10.1038/sj.sc.3100432>
- 33 Hales, M., Biros, E. & Reznik, J. E. Reliability and Validity of the Sensory Component of the International Standards for Neurological Classification of Spinal Cord Injury (ISNCSCI): A Systematic Review. *Top Spinal Cord Inj Rehabil* **21**, 241-249 (2015). <https://doi.org/10.1310/sci2103-241>
- 34 Tigchelaar, S. *et al.* MicroRNA Biomarkers in Cerebrospinal Fluid and Serum Reflect Injury Severity in Human Acute Traumatic Spinal Cord Injury. *J Neurotrauma* **36**, 2358-2371 (2019). <https://doi.org/10.1089/neu.2018.6256>
- 35 Kwon, B. K. *et al.* Cerebrospinal fluid inflammatory cytokines and biomarkers of injury severity in acute human spinal cord injury. *J Neurotrauma* **27**, 669-682 (2010). <https://doi.org/10.1089/neu.2009.1080>
- 36 Kwon, B. K. *et al.* Intrathecal pressure monitoring and cerebrospinal fluid drainage in acute spinal cord injury: a prospective randomized trial. *J Neurosurg Spine* **10**, 181-193 (2009). <https://doi.org/10.3171/2008.10.SPINE08217>
- 37 Kwon, B. K. *et al.* Cerebrospinal Fluid Biomarkers To Stratify Injury Severity and Predict Outcome in Human Traumatic Spinal Cord Injury. *J Neurotrauma* **34**, 567-580 (2017). <https://doi.org/10.1089/neu.2016.4435>
- 38 Papatheodorou, A. *et al.* High-Mobility Group Box 1 (HMGB1) Is Elevated Systemically in Persons with Acute or Chronic Traumatic Spinal Cord Injury. *J Neurotrauma* **34**, 746-754 (2017). <https://doi.org/10.1089/neu.2016.4596>
- 39 Bank, M. *et al.* Elevated circulating levels of the pro-inflammatory cytokine macrophage migration inhibitory factor in individuals with acute spinal cord injury. *Arch Phys Med Rehabil* **96**, 633-644 (2015). <https://doi.org/10.1016/j.apmr.2014.10.021>
- 40 Stukas, S. *et al.* Association of CSF and Serum Neurofilament Light and Glial Fibrillary Acidic Protein, Injury Severity, and Outcome in Spinal Cord Injury. *Neurology* (2023). <https://doi.org/10.1212/WNL.0000000000206744>
- 41 Breasted, J. H. *The Edwin Smith Surgical Papyrus, Volume 2: Facsimile Plates and Line for Line Hieroglyphic Transliteration.*, Vol. 2 (Oriental Institute Publications, 1930).
- 42 van Middendorp, J. J., Sanchez, G. M. & Burridge, A. L. The Edwin Smith papyrus: a clinical reappraisal of the oldest known document on spinal injuries. *Eur Spine J* **19**, 1815-1823 (2010). <https://doi.org/10.1007/s00586-010-1523-6>
- 43 Silver, J. R. History of the treatment of spinal injuries. *Postgrad Med J* **81**, 108-114 (2005). <https://doi.org/10.1136/pgmj.2004.019992>
- 44 Guttmann, L. The principles of physiotherapy in the treatment of spinal paraplegia. *Physiotherapy* **35**, 157-164, illust (1949).
- 45 Guttmann, L. New hope for spinal cord sufferers. *S Afr Med J* **20**, 141-144 (1946).
- 46 Robert R Hansebout, M., FRCS(C), FACSEdward Kachur, MD, FRCS(C). *UpToDate: Acute traumatic spinal cord injury*,

- <https://www.uptodate.com/contents/acute-traumatic-spinal-cord-injury?search=spinal%20cord%20injury&source=search_result&selectedTitle=1~150&usage_type=default&display_rank=1#H3> (2018).
- 47 Fehlings, M. G. *et al.* Early versus delayed decompression for traumatic cervical spinal cord injury: results of the Surgical Timing in Acute Spinal Cord Injury Study (STASCIS). *PLoS One* **7**, e32037 (2012). <https://doi.org/10.1371/journal.pone.0032037>
- 48 Pedro, K. M. & Fehlings, M. G. Time is spine: What's over the horizon. *J Clin Orthop Trauma* **35**, 102043 (2022). <https://doi.org/10.1016/j.jcot.2022.102043>
- 49 Ditunno, J. F., Little, J. W., Tessler, A. & Burns, A. S. Spinal shock revisited: a four-phase model. *Spinal Cord* **42**, 383-395 (2004). <https://doi.org/10.1038/sj.sc.3101603>
- 50 Furlan, J. C. & Fehlings, M. G. Cardiovascular complications after acute spinal cord injury: pathophysiology, diagnosis, and management. *Neurosurg Focus* **25**, E13 (2008). <https://doi.org/10.3171/FOC.2008.25.11.E13>
- 51 Weinberg, J. A. *et al.* Mean arterial pressure maintenance following spinal cord injury: Does meeting the target matter? *J Trauma Acute Care Surg* **90**, 97-106 (2021). <https://doi.org/10.1097/TA.0000000000002953>
- 52 Kakimoto, Y., Matsushima, Y., Tsuboi, A., Seto, Y. & Osawa, M. Nonocclusive mesenteric ischemia secondary to spinal cord injury: an autopsy case. *Spinal Cord Ser Cases* **7**, 37 (2021). <https://doi.org/10.1038/s41394-021-00402-9>
- 53 Hou, S. & Rabchevsky, A. G. Autonomic consequences of spinal cord injury. *Compr Physiol* **4**, 1419-1453 (2014). <https://doi.org/10.1002/cphy.c130045>
- 54 Krassioukov, A. Autonomic function following cervical spinal cord injury. *Respir Physiol Neurobiol* **169**, 157-164 (2009). <https://doi.org/10.1016/j.resp.2009.08.003>
- 55 Galeiras Vazquez, R., Rascado Sedes, P., Mourelo Farina, M., Montoto Marques, A. & Ferreira Velasco, M. E. Respiratory management in the patient with spinal cord injury. *Biomed Res Int* **2013**, 168757 (2013). <https://doi.org/10.1155/2013/168757>
- 56 Lynch, A. C., Antony, A., Dobbs, B. R. & Frizelle, F. A. Bowel dysfunction following spinal cord injury. *Spinal Cord* **39**, 193-203 (2001). <https://doi.org/10.1038/sj.sc.3101119>
- 57 Holmes, G. M. & Blanke, E. N. Gastrointestinal dysfunction after spinal cord injury. *Exp Neurol* **320**, 113009 (2019). <https://doi.org/10.1016/j.expneurol.2019.113009>
- 58 White, A. R. & Holmes, G. M. Anatomical and Functional Changes to the Colonic Neuromuscular Compartment after Experimental Spinal Cord Injury. *J Neurotrauma* **35**, 1079-1090 (2018). <https://doi.org/10.1089/neu.2017.5369>
- 59 Kabatas, S. *et al.* Neural and anatomical abnormalities of the gastrointestinal system resulting from contusion spinal cord injury. *Neuroscience* **154**, 1627-1638 (2008). <https://doi.org/10.1016/j.neuroscience.2008.04.071>
- 60 Liu, J. *et al.* Study of bacterial translocation from gut after paraplegia caused by spinal cord injury in rats. *Spine (Phila Pa 1976)* **29**, 164-169 (2004). <https://doi.org/10.1097/01.BRS.0000107234.74249.CD>
- 61 Yu, B. *et al.* Profile of gut microbiota in patients with traumatic thoracic spinal cord injury and its clinical implications: a case-control study in a rehabilitation setting.

- 62 Pattanakuhar, S., Kaewchur, T., Saiyasit, N., Chattipakorn, N. & Chattipakorn, S. C. Level of injury is an independent determining factor of gut dysbiosis in people with chronic spinal cord injury: A cross-sectional study. *Spinal Cord* **60**, 1115-1122 (2022). <https://doi.org/10.1038/s41393-022-00832-8>
- 63 Kong, G. *et al.* The gut microbiota and metabolite profiles are altered in patients with spinal cord injury. *Mol Brain* **16**, 26 (2023). <https://doi.org/10.1186/s13041-023-01014-0>
- 64 Bazzocchi, G. *et al.* Changes in gut microbiota in the acute phase after spinal cord injury correlate with severity of the lesion. *Sci Rep* **11**, 12743 (2021). <https://doi.org/10.1038/s41598-021-92027-z>
- 65 Myers, S. A. *et al.* Following spinal cord injury, PDE4B drives an acute, local inflammatory response and a chronic, systemic response exacerbated by gut dysbiosis and endotoxemia. *Neurobiol Dis* **124**, 353-363 (2019). <https://doi.org/10.1016/j.nbd.2018.12.008>
- 66 O'Connor, G. *et al.* Investigation of Microbiota Alterations and Intestinal Inflammation Post-Spinal Cord Injury in Rat Model. *J Neurotrauma* **35**, 2159-2166 (2018). <https://doi.org/10.1089/neu.2017.5349>
- 67 Schmidt, E. K. A. *et al.* Fecal transplant prevents gut dysbiosis and anxiety-like behaviour after spinal cord injury in rats. *PLoS One* **15**, e0226128 (2020). <https://doi.org/10.1371/journal.pone.0226128>
- 68 Taweel, W. A. & Seyam, R. Neurogenic bladder in spinal cord injury patients. *Res Rep Urol* **7**, 85-99 (2015). <https://doi.org/10.2147/RRU.S29644>
- 69 Center, N. S. C. I. S. *The 2013 Annual Statistical Report for Spinal Cord Injury Model Systems*, 2013).
- 70 Hachem, L. D., Ahuja, C. S. & Fehlings, M. G. Assessment and management of acute spinal cord injury: From point of injury to rehabilitation. *J Spinal Cord Med* **40**, 665-675 (2017). <https://doi.org/10.1080/10790268.2017.1329076>
- 71 Bracken, M. B. *et al.* Administration of methylprednisolone for 24 or 48 hours or tirilazad mesylate for 48 hours in the treatment of acute spinal cord injury. Results of the Third National Acute Spinal Cord Injury Randomized Controlled Trial. National Acute Spinal Cord Injury Study. *JAMA* **277**, 1597-1604 (1997).
- 72 Bracken, M. B. *et al.* A randomized, controlled trial of methylprednisolone or naloxone in the treatment of acute spinal-cord injury. Results of the Second National Acute Spinal Cord Injury Study. *N Engl J Med* **322**, 1405-1411 (1990). <https://doi.org/10.1056/NEJM199005173222001>
- 73 Bracken, M. B. *et al.* Efficacy of methylprednisolone in acute spinal cord injury. *JAMA* **251**, 45-52 (1984).
- 74 Gerndt, S. J. *et al.* Consequences of high-dose steroid therapy for acute spinal cord injury. *J Trauma* **42**, 279-284 (1997). <https://doi.org/10.1097/00005373-199702000-00017>
- 75 Matsumoto, T. *et al.* Early complications of high-dose methylprednisolone sodium succinate treatment in the follow-up of acute cervical spinal cord injury. *Spine (Phila Pa 1976)* **26**, 426-430 (2001). <https://doi.org/10.1097/00007632-200102150-00020>

- 76 Fehlings, M. G. *et al.* A Clinical Practice Guideline for the Management of Patients With Acute Spinal Cord Injury: Recommendations on the Use of Methylprednisolone Sodium Succinate. *Global Spine J* **7**, 203S-211S (2017). <https://doi.org/10.1177/2192568217703085>
- 77 Wells, J. E., Hurlbert, R. J., Fehlings, M. G. & Yong, V. W. Neuroprotection by minocycline facilitates significant recovery from spinal cord injury in mice. *Brain* **126**, 1628-1637 (2003). <https://doi.org/10.1093/brain/awg178>
- 78 Stirling, D. P. *et al.* Minocycline treatment reduces delayed oligodendrocyte death, attenuates axonal dieback, and improves functional outcome after spinal cord injury. *J Neurosci* **24**, 2182-2190 (2004). <https://doi.org/10.1523/JNEUROSCI.5275-03.2004>
- 79 Lee, S. M. *et al.* Minocycline reduces cell death and improves functional recovery after traumatic spinal cord injury in the rat. *J Neurotrauma* **20**, 1017-1027 (2003). <https://doi.org/10.1089/089771503770195867>
- 80 Casha, S. *et al.* Results of a phase II placebo-controlled randomized trial of minocycline in acute spinal cord injury. *Brain* **135**, 1224-1236 (2012). <https://doi.org/10.1093/brain/aws072>
- 81 Schwartz, G. & Fehlings, M. G. Secondary injury mechanisms of spinal cord trauma: a novel therapeutic approach for the management of secondary pathophysiology with the sodium channel blocker riluzole. *Prog Brain Res* **137**, 177-190 (2002). [https://doi.org/10.1016/s0079-6123\(02\)37016-x](https://doi.org/10.1016/s0079-6123(02)37016-x)
- 82 Katoh-Semba, R. *et al.* Riluzole enhances expression of brain-derived neurotrophic factor with consequent proliferation of granule precursor cells in the rat hippocampus. *FASEB J* **16**, 1328-1330 (2002). <https://doi.org/10.1096/fj.02-0143fje>
- 83 Grossman, R. G. *et al.* A prospective, multicenter, phase I matched-comparison group trial of safety, pharmacokinetics, and preliminary efficacy of riluzole in patients with traumatic spinal cord injury. *J Neurotrauma* **31**, 239-255 (2014). <https://doi.org/10.1089/neu.2013.2969>
- 84 Nagoshi, N., Nakashima, H. & Fehlings, M. G. Riluzole as a neuroprotective drug for spinal cord injury: from bench to bedside. *Molecules* **20**, 7775-7789 (2015). <https://doi.org/10.3390/molecules20057775>
- 85 Fehlings, M. G. *et al.* Rationale, design and critical end points for the Riluzole in Acute Spinal Cord Injury Study (RISCIS): a randomized, double-blinded, placebo-controlled parallel multi-center trial. *Spinal Cord* **54**, 8-15 (2016). <https://doi.org/10.1038/sc.2015.95>
- 86 Lewis, L. J. & Brookhart, J. M. Significance of the crossed phrenic phenomenon. *Am J Physiol* **166**, 241-254 (1951). <https://doi.org/10.1152/ajplegacy.1951.166.2.241>
- 87 Porter, W. T. The Path of the Respiratory Impulse from the Bulb to the Phrenic Nuclei. *J Physiol* **17**, 455-485 (1895). <https://doi.org/10.1113/jphysiol.1895.sp000553>
- 88 Goshgarian, H. G. The crossed phrenic phenomenon and recovery of function following spinal cord injury. *Respir Physiol Neurobiol* **169**, 85-93 (2009). <https://doi.org/10.1016/j.resp.2009.06.005>

- 89 O'Hara, T. E. & Goshgarian, H. G. Quantitative assessment of phrenic nerve functional recovery mediated by the crossed phrenic reflex at various time intervals after spinal cord injury. *Exp Neurol* **111**, 244-250 (1991). [https://doi.org/10.1016/0014-4886\(91\)90012-2](https://doi.org/10.1016/0014-4886(91)90012-2)
- 90 Moreno, D. E., Yu, X. J. & Goshgarian, H. G. Identification of the axon pathways which mediate functional recovery of a paralyzed hemidiaphragm following spinal cord hemisection in the adult rat. *Exp Neurol* **116**, 219-228 (1992). [https://doi.org/10.1016/0014-4886\(92\)90001-7](https://doi.org/10.1016/0014-4886(92)90001-7)
- 91 Goshgarian, H. G. The role of cervical afferent nerve fiber inhibition of the crossed phrenic phenomenon. *Exp Neurol* **72**, 211-225 (1981). [https://doi.org/10.1016/0014-4886\(81\)90139-4](https://doi.org/10.1016/0014-4886(81)90139-4)
- 92 Goshgarian, H. G. The crossed phrenic phenomenon: a model for plasticity in the respiratory pathways following spinal cord injury. *J Appl Physiol* (1985) **94**, 795-810 (2003). <https://doi.org/10.1152/japplphysiol.00847.2002>
- 93 Nantwi, K. D., El-Bohy, A. & Goshgarian, H. G. Actions of systemic theophylline on hemidiaphragmatic recovery in rats following cervical spinal cord hemisection. *Exp Neurol* **140**, 53-59 (1996). <https://doi.org/10.1006/exnr.1996.0114>
- 94 Nantwi, K. D., Basura, G. J. & Goshgarian, H. G. Effects of long-term theophylline exposure on recovery of respiratory function and expression of adenosine A1 mRNA in cervical spinal cord hemisected adult rats. *Exp Neurol* **182**, 232-239 (2003). [https://doi.org/10.1016/s0014-4886\(03\)00109-2](https://doi.org/10.1016/s0014-4886(03)00109-2)
- 95 Hoy, K. C., Jr. & Alilain, W. J. Acute theophylline exposure modulates breathing activity through a cervical contusion. *Exp Neurol* **271**, 72-76 (2015). <https://doi.org/10.1016/j.expneurol.2015.04.024>
- 96 Hayashi, F., Coles, S. K., Bach, K. B., Mitchell, G. S. & McCrimmon, D. R. Time-dependent phrenic nerve responses to carotid afferent activation: intact vs. decerebellate rats. *Am J Physiol* **265**, R811-819 (1993). <https://doi.org/10.1152/ajpregu.1993.265.4.R811>
- 97 Fuller, D. D., Bach, K. B., Baker, T. L., Kinkead, R. & Mitchell, G. S. Long term facilitation of phrenic motor output. *Respir Physiol* **121**, 135-146 (2000). [https://doi.org/10.1016/s0034-5687\(00\)00124-9](https://doi.org/10.1016/s0034-5687(00)00124-9)
- 98 Millhorn, D. E., Eldridge, F. L. & Waldrop, T. G. Prolonged stimulation of respiration by a new central neural mechanism. *Respir Physiol* **41**, 87-103 (1980). [https://doi.org/10.1016/0034-5687\(80\)90025-0](https://doi.org/10.1016/0034-5687(80)90025-0)
- 99 Golder, F. J. & Mitchell, G. S. Spinal synaptic enhancement with acute intermittent hypoxia improves respiratory function after chronic cervical spinal cord injury. *J Neurosci* **25**, 2925-2932 (2005). <https://doi.org/10.1523/JNEUROSCI.0148-05.2005>
- 100 Baker, T. L. & Mitchell, G. S. Episodic but not continuous hypoxia elicits long-term facilitation of phrenic motor output in rats. *J Physiol* **529 Pt 1**, 215-219 (2000). <https://doi.org/10.1111/j.1469-7793.2000.00215.x>
- 101 Vinit, S., Lovett-Barr, M. R. & Mitchell, G. S. Intermittent hypoxia induces functional recovery following cervical spinal injury. *Respir Physiol Neurobiol* **169**, 210-217 (2009). <https://doi.org/10.1016/j.resp.2009.07.023>

- 102 Baker-Herman, T. L. & Mitchell, G. S. Phrenic long-term facilitation requires spinal serotonin receptor activation and protein synthesis. *J Neurosci* **22**, 6239-6246 (2002). <https://doi.org:20026595>
- 103 Baker-Herman, T. L. *et al.* BDNF is necessary and sufficient for spinal respiratory plasticity following intermittent hypoxia. *Nat Neurosci* **7**, 48-55 (2004). <https://doi.org:10.1038/nn1166>
- 104 Bach, K. B. & Mitchell, G. S. Hypoxia-induced long-term facilitation of respiratory activity is serotonin dependent. *Respir Physiol* **104**, 251-260 (1996). [https://doi.org:10.1016/0034-5687\(96\)00017-5](https://doi.org:10.1016/0034-5687(96)00017-5)
- 105 Silver, J. & Miller, J. H. Regeneration beyond the glial scar. *Nat Rev Neurosci* **5**, 146-156 (2004). <https://doi.org:10.1038/nrn1326>
- 106 Cajal, S. R. y. Degeneration and Regeneration of the Nervous System. *Clarendon Press* (1928).
- 107 David, S. & Aguayo, A. J. Axonal elongation into peripheral nervous system "bridges" after central nervous system injury in adult rats. *Science* **214**, 931-933 (1981). <https://doi.org:10.1126/science.6171034>
- 108 Warren, P. M. *et al.* Rapid and robust restoration of breathing long after spinal cord injury. *Nat Commun* **9**, 4843 (2018). <https://doi.org:10.1038/s41467-018-06937-0>
- 109 Tom, V. J. *et al.* Combining peripheral nerve grafts and chondroitinase promotes functional axonal regeneration in the chronically injured spinal cord. *J Neurosci* **29**, 14881-14890 (2009). <https://doi.org:10.1523/JNEUROSCI.3641-09.2009>
- 110 Tom, V. J., Kadakia, R., Santi, L. & Houle, J. D. Administration of chondroitinase ABC rostral or caudal to a spinal cord injury site promotes anatomical but not functional plasticity. *J Neurotrauma* **26**, 2323-2333 (2009). <https://doi.org:10.1089/neu.2009.1047>
- 111 Tom, V. J. & Houle, J. D. Intraspinal microinjection of chondroitinase ABC following injury promotes axonal regeneration out of a peripheral nerve graft bridge. *Exp Neurol* **211**, 315-319 (2008). <https://doi.org:10.1016/j.expneurol.2008.01.021>
- 112 Houle, J. D. *et al.* Combining an autologous peripheral nervous system "bridge" and matrix modification by chondroitinase allows robust, functional regeneration beyond a hemisection lesion of the adult rat spinal cord. *J Neurosci* **26**, 7405-7415 (2006). <https://doi.org:10.1523/JNEUROSCI.1166-06.2006>
- 113 Salewski, R. P., Mitchell, R. A., Shen, C. & Fehlings, M. G. Transplantation of neural stem cells clonally derived from embryonic stem cells promotes recovery after murine spinal cord injury. *Stem Cells Dev* **24**, 36-50 (2015). <https://doi.org:10.1089/scd.2014.0096>
- 114 Salewski, R. P. *et al.* Transplantation of Induced Pluripotent Stem Cell-Derived Neural Stem Cells Mediate Functional Recovery Following Thoracic Spinal Cord Injury Through Remyelination of Axons. *Stem Cells Transl Med* **4**, 743-754 (2015). <https://doi.org:10.5966/sctm.2014-0236>
- 115 Rosenzweig, E. S. *et al.* Restorative effects of human neural stem cell grafts on the primate spinal cord. *Nat Med* **24**, 484-490 (2018). <https://doi.org:10.1038/nm.4502>
- 116 Morita, T. *et al.* Intravenous infusion of mesenchymal stem cells promotes functional recovery in a model of chronic spinal cord injury. *Neuroscience* **335**, 221-231 (2016). <https://doi.org:10.1016/j.neuroscience.2016.08.037>

- 117 McKenna, S. L. *et al.* Ten-year safety of pluripotent stem cell transplantation in acute thoracic spinal cord injury. *J Neurosurg Spine*, 1-10 (2022). <https://doi.org:10.3171/2021.12.SPINE21622>
- 118 Fessler, R. G. *et al.* A phase 1/2a dose-escalation study of oligodendrocyte progenitor cells in individuals with subacute cervical spinal cord injury. *J Neurosurg Spine* **37**, 812-820 (2022). <https://doi.org:10.3171/2022.5.SPINE22167>
- 119 Anderson, K. D. *et al.* Safety of Autologous Human Schwann Cell Transplantation in Subacute Thoracic Spinal Cord Injury. *J Neurotrauma* **34**, 2950-2963 (2017). <https://doi.org:10.1089/neu.2016.4895>
- 120 Ho, C. H. *et al.* Functional electrical stimulation and spinal cord injury. *Phys Med Rehabil Clin N Am* **25**, 631-654, ix (2014). <https://doi.org:10.1016/j.pmr.2014.05.001>
- 121 Harkema, S. J. *et al.* Normalization of Blood Pressure With Spinal Cord Epidural Stimulation After Severe Spinal Cord Injury. *Front Hum Neurosci* **12**, 83 (2018). <https://doi.org:10.3389/fnhum.2018.00083>
- 122 Barra, B. *et al.* Epidural electrical stimulation of the cervical dorsal roots restores voluntary upper limb control in paralyzed monkeys. *Nat Neurosci* **25**, 924-934 (2022). <https://doi.org:10.1038/s41593-022-01106-5>
- 123 Rowald, A. *et al.* Activity-dependent spinal cord neuromodulation rapidly restores trunk and leg motor functions after complete paralysis. *Nat Med* **28**, 260-271 (2022). <https://doi.org:10.1038/s41591-021-01663-5>
- 124 Gad, P. N. *et al.* Neuromodulation of the neural circuits controlling the lower urinary tract. *Exp Neurol* **285**, 182-189 (2016). <https://doi.org:10.1016/j.expneurol.2016.06.034>
- 125 Smith, J. C., Ellenberger, H. H., Ballanyi, K., Richter, D. W. & Feldman, J. L. Pre-Botzinger complex: a brainstem region that may generate respiratory rhythm in mammals. *Science* **254**, 726-729 (1991). <https://doi.org:10.1126/science.1683005>
- 126 Wenninger, J. M. *et al.* Large lesions in the pre-Botzinger complex area eliminate eupneic respiratory rhythm in awake goats. *J Appl Physiol (1985)* **97**, 1629-1636 (2004). <https://doi.org:10.1152/jappphysiol.00953.2003>
- 127 Gray, P. A., Janczewski, W. A., Mellen, N., McCrimmon, D. R. & Feldman, J. L. Normal breathing requires preBotzinger complex neurokinin-1 receptor-expressing neurons. *Nat Neurosci* **4**, 927-930 (2001). <https://doi.org:10.1038/nn0901-927>
- 128 Tan, W., Pagliardini, S., Yang, P., Janczewski, W. A. & Feldman, J. L. Projections of preBotzinger complex neurons in adult rats. *J Comp Neurol* **518**, 1862-1878 (2010). <https://doi.org:10.1002/cne.22308>
- 129 Smith, J. C., Morrison, D. E., Ellenberger, H. H., Otto, M. R. & Feldman, J. L. Brainstem projections to the major respiratory neuron populations in the medulla of the cat. *J Comp Neurol* **281**, 69-96 (1989). <https://doi.org:10.1002/cne.902810107>
- 130 Dobbins, E. G. & Feldman, J. L. Brainstem network controlling descending drive to phrenic motoneurons in rat. *J Comp Neurol* **347**, 64-86 (1994). <https://doi.org:10.1002/cne.903470106>
- 131 Del Negro, C. A., Funk, G. D. & Feldman, J. L. Breathing matters. *Nat Rev Neurosci* **19**, 351-367 (2018). <https://doi.org:10.1038/s41583-018-0003-6>

- 132 DeVries, K. L. & Goshgarian, H. G. Spinal cord localization and characterization of the neurons which give rise to the accessory phrenic nerve in the adult rat. *Exp Neurol* **104**, 88-90 (1989). [https://doi.org:10.1016/0014-4886\(89\)90013-7](https://doi.org:10.1016/0014-4886(89)90013-7)
- 133 Feldman, J. L., Loewy, A. D. & Speck, D. F. Projections from the ventral respiratory group to phrenic and intercostal motoneurons in cat: an autoradiographic study. *J Neurosci* **5**, 1993-2000 (1985). <https://doi.org:10.1523/JNEUROSCI.05-08-01993.1985>
- 134 Ellenberger, H. H., Feldman, J. L. & Goshgarian, H. G. Ventral respiratory group projections to phrenic motoneurons: electron microscopic evidence for monosynaptic connections. *J Comp Neurol* **302**, 707-714 (1990). <https://doi.org:10.1002/cne.903020403>
- 135 Onai, T., Saji, M. & Miura, M. Projections of supraspinal structures to the phrenic motor nucleus in rats studied by a horseradish peroxidase microinjection method. *J Auton Nerv Syst* **21**, 233-239 (1987). [https://doi.org:10.1016/0165-1838\(87\)90026-9](https://doi.org:10.1016/0165-1838(87)90026-9)
- 136 Lipski, J., Zhang, X., Kruszewska, B. & Kanjhan, R. Morphological study of long axonal projections of ventral medullary inspiratory neurons in the rat. *Brain Res* **640**, 171-184 (1994). [https://doi.org:10.1016/0006-8993\(94\)91871-6](https://doi.org:10.1016/0006-8993(94)91871-6)
- 137 Lane, M. A. *et al.* Cervical prephrenic interneurons in the normal and lesioned spinal cord of the adult rat. *J Comp Neurol* **511**, 692-709 (2008). <https://doi.org:10.1002/cne.21864>
- 138 Millhorn, D. E. Stimulation of raphe (obscurus) nucleus causes long-term potentiation of phrenic nerve activity in cat. *J Physiol* **381**, 169-179 (1986). <https://doi.org:10.1113/jphysiol.1986.sp016320>
- 139 Holtman, J. R., Jr., Dick, T. E. & Berger, A. J. Involvement of serotonin in the excitation of phrenic motoneurons evoked by stimulation of the raphe obscurus. *J Neurosci* **6**, 1185-1193 (1986). <https://doi.org:10.1523/JNEUROSCI.06-04-01185.1986>
- 140 Bocchiario, C. M. & Feldman, J. L. Synaptic activity-independent persistent plasticity in endogenously active mammalian motoneurons. *Proc Natl Acad Sci U S A* **101**, 4292-4295 (2004). <https://doi.org:10.1073/pnas.0305712101>
- 141 Hodges, M. R. & Richerson, G. B. The role of medullary serotonin (5-HT) neurons in respiratory control: contributions to eupneic ventilation, CO₂ chemoreception, and thermoregulation. *J Appl Physiol (1985)* **108**, 1425-1432 (2010). <https://doi.org:10.1152/jappphysiol.01270.2009>
- 142 Teran, F. A., Massey, C. A. & Richerson, G. B. Serotonin neurons and central respiratory chemoreception: where are we now? *Prog Brain Res* **209**, 207-233 (2014). <https://doi.org:10.1016/B978-0-444-63274-6.00011-4>
- 143 Guyenet, P. G., Stornetta, R. L. & Bayliss, D. A. Central respiratory chemoreception. *J Comp Neurol* **518**, 3883-3906 (2010). <https://doi.org:10.1002/cne.22435>
- 144 Veasey, S. C., Fornal, C. A., Metzler, C. W. & Jacobs, B. L. Response of serotonergic caudal raphe neurons in relation to specific motor activities in freely moving cats. *J Neurosci* **15**, 5346-5359 (1995). <https://doi.org:10.1523/JNEUROSCI.15-07-05346.1995>

- 145 Taylor, N. C., Li, A. & Nattie, E. E. Medullary serotonergic neurones modulate the ventilatory response to hypercapnia, but not hypoxia in conscious rats. *J Physiol* **566**, 543-557 (2005). <https://doi.org:10.1113/jphysiol.2005.083873>
- 146 Lindsey, B. G., Nuding, S. C., Segers, L. S. & Morris, K. F. Carotid Bodies and the Integrated Cardiorespiratory Response to Hypoxia. *Physiology (Bethesda)* **33**, 281-297 (2018). <https://doi.org:10.1152/physiol.00014.2018>
- 147 Fogarty, M. J. & Sieck, G. C. Evolution and Functional Differentiation of the Diaphragm Muscle of Mammals. *Compr Physiol* **9**, 715-766 (2019). <https://doi.org:10.1002/cphy.c180012>
- 148 Dutschmann, M., Jones, S. E., Subramanian, H. H., Stanic, D. & Bautista, T. G. The physiological significance of postinspiration in respiratory control. *Prog Brain Res* **212**, 113-130 (2014). <https://doi.org:10.1016/B978-0-444-63488-7.00007-0>
- 149 Aliverti, A. The respiratory muscles during exercise. *Breathe (Sheff)* **12**, 165-168 (2016). <https://doi.org:10.1183/20734735.008116>
- 150 Ghali, M. G. Z. The bulbospinal network controlling the phrenic motor system: Laterality and course of descending projections. *Neurosci Res* **121**, 7-17 (2017). <https://doi.org:10.1016/j.neures.2017.03.004>
- 151 Duron, B., Marlot, D., Larnicol, N., Jung-Caillol, M. C. & Macron, J. M. Somatotopy in the phrenic motor nucleus of the cat as revealed by retrograde transport of horseradish peroxidase. *Neurosci Lett* **14**, 159-163 (1979). [https://doi.org:10.1016/0304-3940\(79\)96141-x](https://doi.org:10.1016/0304-3940(79)96141-x)
- 152 DeVivo, M. J. & Ivie, C. S. Life expectancy of ventilator-dependent persons with spinal cord injuries. *Chest* **108**, 226-232 (1995). <https://doi.org:10.1378/chest.108.1.226>
- 153 Truflandier, K. *et al.* Mechanical ventilation modulates pro-inflammatory cytokine expression in spinal cord tissue after injury in rats. *Neurosci Lett* **671**, 13-18 (2018). <https://doi.org:10.1016/j.neulet.2018.01.028>
- 154 Velmahos, G. C. *et al.* Intubation after cervical spinal cord injury: to be done selectively or routinely? *Am Surg* **69**, 891-894 (2003).
- 155 Winslow, C. & Rozovsky, J. Effect of spinal cord injury on the respiratory system. *Am J Phys Med Rehabil* **82**, 803-814 (2003). <https://doi.org:10.1097/01.PHM.0000078184.08835.01>
- 156 Warren, P. M. & Alilain, W. J. The challenges of respiratory motor system recovery following cervical spinal cord injury. *Prog Brain Res* **212**, 173-220 (2014). <https://doi.org:10.1016/B978-0-444-63488-7.00010-0>
- 157 Sharma, H., Alilain, W. J., Sadhu, A. & Silver, J. Treatments to restore respiratory function after spinal cord injury and their implications for regeneration, plasticity and adaptation. *Exp Neurol* **235**, 18-25 (2012). <https://doi.org:10.1016/j.expneurol.2011.12.018>
- 158 Oo, T., Watt, J. W., Soni, B. M. & Sett, P. K. Delayed diaphragm recovery in 12 patients after high cervical spinal cord injury. A retrospective review of the diaphragm status of 107 patients ventilated after acute spinal cord injury. *Spinal Cord* **37**, 117-122 (1999). <https://doi.org:10.1038/sj.sc.3100775>
- 159 Alilain, W. J. & Goshgarian, H. G. Glutamate receptor plasticity and activity-regulated cytoskeletal associated protein regulation in the phrenic motor nucleus may mediate spontaneous recovery of the hemidiaphragm following chronic

- cervical spinal cord injury. *Exp Neurol* **212**, 348-357 (2008).
<https://doi.org:10.1016/j.expneurol.2008.04.017>
- 160 Alilain, W. J. *et al.* Light-induced rescue of breathing after spinal cord injury. *J Neurosci* **28**, 11862-11870 (2008). <https://doi.org:10.1523/JNEUROSCI.3378-08.2008>
- 161 Fuller, D. D. *et al.* Modest spontaneous recovery of ventilation following chronic high cervical hemisection in rats. *Exp Neurol* **211**, 97-106 (2008).
<https://doi.org:10.1016/j.expneurol.2008.01.013>
- 162 Fuller, D. D. & Mitchell, G. S. Respiratory neuroplasticity - Overview, significance and future directions. *Exp Neurol* **287**, 144-152 (2017).
<https://doi.org:10.1016/j.expneurol.2016.05.022>
- 163 Loveridge, B., Sanii, R. & Dubo, H. I. Breathing pattern adjustments during the first year following cervical spinal cord injury. *Paraplegia* **30**, 479-488 (1992).
<https://doi.org:10.1038/sc.1992.102>
- 164 Fuller, D. D., Johnson, S. M., Olson, E. B., Jr. & Mitchell, G. S. Synaptic pathways to phrenic motoneurons are enhanced by chronic intermittent hypoxia after cervical spinal cord injury. *J Neurosci* **23**, 2993-3000 (2003).
<https://doi.org:10.1523/JNEUROSCI.23-07-02993.2003>
- 165 Fuller, D. D., Golder, F. J., Olson, E. B., Jr. & Mitchell, G. S. Recovery of phrenic activity and ventilation after cervical spinal hemisection in rats. *J Appl Physiol* (1985) **100**, 800-806 (2006). <https://doi.org:10.1152/jappphysiol.00960.2005>
- 166 Stripling, J. & Rodriguez, M. Current Evidence in Delivery and Therapeutic Uses of Fecal Microbiota Transplantation in Human Diseases-Clostridium difficile Disease and Beyond. *Am J Med Sci* **356**, 424-432 (2018).
<https://doi.org:10.1016/j.amjms.2018.08.010>
- 167 EISEMAN, B., SILEN, W., BASCOM, G. S. & KAUVAR, A. J. Fecal enema as an adjunct in the treatment of pseudomembranous enterocolitis. *Surgery* **44**, 854-859 (1958).
- 168 Valdes, A. M., Walter, J., Segal, E. & Spector, T. D. Role of the gut microbiota in nutrition and health. *BMJ* **361**, k2179 (2018). <https://doi.org:10.1136/bmj.k2179>
- 169 Khot, P. D. & Fisher, M. A. Novel approach for differentiating Shigella species and Escherichia coli by matrix-assisted laser desorption ionization-time of flight mass spectrometry. *J Clin Microbiol* **51**, 3711-3716 (2013).
<https://doi.org:10.1128/JCM.01526-13>
- 170 Arumugam, M. *et al.* Enterotypes of the human gut microbiome. *Nature* **473**, 174-180 (2011). <https://doi.org:10.1038/nature09944>
- 171 Tremaroli, V. & Backhed, F. Functional interactions between the gut microbiota and host metabolism. *Nature* **489**, 242-249 (2012).
<https://doi.org:10.1038/nature11552>
- 172 Turnbaugh, P. J. *et al.* An obesity-associated gut microbiome with increased capacity for energy harvest. *Nature* **444**, 1027-1031 (2006).
<https://doi.org:10.1038/nature05414>
- 173 Ley, R. E. *et al.* Obesity alters gut microbial ecology. *Proc Natl Acad Sci U S A* **102**, 11070-11075 (2005). <https://doi.org:10.1073/pnas.0504978102>

- 174 De Palma, G. *et al.* Transplantation of fecal microbiota from patients with irritable
bowel syndrome alters gut function and behavior in recipient mice. *Sci Transl Med*
9 (2017). <https://doi.org:10.1126/scitranslmed.aaf6397>
- 175 Zajac, D. J., Green, S. J., Johnson, L. A. & Estus, S. APOE genetics influence
murine gut microbiome. *Sci Rep* **12**, 1906 (2022). <https://doi.org:10.1038/s41598-022-05763-1>
- 176 Chang, C. & Lin, H. Dysbiosis in gastrointestinal disorders. *Best Pract Res Clin
Gastroenterol* **30**, 3-15 (2016). <https://doi.org:10.1016/j.bpg.2016.02.001>
- 177 Carabotti, M., Scirocco, A., Maselli, M. A. & Severi, C. The gut-brain axis:
interactions between enteric microbiota, central and enteric nervous systems. *Ann
Gastroenterol* **28**, 203-209 (2015).
- 178 Bistoletti, M. *et al.* Antibiotic treatment-induced dysbiosis differently affects
BDNF and TrkB expression in the brain and in the gut of juvenile mice. *PLoS One*
14, e0212856 (2019). <https://doi.org:10.1371/journal.pone.0212856>
- 179 Yano, J. M. *et al.* Indigenous bacteria from the gut microbiota regulate host
serotonin biosynthesis. *Cell* **161**, 264-276 (2015).
<https://doi.org:10.1016/j.cell.2015.02.047>
- 180 Bercik, P. *et al.* The intestinal microbiota affect central levels of brain-derived
neurotrophic factor and behavior in mice. *Gastroenterology* **141**, 599-609, 609.e591-
593 (2011). <https://doi.org:10.1053/j.gastro.2011.04.052>
- 181 Jiang, H. *et al.* Altered fecal microbiota composition in patients with major
depressive disorder. *Brain Behav Immun* **48**, 186-194 (2015).
<https://doi.org:10.1016/j.bbi.2015.03.016>
- 182 Singh, V. *et al.* Microbiota Dysbiosis Controls the Neuroinflammatory Response
after Stroke. *J Neurosci* **36**, 7428-7440 (2016).
<https://doi.org:10.1523/JNEUROSCI.1114-16.2016>
- 183 Kelly, J. R. *et al.* Transferring the blues: Depression-associated gut microbiota
induces neurobehavioural changes in the rat. *J Psychiatr Res* **82**, 109-118 (2016).
<https://doi.org:10.1016/j.jpsychires.2016.07.019>
- 184 Zeng, Q. *et al.* The alteration of gut microbiome and metabolism in amyotrophic
lateral sclerosis patients. *Sci Rep* **10**, 12998 (2020). <https://doi.org:10.1038/s41598-020-69845-8>
- 185 Barandouzi, Z. A. *et al.* Associations of neurotransmitters and the gut microbiome
with emotional distress in mixed type of irritable bowel syndrome. *Sci Rep* **12**, 1648
(2022). <https://doi.org:10.1038/s41598-022-05756-0>
- 186 Houlden, A. *et al.* Brain injury induces specific changes in the caecal microbiota of
mice via altered autonomic activity and mucoprotein production. *Brain Behav
Immun* **57**, 10-20 (2016). <https://doi.org:10.1016/j.bbi.2016.04.003>
- 187 Howard, B. M. *et al.* Characterizing the gut microbiome in trauma: significant
changes in microbial diversity occur early after severe injury. *Trauma Surg Acute
Care Open* **2**, e000108 (2017). <https://doi.org:10.1136/tsaco-2017-000108>
- 188 Zhu, C. S., Grandhi, R., Patterson, T. T. & Nicholson, S. E. A Review of Traumatic
Brain Injury and the Gut Microbiome: Insights into Novel Mechanisms of
Secondary Brain Injury and Promising Targets for Neuroprotection. *Brain Sci* **8**
(2018). <https://doi.org:10.3390/brainsci8060113>

- 189 Gungor, B., Adiguzel, E., Gursel, I., Yilmaz, B. & Gursel, M. Intestinal Microbiota
in Patients with Spinal Cord Injury. *PLoS One* **11**, e0145878 (2016).
<https://doi.org/10.1371/journal.pone.0145878>
- 190 Wallace, D. J. *et al.* Spinal cord injury and the human microbiome: beyond the
brain-gut axis. *Neurosurg Focus* **46**, E11 (2019).
<https://doi.org/10.3171/2018.12.FOCUS18206>
- 191 Veeravagu, A. *et al.* Acute respiratory distress syndrome and acute lung injury in
patients with vertebral column fracture(s) and spinal cord injury: a nationwide
inpatient sample study. *Spinal Cord* **51**, 461-465 (2013).
<https://doi.org/10.1038/sc.2013.16>
- 192 Dickson, R. P. *et al.* Enrichment of the lung microbiome with gut bacteria in sepsis
and the acute respiratory distress syndrome. *Nat Microbiol* **1**, 16113 (2016).
<https://doi.org/10.1038/nmicrobiol.2016.113>
- 193 Dang, A. T. & Marsland, B. J. Microbes, metabolites, and the gut-lung axis.
Mucosal Immunol **12**, 843-850 (2019). <https://doi.org/10.1038/s41385-019-0160-6>
- 194 Gershon, M. D. & Tack, J. The serotonin signaling system: from basic
understanding to drug development for functional GI disorders. *Gastroenterology*
132, 397-414 (2007). <https://doi.org/10.1053/j.gastro.2006.11.002>
- 195 Tran, T. T. T. *et al.* genotype influences the gut microbiome structure and function
in humans and mice: relevance for Alzheimer's disease pathophysiology. *FASEB J*
33, 8221-8231 (2019). <https://doi.org/10.1096/fj.201900071R>
- 196 Wang, X. *et al.* Sodium oligomannate therapeutically remodels gut microbiota and
suppresses gut bacterial amino acids-shaped neuroinflammation to inhibit
Alzheimer's disease progression. *Cell Res* **29**, 787-803 (2019).
<https://doi.org/10.1038/s41422-019-0216-x>
- 197 Zajac, D. J. *et al.* Exogenous Short Chain Fatty Acid Effects in APP/PS1 Mice.
Front Neurosci **16**, 873549 (2022). <https://doi.org/10.3389/fnins.2022.873549>
- 198 Serbanescu, M. A. *et al.* General Anesthesia Alters the Diversity and Composition
of the Intestinal Microbiota in Mice. *Anesth Analg* **129**, e126-e129 (2019).
<https://doi.org/10.1213/ANE.0000000000003938>
- 199 Gicquelais, R. E., Bohnert, A. S. B., Thomas, L. & Foxman, B. Opioid agonist and
antagonist use and the gut microbiota: associations among people in addiction
treatment. *Sci Rep* **10**, 19471 (2020). <https://doi.org/10.1038/s41598-020-76570-9>
- 200 Li, Y. J., Dai, C. & Jiang, M. Mechanisms of Probiotic VSL#3 in a Rat Model of
Visceral Hypersensitivity Involves the Mast Cell-PAR2-TRPV1 Pathway. *Dig Dis
Sci* **64**, 1182-1192 (2019). <https://doi.org/10.1007/s10620-018-5416-6>
- 201 Dai, C. *et al.* VSL#3 probiotics exerts the anti-inflammatory activity via PI3k/Akt
and NF-kappaB pathway in rat model of DSS-induced colitis. *Mol Cell Biochem*
374, 1-11 (2013). <https://doi.org/10.1007/s11010-012-1488-3>
- 202 Chang, B. *et al.* The protective effect of VSL#3 on intestinal permeability in a rat
model of alcoholic intestinal injury. *BMC Gastroenterol* **13**, 151 (2013).
<https://doi.org/10.1186/1471-230X-13-151>
- 203 Wang, H. *et al.* Mechanism of Probiotic VSL#3 Inhibiting NF-kappaB and TNF-
alpha on Colitis through TLR4-NF-kappaB Signal Pathway. *Iran J Public Health*
48, 1292-1300 (2019).

- 204 Bialkowska, A. B., Ghaleb, A. M., Nandan, M. O. & Yang, V. W. Improved Swiss-rolling Technique for Intestinal Tissue Preparation for Immunohistochemical and Immunofluorescent Analyses. *J Vis Exp* (2016). <https://doi.org:10.3791/54161>
- 205 Moolenbeek, C. & Ruitenber, E. J. The "Swiss roll": a simple technique for histological studies of the rodent intestine. *Lab Anim* **15**, 57-59 (1981). <https://doi.org:10.1258/002367781780958577>
- 206 Quaedackers, J. S. *et al.* An evaluation of methods for grading histologic injury following ischemia/reperfusion of the small bowel. *Transplant Proc* **32**, 1307-1310 (2000). [https://doi.org:10.1016/s0041-1345\(00\)01238-0](https://doi.org:10.1016/s0041-1345(00)01238-0)
- 207 Rinninella, E. *et al.* What is the Healthy Gut Microbiota Composition? A Changing Ecosystem across Age, Environment, Diet, and Diseases. *Microorganisms* **7** (2019). <https://doi.org:10.3390/microorganisms7010014>
- 208 Doelman, A. *et al.* Correction to: Characterization of the gut microbiome in a porcine model of thoracic spinal cord injury. *BMC Genomics* **22**, 879 (2021). <https://doi.org:10.1186/s12864-021-08202-z>
- 209 Besecker, E. M., Deiter, G. M., Pironi, N., Cooper, T. K. & Holmes, G. M. Mesenteric vascular dysregulation and intestinal inflammation accompanies experimental spinal cord injury. *Am J Physiol Regul Integr Comp Physiol* **312**, R146-R156 (2017). <https://doi.org:10.1152/ajpregu.00347.2016>
- 210 Park, P. O., Haglund, U., Bulkley, G. B. & Falt, K. The sequence of development of intestinal tissue injury after strangulation ischemia and reperfusion. *Surgery* **107**, 574-580 (1990).
- 211 Chiu, C. J., McArdle, A. H., Brown, R., Scott, H. J. & Gurd, F. N. Intestinal mucosal lesion in low-flow states. I. A morphological, hemodynamic, and metabolic reappraisal. *Arch Surg* **101**, 478-483 (1970). <https://doi.org:10.1001/archsurg.1970.01340280030009>
- 212 Grootjans, J., Lenaerts, K., Buurman, W. A., Dejong, C. H. & Derikx, J. P. Life and death at the mucosal-luminal interface: New perspectives on human intestinal ischemia-reperfusion. *World J Gastroenterol* **22**, 2760-2770 (2016). <https://doi.org:10.3748/wjg.v22.i9.2760>
- 213 Hang, C. H., Shi, J. X., Li, J. S., Wu, W. & Yin, H. X. Alterations of intestinal mucosa structure and barrier function following traumatic brain injury in rats. *World J Gastroenterol* **9**, 2776-2781 (2003). <https://doi.org:10.3748/wjg.v9.i12.2776>
- 214 Strange, R. E. Bacterial "glycogen" and survival. *Nature* **220**, 606-607 (1968). <https://doi.org:10.1038/220606a0>
- 215 Young, L. E. A. *et al.* In situ mass spectrometry imaging reveals heterogeneous glycogen stores in human normal and cancerous tissues. *EMBO Mol Med* **14**, e16029 (2022). <https://doi.org:10.15252/emmm.202216029>
- 216 Sun, R. C. *et al.* Brain glycogen serves as a critical glucosamine cache required for protein glycosylation. *Cell Metab* **33**, 1404-1417 e1409 (2021). <https://doi.org:10.1016/j.cmet.2021.05.003>
- 217 Roberti, M. P., Rauber, C., Kroemer, G. & Zitvogel, L. Impact of the ileal microbiota on colon cancer. *Semin Cancer Biol* **86**, 955-966 (2022). <https://doi.org:10.1016/j.semcancer.2021.09.016>

- 218 Pelaseyed, T. & Hansson, G. C. Membrane mucins of the intestine at a glance. *J Cell Sci* **133** (2020). <https://doi.org/10.1242/jcs.240929>
- 219 Liu, X. *et al.* Hyperbaric Oxygen Treatment Improves Intestinal Barrier Function After Spinal Cord Injury in Rats. *Front Neurol* **11**, 563281 (2020). <https://doi.org/10.3389/fneur.2020.563281>
- 220 Jaglal, S. B. *et al.* Health system factors associated with rehospitalizations after traumatic spinal cord injury: a population-based study. *Spinal Cord* **47**, 604-609 (2009). <https://doi.org/10.1038/sc.2009.9>
- 221 Anderson, K. D. Targeting recovery: priorities of the spinal cord-injured population. *J Neurotrauma* **21**, 1371-1383 (2004). <https://doi.org/10.1089/neu.2004.21.1371>
- 222 Krause, J. S. & Saunders, L. L. Risk of hospitalizations after spinal cord injury: relationship with biographical, injury, educational, and behavioral factors. *Spinal Cord* **47**, 692-697 (2009). <https://doi.org/10.1038/sc.2009.16>
- 223 Ng, C. *et al.* Gastrointestinal symptoms in spinal cord injury: relationships with level of injury and psychologic factors. *Dis Colon Rectum* **48**, 1562-1568 (2005). <https://doi.org/10.1007/s10350-005-0061-5>
- 224 Deitch, E. A., Xu, D. & Kaise, V. L. Role of the gut in the development of injury- and shock induced SIRS and MODS: the gut-lymph hypothesis, a review. *Front Biosci* **11**, 520-528 (2006). <https://doi.org/10.2741/1816>
- 225 de Mello Rieder, M. *et al.* Serum Biomarkers and Clinical Outcomes in Traumatic Spinal Cord Injury: Prospective Cohort Study. *World Neurosurg* **122**, e1028-e1036 (2019). <https://doi.org/10.1016/j.wneu.2018.10.206>
- 226 Davies, A. L., Hayes, K. C. & Dekaban, G. A. Clinical correlates of elevated serum concentrations of cytokines and autoantibodies in patients with spinal cord injury. *Arch Phys Med Rehabil* **88**, 1384-1393 (2007). <https://doi.org/10.1016/j.apmr.2007.08.004>
- 227 Huxtable, A. G., Smith, S. M., Vinit, S., Watters, J. J. & Mitchell, G. S. Systemic LPS induces spinal inflammatory gene expression and impairs phrenic long-term facilitation following acute intermittent hypoxia. *J Appl Physiol (1985)* **114**, 879-887 (2013). <https://doi.org/10.1152/japplphysiol.01347.2012>
- 228 Gutierrez, D. V., Clark, M., Nwanna, O. & Alilain, W. J. Intermittent hypoxia training after C2 hemisection modifies the expression of PTEN and mTOR. *Exp Neurol* **248**, 45-52 (2013). <https://doi.org/10.1016/j.expneurol.2013.05.013>
- 229 Warren, P. M. & Alilain, W. J. Plasticity Induced Recovery of Breathing Occurs at Chronic Stages after Cervical Contusion. *J Neurotrauma* **36**, 1985-1999 (2019). <https://doi.org/10.1089/neu.2018.6186>
- 230 Grill, R., Murai, K., Blesch, A., Gage, F. H. & Tuszynski, M. H. Cellular delivery of neurotrophin-3 promotes corticospinal axonal growth and partial functional recovery after spinal cord injury. *J Neurosci* **17**, 5560-5572 (1997). <https://doi.org/10.1523/JNEUROSCI.17-14-05560.1997>
- 231 Liu, Y. *et al.* Transplants of fibroblasts genetically modified to express BDNF promote regeneration of adult rat rubrospinal axons and recovery of forelimb function. *J Neurosci* **19**, 4370-4387 (1999). <https://doi.org/10.1523/JNEUROSCI.19-11-04370.1999>

- 232 Liu, K. *et al.* PTEN deletion enhances the regenerative ability of adult corticospinal neurons. *Nat Neurosci* **13**, 1075-1081 (2010). <https://doi.org:10.1038/nn.2603>
- 233 Kelly, M. N. *et al.* Circadian clock genes and respiratory neuroplasticity genes oscillate in the phrenic motor system. *Am J Physiol Regul Integr Comp Physiol* **318**, R1058-R1067 (2020). <https://doi.org:10.1152/ajpregu.00010.2020>
- 234 Gwak, Y. S., Hains, B. C., Johnson, K. M. & Hulsebosch, C. E. Effect of age at time of spinal cord injury on behavioral outcomes in rat. *J Neurotrauma* **21**, 983-993 (2004). <https://doi.org:10.1089/0897715041650999>
- 235 Friswell, M. K. *et al.* Site and strain-specific variation in gut microbiota profiles and metabolism in experimental mice. *PLoS One* **5**, e8584 (2010). <https://doi.org:10.1371/journal.pone.0008584>
- 236 Binda, C. *et al.* Actinobacteria: A relevant minority for the maintenance of gut homeostasis. *Dig Liver Dis* **50**, 421-428 (2018). <https://doi.org:10.1016/j.dld.2018.02.012>
- 237 Gryaznova, M. *et al.* Dynamics of Changes in the Gut Microbiota of Healthy Mice Fed with Lactic Acid Bacteria and Bifidobacteria. *Microorganisms* **10** (2022). <https://doi.org:10.3390/microorganisms10051020>
- 238 Tasnim, N., Abulizi, N., Pither, J., Hart, M. M. & Gibson, D. L. Linking the Gut Microbial Ecosystem with the Environment: Does Gut Health Depend on Where We Live? *Front Microbiol* **8**, 1935 (2017). <https://doi.org:10.3389/fmicb.2017.01935>
- 239 Vinit, S., Stamegna, J. C., Boulenguez, P., Gauthier, P. & Kastner, A. Restorative respiratory pathways after partial cervical spinal cord injury: role of ipsilateral phrenic afferents. *Eur J Neurosci* **25**, 3551-3560 (2007). <https://doi.org:10.1111/j.1460-9568.2007.05619.x>
- 240 Kigerl, K. A., Zane, K., Adams, K., Sullivan, M. B. & Popovich, P. G. The spinal cord-gut-immune axis as a master regulator of health and neurological function after spinal cord injury. *Exp Neurol* **323**, 113085 (2020). <https://doi.org:10.1016/j.expneurol.2019.113085>
- 241 Clemente, J. C., Manasson, J. & Scher, J. U. The role of the gut microbiome in systemic inflammatory disease. *BMJ* **360**, j5145 (2018). <https://doi.org:10.1136/bmj.j5145>
- 242 Brandsma, E. *et al.* A Proinflammatory Gut Microbiota Increases Systemic Inflammation and Accelerates Atherosclerosis. *Circ Res* **124**, 94-100 (2019). <https://doi.org:10.1161/CIRCRESAHA.118.313234>
- 243 Zysset-Burri, D. C., Morandi, S., Herzog, E. L., Berger, L. E. & Zinkernagel, M. S. The role of the gut microbiome in eye diseases. *Prog Retin Eye Res* **92**, 101117 (2023). <https://doi.org:10.1016/j.preteyeres.2022.101117>
- 244 Valentino, T. R. *et al.* Dysbiosis of the gut microbiome impairs mouse skeletal muscle adaptation to exercise. *J Physiol* **599**, 4845-4863 (2021). <https://doi.org:10.1113/JP281788>
- 245 Bhargava, S., Merckelbach, E., Noels, H., Vohra, A. & Jankowski, J. Homeostasis in the Gut Microbiota in Chronic Kidney Disease. *Toxins (Basel)* **14** (2022). <https://doi.org:10.3390/toxins14100648>

- 246 Voroneanu, L. *et al.* Gut Microbiota in Chronic Kidney Disease: From Composition to Modulation towards Better Outcomes-A Systematic Review. *J Clin Med* **12** (2023). <https://doi.org:10.3390/jcm12051948>
- 247 Kocot, A. M., Jarocka-Cyrta, E. & Drabinska, N. Overview of the Importance of Biotics in Gut Barrier Integrity. *Int J Mol Sci* **23** (2022). <https://doi.org:10.3390/ijms23052896>
- 248 Appleton, J. The Gut-Brain Axis: Influence of Microbiota on Mood and Mental Health. *Integr Med (Encinitas)* **17**, 28-32 (2018).
- 249 Beattie, E. C. *et al.* Control of synaptic strength by glial TNF α . *Science* **295**, 2282-2285 (2002). <https://doi.org:10.1126/science.1067859>
- 250 Stellwagen, D. & Malenka, R. C. Synaptic scaling mediated by glial TNF- α . *Nature* **440**, 1054-1059 (2006). <https://doi.org:10.1038/nature04671>
- 251 Parameswaran, N. & Patial, S. Tumor necrosis factor- α signaling in macrophages. *Crit Rev Eukaryot Gene Expr* **20**, 87-103 (2010). <https://doi.org:10.1615/critreveukargeneexpr.v20.i2.10>
- 252 Parker, A. *et al.* Fecal microbiota transfer between young and aged mice reverses hallmarks of the aging gut, eye, and brain. *Microbiome* **10**, 68 (2022). <https://doi.org:10.1186/s40168-022-01243-w>
- 253 Sun, J. *et al.* Fecal microbiota transplantation alleviated Alzheimer's disease-like pathogenesis in APP/PS1 transgenic mice. *Transl Psychiatry* **9**, 189 (2019). <https://doi.org:10.1038/s41398-019-0525-3>
- 254 Jenkins, T. A., Nguyen, J. C., Polglaze, K. E. & Bertrand, P. P. Influence of Tryptophan and Serotonin on Mood and Cognition with a Possible Role of the Gut-Brain Axis. *Nutrients* **8** (2016). <https://doi.org:10.3390/nu8010056>
- 255 Ge, X. *et al.* Antibiotics-induced depletion of mice microbiota induces changes in host serotonin biosynthesis and intestinal motility. *J Transl Med* **15**, 13 (2017). <https://doi.org:10.1186/s12967-016-1105-4>
- 256 Kohl, H. M., Castillo, A. R. & Ochoa-Reparaz, J. The Microbiome as a Therapeutic Target for Multiple Sclerosis: Can Genetically Engineered Probiotics Treat the Disease? *Diseases* **8** (2020). <https://doi.org:10.3390/diseases8030033>
- 257 Erny, D. *et al.* Host microbiota constantly control maturation and function of microglia in the CNS. *Nat Neurosci* **18**, 965-977 (2015). <https://doi.org:10.1038/nn.4030>
- 258 Yanckello, L. M. *et al.* Inulin supplementation prior to mild traumatic brain injury mitigates gut dysbiosis, and brain vascular and white matter deficits in mice. *Front Microbiomes* **1** (2022). <https://doi.org:10.3389/frmbi.2022.986951>

VITA

EDUCATION

- UNIVERSITY OF KENTUCKY LEXINGTON, KY
Doctor of Philosophy – Neuroscience 2018 - Present
- Concentration: Traumatic Spinal Cord Injury
 - Advisor: Warren Alilain, Ph.D.
- UNIVERSITY OF KENTUCKY LEXINGTON, KY
Graduate Certificate in Anatomical Sciences Instruction 2021 - 2022
- Teaching Certificate in Gross Anatomy
 - Teaching Certificate in Neuroanatomy
- UNIVERSITY OF KENTUCKY LEXINGTON, KY
Master of Science – Medical Science 2015 - 2017
- Concentration: Alcoholism and Neurogenesis
 - Advisor: Kimberly Nixon, Ph.D.
- UNIVERSITY OF ROCHESTER ROCHESTER, NY
Bachelor of Science - Neuroscience 2009 - 2013
- Minor in Psychology
 - Three-course Cluster completed in American Sign Language
 - Member of the University of Rochester Women’s Soccer Team

CLINICAL AND RESEARCH EXPERIENCE

- REHABILITATION SCIENCE/ORTHOPAEDIC CLINIC LEXINGTON, KY
Clinical Research Coordinator 2017-2018
- MEDICINE SPECIALTIES CLINIC LEXINGTON, KY
Clinical Services Technician 2014-2017
- NEUROLOGY CLINIC ROCHESTER, NY
Medical Technician 2013-2014
- ROCHESTER BABY LAB ROCHESTER, NY
Research Assistant 2011

PROFESSIONAL MEMBERSHIPS AND AFFILIATIONS

- Students in Neuroscience Advancement and Professional Development Society (SINAPS)
 - Outreach Coordinator 2021- present
 - New Student Representative 2019 – 2021
- International Society for Serotonin Research 2/4/2020 – present
- American Spinal Injury Association 1/14/2020 – present
- American Physiological Society 1/1/2020 – present
- Society for Neuroscience 5/2/2019 – present
- Women In Medicine and Science (WIMS) member 2019 – present
- Biomedical Graduate Student Organization member 2018 – present

FUNDING

- NIH Training Grant T32 - Neurobiology of CNS Injury and Repair
9/1/2020 – 8/31/2022

INVITED TALKS

- Ohio River Control of Breathing Seminar, University of Kentucky, Lexington, KY. Trainee Talk. *The Impact of Gut Dysbiosis on Recovery of Breathing After Cervical SCI and Respiratory Motor Plasticity*, September 30, 2022
- Kentucky Spinal Cord and Head Injury Research (KSCHIRT) Symposium, Louisville, KY. Invited Speaker. *The Impact of Gut Dysbiosis on Recovery of Breathing After Cervical SCI*, May 5, 2022
- Department of Neuroscience Student Seminar, University of Kentucky, Lexington, KY. Trainee Talk. *The Impact of Gut Dysbiosis on Recovery of Breathing After Cervical SCI and Respiratory Motor Plasticity*, May 2, 2022
- Department of Neuroscience Student Seminar, University of Kentucky, Lexington, KY. Trainee Talk. *The Impact of Gut Dysbiosis on Recovery of Breathing After Cervical SCI and Respiratory Motor Plasticity*, May 24, 2021
- Department of Neuroscience Student Seminar, University of Kentucky, Lexington, KY. Trainee Talk. *The Impact of Gut Dysbiosis on Recovery of Breathing After Cervical SCI and Respiratory Motor Plasticity*, March 2, 2020

- Department of Neurobiology and Anatomy, Drexel University, Philadelphia, PA. Invited Speaker. *The Impact of Gut Dysbiosis on Recovery of Breathing After Cervical SCI and Respiratory Motor Plasticity*, February 21, 2020
- Ohio River Control of Breathing Seminar, University of Louisville, Louisville, KY. Trainee Talk. *The Impact of Gut Dysbiosis on Recovery of Breathing After Cervical SCI and Respiratory Motor Plasticity*, January 17, 2020

PUBLICATIONS

Chase E. Taylor, Laura E. Mendenhall, Michael D. Sunshine, **Jessica N. Wilson**, Chris M. Calulot, Lance A. Johnson, Warren J. Alilain. (2023) *Sex and APOE Genotype Influence Respiratory Function Under Hypoxic and Hypoxic-Hypercapnic Conditions*. Scientific Reports (submitted, under review)

Book chapters

Olsufka, R. Peng, H. **Newton, J.** & Nixon, K. (2018). Alcohol Effects on Adult Neural Stem Cells – A Novel Mechanism of Neurotoxicity in Alcohol Use Disorders. Invited submission for T. Rasmussen (Ed.) *Stem Cells in Birth Defects Research and Developmental Toxicology* (pp. 173-222). John Wiley and Sons (New York).

CONFERENCE PRESENTATIONS

1. **Newton, J.S.**, Taylor, C.E., Sunshine, M.D., Mendenhall, L.E, Speed, S.L., Rose, B.C., Calulot, C.M., Little, B., Young L., Hawkinson, T., Randelman, M., Fortino, T.A, Kigerl, K.A., Sun, R., Waters, C., Lane, M., Popovich, P.G., Alilain, W.J. (2022, September). *The Effects of Gut Dysbiosis on Respiratory Motor Recovery Following Cervical Spinal Cord Injury*. Poster presentation at International Spinal Research Trust (ISRT) 2022, London, England.
2. **Newton, J.S.**, Taylor, C.E., Sunshine, M.D., Mendenhall, L.E, Speed, S.L., Rose, B.C., Calulot, C.M., Little, B., Young L., Hawkinson, T., Randelman, M., Fortino, T.A, Kigerl, K.A., Sun, R., Waters, C., Lane, M., Popovich, P.G., Alilain, W.J. (2022, July). *The Effects of Gut Dysbiosis on Respiratory Motor Recovery Following Cervical Spinal Cord Injury*. Poster presentation at SCI Neuromodulation Symposium 2022, Louisville, KY.

3. **Newton, J.S.**, Taylor, C.E., Mendenhall, L.E, Speed, S.L., Britsch, D.R.S., Calulot, C.M., Alilain, W.J. (2022, April). *The Effects of Gut Dysbiosis on Respiratory Motor Recovery Following Cervical Spinal Cord Injury*. Poster presentation at Experimental Biology 2022, Philadelphia, PA.
4. **Newton, J.S.**, Huffman, E.H., Britsch, D.R.S., Strattan, L.E., Maggard, R.S.J., Mendenhall, L.E., Calulot, C.M., Alilain, W.J. (2021, November). *Cervical spinal cord injury induces distinct changes in gut microbiome composition over time in rats*. Poster presented virtually at Neuroscience 2021 - Society for Neuroscience 50th Annual Meeting.
5. **Newton, J.S.**, Huffman, E.H., Britsch, D.R.S., Strattan, L.E., Maggard, R.S.J., Mendenhall, L.E., Calulot, C.M., Alilain, W.J. (2021, October). *Cervical spinal cord injury induces distinct changes in gut microbiome composition over time in rats*. Poster presented virtually at the Neuroscience Clinical translational Research Symposium, Lexington, KY.
6. **Newton, J.S.**, Huffman, E.H., Britsch, D.R.S., Strattan, L.E., Maggard, R.S.J., Mendenhall, L.E., Calulot, C.M., Alilain, W.J. (2021, May). *Longitudinal analysis of gut microbiome composition after experimental cervical spinal cord injury*. Poster presented at the 26th Annual Kentucky Spinal Cord and Head Injury Research Trust (KSCHIRT) Virtual Symposium, Lexington, KY.
7. **Newton, J.S.**, Huffman, E.H., Britsch, D.R.S., Strattan, L.E., Maggard, R.S.J., Mendenhall, L.E., Calulot, C.M., Alilain, W.J. (2021, April). *Longitudinal analysis of gut microbiome composition after experimental cervical spinal cord injury*. Poster presented at the 14th Annual College of Medicine Trainee Poster Session, Lexington, KY.
8. **Newton, J.S.**, Huffman, E.H., Britsch, D.R.S., Strattan, L.E., Maggard, R.S.J., Mendenhall, L.E., Calulot, C.M., Alilain, W.J. (2020, January). *Longitudinal analysis of gut microbiome composition after experimental cervical spinal cord injury*. Poster presented at the International Symposium of Neural Regeneration 2020, Asilomar, CA.
9. Huffman E.E., **Newton J.S.**, Britsch D.R., Waters C.M. Alilain W.J. (2020, January) *Investigating the link between cervical spinal cord injury and lung injury*. Poster presented at the International Symposium of Neural Regeneration 2020, Asilomar, CA.

10. **Newton, J.S.**, Huffman, E.H., Britsch, D.R.S., Strattan, L.E., Maggard, R.S.J., Mendenhall, L.E., Calulot, C.M., Alilain, W.J. (2019, October). *Longitudinal analysis of gut microbiome composition after experimental cervical spinal cord injury*. Poster presented at Society for Neuroscience 2019 Conference, Chicago, IL.
11. Huffman E.E., **Newton J.S.**, Stoltz D.R., Hager L., Alilain W.J. (2019, October) *Investigating the link between cervical spinal cord injury and lung injury/respiratory distress syndrome*. Poster presented at Society for Neuroscience 2019 Conference, Chicago, IL.
12. **Newton, J.S.**, Huffman, E.H., Britsch, D.R.S., Strattan, L.E., Maggard, R.S.J., Mendenhall, L.E., Calulot, C.M., Alilain, W.J. (2019, October). *Longitudinal analysis of gut microbiome composition after experimental cervical spinal cord injury*. Poster presented at the Kentucky Neuroscience Institute Clinical-Translational Research Symposium, Lexington, KY.